Abstract

Title of Dissertation: ISOTHERMAL DNA DETECTION UTILIZING BICYCLIC AMPLIFICATION OF PADLOCK PROBES

Alessandra Christelle Zimmermann
Doctor of Philosophy, 2019

Dissertation Directed by:

Professor Ian M. White

Department of Bioengineering

Professor Jason D. Kahn

Department of Chemistry and Biochemistry

As healthcare worldwide changes to more patient-centric models, medical diagnostics need to adapt to being used in settings outside of the central lab. Current strategies to bring diagnostics to the patient's bedside involve miniaturizing complicated amplification techniques, such as polymerase chain reaction, or building convoluted microfluidic assays that are difficult to operate. Ideally, a patient-centric diagnostic would require little instrumentation or training to operate, for which isothermal amplification techniques are ideal. Recent developments in catalytic DNA have enabled novel ways of iterating on amplification strategies to detect medically-relevant target sequences in systems that require little manipulation to operate.

In this thesis we improve upon the body of research on DNAzymes, catalytic DNAs that can self-cleave in the presence of a cofactor, used in concert with amplification techniques. We create a one-pot, bicyclic amplification assay capable of detecting single-stranded oligonucleotides, with straightforward extensions to double-stranded targets, multiplexing, and integration into advanced detection platforms. The target is detected through its hybridization to a circle template, using the sequence specificity of DNA to splint the ligation of this 'Template I,' with minimal detection of off-target sequences. The circular Template I is copied through rolling circle amplification (RCA), with the amplicon containing a DNAzyme that will self-cleave in the presence of copper ions. This generates a second primer in situ that can be used to prime a second, pre-ligated, Template II to elevate the RCA amplification scheme from a linear method to a polynomial one.

This Circle II template can then be used in a variety of detection modalities. The second amplicon can be used to cleave a hybridized FRET probe through the same copper ion cleavage mechanism as the primer generation, resulting in real-time fluorescence tracking. Alternatively, the RCA of the second circle can produce G-quadruplexes, which can be visualized with ABTS as a colorimetric endpoint that can be seen by eye, reducing the need for peripheral electronics. Finally, this thesis demonstrates the performance of the bicyclic RCA system in a phase-change system providing sequential mixing of components separated by wax layers, allowing the assay to proceed without any user interaction other than heating.

ISOTHERMAL DNA DETECTION UTILIZING BICYCLIC AMPLIFICATION OF PADLOCK PROBES

By

Alessandra Christelle Zimmermann

Dissertation submitted to the Faculty of the Graduate School of the
University of Maryland, College Park, in partial fulfillment
of the requirements for the degree of
Doctor of Philosophy
2019

Advisory Committee:

Associate Professor Jason D. Kahn, co-Chair

Associate Professor Ian M. White, co-Chair

Professor David Fushman

Associate Professor Douglas Julin

Associate Professor Vincent Lee

Acknowledgements

Thanks to a lot of people without which this would have been significantly more complicated, veering on impossible.

Dr. Jason Kahn and Dr. Ian White, my advisors who provided insight and direction to make this dissertation a reality.

Drs. John Goertz, Imaly Nanayakkara, and Hieu Nguyen, my bioengineering lab members who helped with intellectual and skill development for these projects. Aviva Borison and Nikita Singh, who helped perform the experiments for Chapter 5.

Jason Hustedt and Ian Ferencz, my biochemistry lab members whose comments and critiques helped shape the projects.

Dr. Maithili Saoji, Dr. Diana Zhang, and Ron McNeil, for helping me when I first learned my wet-lab skills and giving me the confidence to move forward with my career.

Marina Pranda, Haleigh Eppler, and Hemanshi Chawla, for their intellectual contributions and listening to me verbally process my data despite not needing to sit through that nonsense.

Christian, Veronique, and Sophie Zimmermann for raising me and continuing to do so from a distance.

James Cassarino for doing all the cleaning so that I don't have to deal with that.

Table of Contents

ACKNOWLEDGEMENTS ..... **II**

TABLE OF CONTENTS ..... **III**

LIST OF FIGURES ..... **VI**

LIST OF ABBREVIATIONS ..... **XIV**

1 INTRODUCTION **1**

2 A REVIEW OF DNAZYME CANDIDATES FOR IMPLEMENTATION IN THE AMPLIFICATION SYSTEM **9**

2.1 Introduction **9**

2.2 Oligonucleotide-cleaving DNAzymes **11**

2.2.1 RNA-Cleaving DNAzyme 11

2.2.1.1 Full RNA Substrate Cleaving DNAzyme 11

2.2.1.2 Chimera-cleaving DNAzymes 15

2.2.2 DNA-Cleaving DNAzymes 23

2.2.3 Allosteric DNAzymes 25

2.3 Emerging Sensing Applications for DNA-Catalyzed Cleavage **27**

2.3.1 Ion Sensors 28

2.3.2 Biosensors 31

2.4 Conclusion **34**

3 EXPERIMENTAL EVALUATION OF POTENTIAL DNAZYME SEQUENCES FOR USE IN TWO-STAGE RCA **37**

3.1 Introduction **37**

3.2 Different cleavage mechanisms of DNAzymes **38**

3.3 10-23: DNAzyme that cleaves chimeric DNA/RNA, leaving a 2′,3′ cyclic phosphate end **40**

3.3.1 Materials and Methods 41

3.3.2 Cleaving from a minimal sequence 42

3.3.3 Cleaving off the amplicon 43
3.3.4 Cleaved End Extension 45
3.3.5 10-23 summary 47

3.4 1-R3: DNAzyme that cleaves DNA through hydrolysis, leaving a 3′ OH 47
3.4.1 Materials and Methods 47
3.4.2 Cleaving in a minimal sequence 49
3.4.3 Cleaving from the amplicon 50
3.4.4 I-R3 summary 52

3.5 46mer Pistol-like: DNA-cleaving DNAzyme generating a phosphoglycolate 3′ end 52
3.5.1 Materials and Methods 53
3.5.2 Cleaving in a minimal sequence 54
3.5.3 Cleaving from the amplicon 55
3.5.4 Pistol-like summary 57

3.6 F8-X: DNA-cleaving DNAzyme with both a 3′ and 5′ phosphate 57
3.6.1 Materials and Methods 58
3.6.2 Cleaving in a minimal sequence 59
3.6.3 Cleaving from the amplicon 60
3.6.4. F8-X summary 62

3.7 Conclusion 62

4 BICYCLIC RCA: RAPID AMPLIFICATION AND REAL-TIME READOUT WITH A TWO-STAGE RCA SYSTEM 64

4.1 Introduction 64

4.2 Materials and Methods 66
Methods and Procedures 67

4.3 Results and Discussion 69
4.3.1 Specificity of RCA Amplification 69
4.3.2 Template I to Template II transition 72
4.3.3 Cleavage of bimolecular F8-X 73
4.3.4 One-Pot Reaction 76

4.4 Conclusion 78

5 INTEGRATION OF THE BICYCLIC RCA INTO A PHASE CHANGE PLATFORM FOR POC APPLICATIONS..... 79

5.1 Introduction 79

5.2 Materials and Methods 82

5.3 Results and Discussion 86

5.3.1 Selecting G-quadruplexes for High Temperature Use 86

5.3.2 G-quadruplex Generation from RCA.....89

5.3.3 Colorimetric output optimization.....92

5.3.4 RCA in layers.....95

5.4 Conclusion.....103

6 SIGNIFICANCE OF RESULTS AND FUTURE PROSPECTS 104

6.1 Development of a one-pot bicyclic nucleic acid amplification assay using DNAzyme-generated primers for Rolling Circle Amplification 104

6.2 Integration of an amplification multi-step assay into a one-pot, hands-free system 106

6.4 Future Directions – Expansion to double stranded nucleic acids.....108

6.5 Final advice for others embarking on PoC DNA amplification assay design.....109

APPENDICES..... 112

List of Sequences 112

List of Buffers 117

REFERENCES..... 118

List of Figures

Figure 1: Minimalist renderings of various nucleic acid amplification techniques: PCR (A), 3SR (B), EXPAR (C), LAMP (D) and HDA (E). PCR is shown as primers (red) annealing to a melted target duplex (black) and being extended by a DNA polymerase, creating two new duplexes (A). 3SR shows a target RNA (blue) annealing to a DNA primer (red) with a T7 RNA polymerase promoter sequence (orange), and extension by reverse transcriptase. The RNA is then degraded by the RNAse H activity of reverse transcriptase, allowing a second primer to anneal and to be extended. The now double stranded promoter can recruit T7 RNA polymerase and multiple RNA copies (blue) are produced, which can then each support extension of the red primer (B). EXPAR occurs through the binding of a template (bottom strand, with a repeated segment in red) with a T7 promoter or nicking enzyme recognition sequence (orange) to the target oligonucleotide (black). The target is extended across the template by a DNA polymerase. The product is either cut and refilled, or T7 RNAP binds and generates RNA (blue). The RNA or released segment can then serve as a primer at the 3′ end of another template and the cycle repeats (C). LAMP includes the interplay of inner (orange-blue and green-purple) as well as outer (orange and pink) primers extending from binding sites adjacent to the target sequence (black) via toe-hold exchange. The primers are designed so that a dumbbell template is generated, allowing loop primers (red/blue and purple/green) to bind and extend (D). HDA uses helicase (green) and accessory proteins (orange) to open double stranded target DNA (black) so that primers (red) can bind and be extended by DNA polymerase, generating new double stranded duplexes, which are then again opened by helicases (E). 3

Figure 2: Scheme of the mechanism of RCA amplification: (A) target hybridization to the padlock template and subsequent ligation of the template into a circular DNA, (B) hybridization of a primer to the circular template, and (C) the amplification of the circular template by a DNA polymerase (orange) lacking 5′ to 3′ exonuclease activity. 6

Figure 3: Hybridization of the linear Template I to the Target Sequence and ligation of the template ends (A), followed by priming of the template (B) and RCA amplification (C), generating a DNAzyme that self-cleaves in the presence of Cu^{2+} (D). The cleaved amplicon can then be hybridized to another Template I, allowing for the ligation of another circle and generating more primer for RCA (E) of either/both Template I or/and preformed Template II (F), shifting the reaction from linear to near-exponential amplification..... 7

Figure 4: Sequences and structures of full-RNA cleaving DNAzymes: the Pb^{2+} dependent 8-17 and its consensus sequence, along with Mg^{2+} dependent 10-23 and its consensus sequence, determined through selective mutation studies. The consensus sequences are shown binding to a full-RNA substrate to demonstrate the ability of these DNAzymes to cleave both full-RNA and chimeras. The GC DNAzyme is a Mg^{2+}-dependent analogue of

8-17 constructed of only GC bases,[54] and the modified 10-23 known as MNAzyme.[55] Highly conserved bases (red) are required for catalytic activity, moderately conserved bases (orange) are believed to specify the catalytic cation. The dashed outlines indicate the conserved cataltic sequence of the 8-17, and the appearance of that same sequence in the 10-23 DNAzyme. 13

Figure 5: Sequences and structures of the full RNA substrate cleaving DNAzymes that do not belong to the 8-17 family: S4, S9 and S21. All require Mn^{2+}. The GUG sequence in each of the substrate strands is a remnant of the primers used to generate the SELEX pool, so it is not known if the sequence is strictly required for DNAzyme activity. 15

Figure 6: Shown are the sequences and structures of the magnesium- and manganese-dependent DNAzymes E6,[58] CT10.3.29M5[61] and S15.[60] Conserved bases for CT10.3.29.M5 are identified by comparing all hits within a selection pool for consensus. The changing the orange base to G (M4 variant) alters the sequence preference for the RNA base (light blue) at the cleavage site. 17

Figure 7: Sequences and structures of transition metal dependent chimeric substrate cleaving DNAzymes: the Ag^{2+} dependent Ag10c, [36] Hg^{2+} dependent $E_{Hg}0T$,[37] UO_2^{2+} dependent 39,[38] Pb^{2+} dependent GR-5,[39] and Co^{2+} dependent DEC22-18.[41] PSCu10 is a DNAzyme with a phosphorotioate linkage (indicated by an asterisk) that confers dependence on Cu^{2+} for self-cleavage.[40] DZ1 and DZ7 catalysis can be assisted by a range of metal ions (Mn, Ni, Co, Zn, Pb, Cd).[44] Conserved bases are identified by comparing all hits within a selection pool for consensus..... 19

Figure 8: Sequences and structures of the monovalent ion chimeric substrate DNAzymes: the Na^+ or NH_4^+ dependent G3,[71] Na^+ dependent NaA43[72] and EtNa,[59] and Ce13d,[57] a variant of NaA43 that prefers $Ce3^+$ over Na^+. There is a strong but essentially accidental sequence homology to the substrates of the previously listed DNAzymes: TrAGGAA is in these sequences due to the selection conditions used in these various publications – it is the substrate sequence of 8-17. Due to the knowledge that 8-17 is dependent on divalent transition metal ions, most DNAzymes designed for ion specificity instead of cleavage sequence variety were screened against the 8-17 substrate. 21

Figure 9: Sequences and structures of DNAzymes capable of cleavage in low pH conditions: pH 4 responsive DZ15W5,[73] pH 4.5 responsive DZ27WS,[73] pH 3 responsive pH3DZ1[75] and pH4 responsive pH4DZ1. [75] Conserved bases are identified by comparing all positive hits within a selection pool for consensus. pH5DZ1 and pH6DZ1 are not shown, however all sequences are available in Table 1. 22

Figure 10: Sequences and structures of DNA-cleaving DNAzymes: the Cu^{2+} mediated Pistol-Like DNAzyme,[76] PLDz,[78] and F8-X,[79] as well as the Mn^{2+} and Zn^{2+} dependent 10MD5[80] and Zn^{2+} dependent Class I and II.[81] Conserved bases are identified by comparing all positive hits within a selection pool for consensus. 24

Figure 11: Sequences and structure representations of several allosteric DNAzymes. The 8-17 and pistol-like DNAzyme hybrid, DRc, that can cleave through either mechanisms depending on the available analyte.[84] The Dual DNAzyme undergoes pistol-like cleavage that allows for refolding to form a G-quadruplex for subsequent colorimetric signal generation through TMB.[85] Instead of introducing another DNAzyme's functionality, the addition of T-T mismatches to the DNAzyme 39 sequence led to a requirement for Hg^{2+} for cleavage, generating a DNAzyme that can detect the presence of either analyte: mercury and uranium.[63] 26

Figure 12: Utilization of an immobilized pistol-like DNAzyme to cleave HRP-conjugated streptavidin-biotin concatemers, allowing the HRP to be washed away upon copper ion mediated cleavage, and thus preventing the activation of the TMB and resulting in the absence of a colorimetric output. 30

Figure 13: The utilization of the 8-17 DNAzyme as a lead-sensitive readout following a traditional ELISA. The lead ions generated in solution from the capture antibody's binding cleave the 8-17, allowing for a ferrocene molecule to come in contact with the gold electrode, generating a detectable electrical signal.[99] 32

Figure 14: This assay demonstrates the use of a DNAzyme to generate a primer for Rolling Circle Amplification (RCA). The cleavage of the EC1 DNAzyme leaves a cyclic phosphate on the 3′ end. Upon end processing with PNK, the φ29 DNA polymerase (green) can excise back to a region that can pair with the other circle, and then it can extend the primer using the second concatenated circle as a template.[103] 34

Figure 15: Mechanism of cleavage of an RNA base by DNA[92] (A) and several proposed mechanisms of cleavage of DNA by DNA. The hydrolysis of the 3′ phosphate (B),[98] the additional hydrolysis of the 5′ phosphate resulting in a base excision (C)[66] and cleaving across the nucleotide resulting in a phosphoglycolate (D).[65] The mechanism for (D) is infered from several sources, including bleomycin-induced DNA scission.[95–97] 38

Figure 16: Structure of the 10-23 DNAzyme (A). Demonstration of 10-23 Substrate cleavage in the presence of the 10-23 Enzyme sequence and 10 mM $MgCl_2$ (B). Color-coding is as described in Figure 4. 43

Figure 17: Testing the ability of the 10-23 extended substrate to be cleaved in the simple Enzyme-Substrate, Circle Complement-Substrate, and RCA Amplicon-Substrate design respectively. Mg^{2+} ranges from 10 to 40 mM across the reactions (A). Demonstrating that the 10-23 Substrate is capable of being cleaved in the RCA mixture (B). Employment of an interfering DNA to remove possible secondary structures blocking the cleavage of the 10-23 Substrate in the RCA Amplicon. Mg^{2+} concentration is 30 and 60 mM (C). Showing that the RCA Amplicon is accessible to the 10-23 Substrate by demonstrating cleavage with HinfI at one site within the Amplicon (D). 44

Figure 18: Extension of pre-cleaved 10-23 Substrate from the 10-23 Enzyme in reaction buffer at pH 8.8 to 7.0, with control lanes of the Enzyme and Substrate in isolation, and a pH 7.9 reaction to represent standard protocol (A). Incubation of pre-cleaved 10-23 Enzyme and Substrate with Klenow DNA polymerase (3′→5′ exo⁻) in the presence (1), and absence (2) or dNTPs and in the presence of dNTPs and PNK (3). 46

Figure 19: Structure of the I-R3 DNAzyme with conserved sequence shown in red and cleavage point shown with an arrow (A). I-R3 cleavage efficiency in the presence of 10-1 mM $ZnCl_2$ in Reaction Buffer at 25 °C for 30 min. I-R3 in the absence of any zinc is shown on left as a control (B). Increasing concentration (0 to 16 mM) of $ZnCl_2$ to overcome the sequestering effects of 0.1 mM ATP, with I-R3 in the presence of 10 mM $ZnCl_2$ and no ATP on the left as a control (C). Increasing DTT concentration (0 to 10 µM) to determine the inhibitory effect on available $ZnCl_2$ (D). Analysis of (B), (C) and (D) were done on denaturing PAGE. 50

Figure 20: A schematic of the I-R3 DNAzyme in the bicyclic padlock system (A). A demonstration of the inhibitory effect of zinc on the polymerase, with the ligation and RCA in the absence of zinc on the left, followed by the increasing presence of $ZnCl_2$ (4 to 16 mM) during RCA (B). The effect of potential secondary structures competing with hybridization to the second circle, ligation of the first circle, Exonuclease I cleanup to demonstrate the presence of the circle, RCA in the absence of zinc, simultaneous or subsequent addition of the second circle to the RCA amplicon and ligation of the second circle and proof of the circle's presence (C). Analysis of (B) and (C) were done on denaturing PAGE. 51

Figure 21: Structure of the 46mer pistol-like DNAzyme (A). Cleavage in the presence of 1 µM-1 mM $CuSO_4$ overnight (B). 55

Figure 22: Scheme of the cleavage of the 46mer within the RCA amplicon (A). Off-amplicon cleavage of the 46mer DNAzyme post RCA in 1 mM $CuSO_4$ with either 100 µM ammonium sulfate, 500 µM betaine, or 1 % glycerol for 48 hours (B). Post-RCA cleavage of the 46mer DNAzyme in the amplicon in the same conditions during a 2 hour incubation (C). 56

Figure 23: Structure of the F8-X DNAzyme Enzyme and Substrate sequences (without loop) and F8-X Full (with loop) (A). Cleavage of the F8-X Substrate sequence from the Enzyme strand in 1 mM to 1 nM copper sulfate (B). Cleavage of the F8-X Full sequence in 1 mM to 10 nM copper sulfate (C). Both are 1 hour incubations. 60

Figure 24: Demonstration of bimolecular F8-X cleavage from the RCA Amplicon via visualization of the 5′ FAM labeled Substrate strand. Reactions were performed in either 0.1 or 0.2 mM copper sulfate and in the presence or absence of PNK as labeled (A). Demonstration of unimolecular F8-X cleavage in the presence of 10-1000 µM Cu^{2+} from amplicons generated by Klenow (exo⁻) or BST 2.0 DNA polymerases (B). Testing the 3′

phosphate cleanup by Shrimp Alkaline Phosphatase (rSAP) and PNK and visualizing extension via the 5′ FAM label. Reactions were performed in standard reaction buffer (--) or in the presence of 100 μM ammonium sulfate (N) or 500 μM betaine (“B”); (panel C). 61

Figure 25: The scheme representing the bicyclic reaction, starting with ligation of the padlock probe hybridized to a target DNA or RNA sequence (A), priming of the newly circularized Template I (B) and RCA (C) that generates an in-amplicon DNAzyme capable of cleavage in the presence of low concentrations of copper ion (D). This newly cleaved amplicon has its 3′ phosphate removed by T4 PNK and is used as a primer for a pre-circularized Template II (E), initiating a second round of RCA (F) and generating an amplicon that contains the enzymatic portion of the same DNAzyme, allowing for the fluorophore-quencher FRET probe DNA to bind to the amplicon (G) and to be cleaved, generating a fluorescent readout (H) or allowing for separation of a small labeled fragment. 65

Figure 26: Ligation and RCA reactions amplifying Template I in the presence and absence of the Target Sequence. Lane (1) is the linear Template I DNA alone as a control. Subsequent lanes are the ligation of Template I in the presence (2) or absence (3) of the Target Sequence, and the RCA reaction of the two ligation reactions respectively (4,5). This was analyzed on a PAGE gel as specified in methods. 70

Figure 27: Testing the processivity of RCA using 4 different variants of the Template II (Circle II F8X and Circle II G Version I, II and III). The ligated circles are shown in the four lanes at the far left, followed by the RCA reaction in either the absence or presence of a primer, showing that the long amplicon forms only when the primer is present (A). The dependence on the primer is additionally emphasized by showing the dependence of the amount of RCA amplicon formed upon initial primer concentration, as demonstrated through RCA reactions run with 1 μM to 1 nM copper ion-cleaved F8-X and a constant 0.1 μM ligated Template II (B)..... 71

Figure 28: Extension of two variants of Template II by a precut F8-X primer that has a functional 3′ end (primer) and the cleaved and T4 PNK cleaned F8-X DNAzyme (F8-X) (A). Extension of variants of Template II from cleaved and cleaned Template I, with two concentrations of starting primer shown (B). 72

Figure 29: FAM fluorescence signal from the FRET probe in the presence of various DNAs and 10 μM $CuSO_4$. The DNAs are the RCA Amplicon of Circle II, the minimal sequence Enzyme moiety of the F8-X DNAzyme, and an artificial Circle II complement. The FRET probe alone is shown as the lower bound for fluorescence, and an unquenched FAM sequence is a positive control (A). The denaturing PAGE gel of the reaction with a FAM only (B) and SYBR-stained view (C), showing the cleavage products in the presence of the complement and the enzyme sequence..... 74

Figure 30: Time course of FAM signal during RCA of Template II, demonstrating the signal generation from the FRET probe as it hybridizes to the RCA amplicon. 'Target' is the Template II splint acting as a target for this assay. 76

Figure 31: Realtime FRET of the bicyclic assay initiated by a pre-ligated Circle I RCA amplicon. Fluorescence is background subtracted by setting the reading at $t_0 = 0$ for all runs..... 77

Figure 32: Full bicyclic RCA reaction performed in real time with a range of Target concentrations. Fluorescence is background subtracted by setting the reading at $t_0 = 0$ for all runs..... 78

Figure 33: Scheme of the phase-change partitioned bicyclic RCA assay. This scheme demonstrates the partitioned reagents prior to addition of the target sequence, separated by pure alkanes represented by grey bands (A). The reaction is initiated through the addition of the target sample (B) and subsequent heating to 37 °C, melting the octadecane layer allowing mixing of the target with the linear Circle I precursor and T4 DNA ligase (C). The ligation occurs as the temperature ramps up to 40 °C, allowing the eicosane layers to melt and revealing Klenow (exo$^-$) and the Circle I primer to initiate RCA and T4 PNK to clean up the 3′ end of the in situ generated primers (D). The transition to 50 °C melts the docosane layer, revealing Circle II and BST 2.0, kicking off the second round of RCA, in which the amplicon is a G-quadruplex sequence. Hemin in this RCA mixture stabilizes the G-quadruplexes as they form, and Nb.BsmI allows for nicking of the amplicon to increase the G-quadruplex color output (E). Finally, heating to 55 °C melts the tetracosane layers, revealing the ABTS, additional hemin and the hydrogen peroxide. The reaction is then removed from the heating element and the colorimetric output develops for 30 minutes before analysis (F)..... 81

Figure 34: Testing various known G-quadruplexes in standard (pH 7.9) buffer at 65, 55 and 37 °C to determine thermal limits for their use (A). Testing CatG4 at pH 9.5 to 7.0 at 25 °C to determine optimal pH for colorimetric analysis (B). Generation of the G5A5G5 G-quadruplex from a linear template using BST 2.0 Polymerase at pH 8.8-6.5, incubated during the synthesis at 37, 45, or 55 °C before analysis with PAGE (C). 88

Figure 35: Ligation of an RCA template containing the complement to either G5A5G5, G4T4G4 or CatG4 and subsequent RCA at 55 °C for 2 hours in the absence or presence of Nb.BsmI, a nicking enzyme (A). RCA of the same templates, with the addition of a template (NG) that does not contain a G-quadruplex, in the presence and absence of Nb.BsmI. The outputs were analyzed after 30 minutes by denaturing PAGE and colorimetric output through complexing with Hemin and ABTS (B). 90

Figure 36: Stabilizing the formation of the G-quadruplexes on the amplicon using 10-20 μM hemin, with or without 10 mM ammonium sulfate, in the RCA mixture, followed by additional hemin during the colorimetric assay. RCA was performed with a primer ordered

from IDT (primer) or a primer created through F8-X cleavage (cut F8-X). Only the cleaved primers are shown in the colorimetric traces (A). The addition of 10 μM hemin, 10 μM hemin and 10 mM ammonium sulfate, 20 μM hemin or the base RCA mixture to a Circle II variant that generates the G5A5G5 sequence instead of CatG4, with both absorbance scan and PAGE gel of the resulting RCA amplicon (B). 91

Figure 37: Concentration scale of in situ generated primer initializing Circle II RCA, visualized through endpoint ABTS absorbance. The absorbance at 420 nm is background subtracted against its baseline at 550 nm. 92

Figure 38: (A) Several compounds were tested for their G-quadruplex stabilizing and background reducing qualities, with the background subtracted absorbance at 420 nm shown. All G-quadruplex samples have 10 μM CatG4 in reaction buffer. (B) Changing to a pH 7.0 assay buffer from the pH 7.9 reaction buffer increases the colorimetric output of the G-quadruplexes. (C) Demonstrating the quantitation and limit of detection of the ABTS-hemin colorimetric output. The full absorbance scan of the colorimetric output is shown, baseline adjusted to zero absorbance at 550 nm. (D) The absorbance at 420 nm of an extended CatG4 concentration range is shown separately, demonstrating the background intrinsic to the reaction. Of note is the no buffer control showcasing that the buffer, and particularly KCl, is instrumental in decreasing the background absorption. 94

Figure 39: The order of layer assembly with the different wax layers identified (A) and a demonstration of the sequential melt layers on PAGE gel (B). Numbers on the gel correlate to the different stages of assembly indicated in (A). 96

Figure 40: Optimization of the hydrogen peroxide addition by depositing 4 or 10 μL of 2 mM hydrogen peroxide in water (A). 20-60 μM of hemin and 4-10 mM of ABTS were tested to increase the output difference between negative and G-quadruplex positive samples (B), as well as varying the enzyme solution' glycerol composition (C), and either depositing 4 or 10 μL of the 100 % glycerol enzyme solution (D) in the layered reaction. 98

Figure 41: Photograph of the prepared alkane layers prior to target addition and melting (A). ABTS output from a pre-initiated reaction (Circle I ligated ahead of time), the full reaction in the presence and absence of the Target, as well as a reaction supplemented with 0.1 μM CatG4 (B). Significant improvement is then observed upon the addition of 20 % v/v organic solvents to the Hemin-ABTS layer (C). Background subtraction was done by subtracting the absorbance at 550 nm from that at 420 nm. 100

Figure 42: Bicyclic reaction performed in layers from pre-incubated Circle I RCA Amplicon or synthetic Circle II primer (A). Full bicyclic reaction performed in layers, either melted in one go (full) or stopped at the $CuSO_4$ stage and left to cleave overnight before continuing (B). Background subtraction was done by subtracting the absorbance at 550 nm from that at 420 nm. 102

Figure 43: Proposed multiplexing of bicyclic RCA. The design of the Target I and II detection circles is shown (A) as well as a scheme demonstrating the parallel reactions with no consensus sequences, allowing for both targets to be detected in a single reaction with no crosstalk. Separate FRET probes designed with different fluorophores are used to quantitate which, or both, of the Targets are present in solution (B). Previous work testing the sequence specificity of the DNAzyme is shown in (C) with the arm sequences varied to have only a certain number of matched bases flanking the cut site. 106

Figure 44: Proposal for opening the dsDNA helix using strand invasion by short PNA or LNA brackets (pink). The PNA or LNA brackets invade the dsDNA helix due to their higher binding affinity (A), thus allowing Circle I precursor to hybridize and ligate (B). 109

List of Abbreviations

3SR – Self-Sustained Sequence Replication

ABTS – 2,2′-azino-bis(3-ethylbenzothiazoline-6-sulphonic acid)

DNAzyme – DNA enzyme

DTT – Dithiothreitol

EXPAR – EXPonential Amplification Reaction

FAM – Fluorescein

FRET – Förster Resonance Energy Transfer

HDA – Helicase Dependent Amplification

LAMP – Loop-mediated isothermal AMPlification

PAGE – Poly-Acrylamide Gel Electrophoresis

PCR – Polymerase Chain Reaction

PNK – PolyNucleotide Kinase

PoC – Point of Care

RCA – Rolling Circle Amplification

rSAP – Shrimp Alkaline Phosphatase

SERS – Surface Enhanced Raman Spectroscopy

TMB – 3,3′,5,5′-Tetramethylbenzidine

1
Introduction

Healthcare in the modern world is changing. With more patients, more tests, and tighter budgets, the central laboratory model is becoming an economic burden. Already, many areas are adopting a more primary care oriented model,[1] but with the new model comes new requirements for medical tests. In the absence of the resources of a central laboratory, diagnostic assays need to be simple enough to be completed by anyone employed by a clinic, but still accurate enough to be trusted in comparison to an established standard test. In some areas where even a permanent office is not cost-effective, or even in locations that do not have the freezer space to store anything more than vaccines, the diagnostic kit needs to be capable of being stored and transported in the wide range of conditions that face roving clinics. Point-of-care (PoC) testing has been at the forefront of this primary care revolution. Some PoC tests, such as the pregnancy test[2] or the blood-glucose monitor,[3] also allow for individuals to monitor their own health without the need to see a physician, alleviating an enormous barrier to care in some regions. In other cases, such as the HIV mucosal swab, the test is performed by a medical professional in the presence of the patient, to guarantee an accurate diagnosis.[4]

The World Health Organization, in a move to guide the design of PoC devices towards practical applications, has provided guidelines for PoC devices with a specific focus on sexually transmitted infection testing. These requirements are known as the ASSURED guidelines,[5] listed below:

Affordable – for those at risk of infection

Sensitive – minimal false negatives

Specific – minimal false positives

User-friendly – minimal number of steps to carry out

Rapid and **R**obust – short turnaround time and no need for refrigerated storage

Equipment-free – no complex or bulky equipment

Delivered – to end users

Enzymatic DNA or RNA amplification using specific DNA primers is a natural answer to the ASSURED guidelines, as it checks nearly all the boxes. Synthetic DNA is no longer prohibitively expensive, and enzymes need only be present in catalytic amounts. The sequence-dependent nature of DNA hybridization allows for both sensitivity and specificity of the assay, and enzymes and DNA are both shelf-stable in a wide range of conditions when lyophilized,[6–8] allowing for the robustness of the assay. The two main concerns when designing a DNA amplification assay for PoC use then become managing the assay's complexity in terms of manipulation and equipment (i.e., user friendliness) as well as its speed.

The Polymerase Chain Reaction (PCR) is the gold standard for DNA amplification reactions, however there is a limit when it comes to complexity. Its design is theoretically simple: melt a double stranded sequence, allow specially designed primers to bind to the melted ends, extend with a thermostable DNA polymerase, and repeat 30-40 times (Figure 1A).[9,10] PCR has been adapted for PoC settings,[11] but the core concept of PCR still requires rapid heating and cooling of the assay mixture, and thus relies on having a source of power

nearby. Miniaturizing the electronics so that the instrument can be carried to the patient's bedside has also caused the device to be prohibitively expensive for many rural areas.[12]

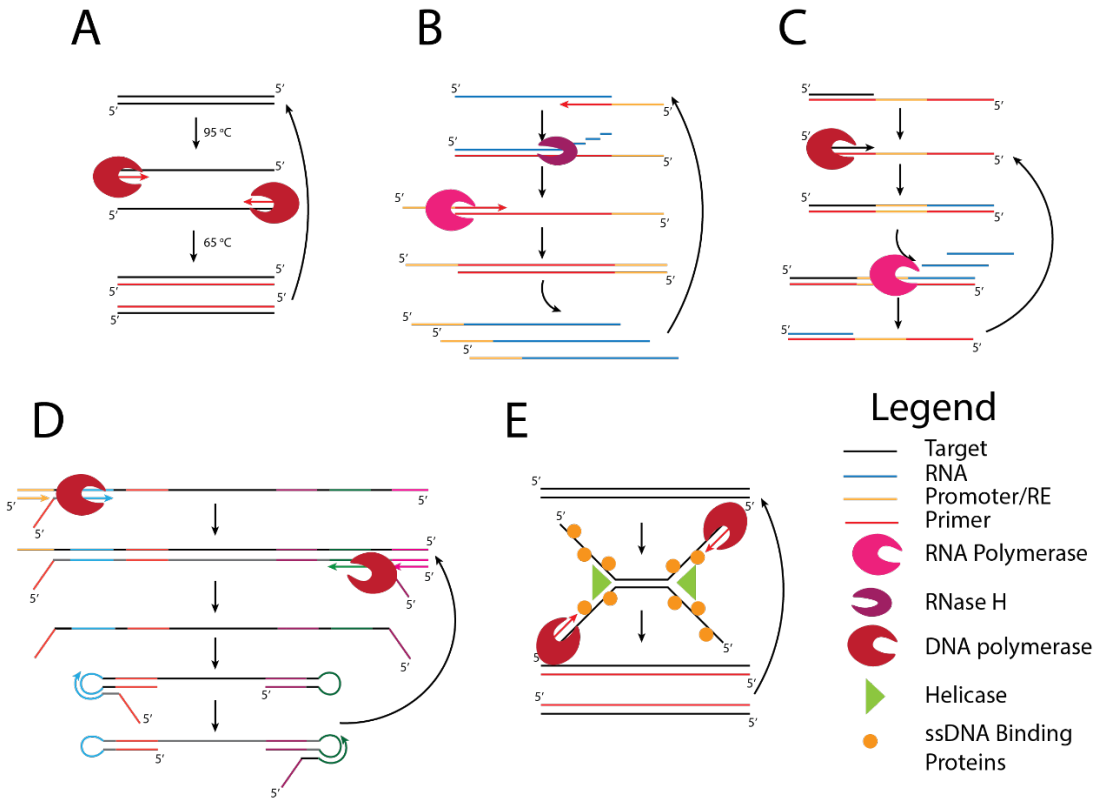

Figure 1: Minimalist renderings of various nucleic acid amplification techniques: PCR (A), 3SR (B), EXPAR (C), LAMP (D) and HDA (E).
PCR is shown as primers (red) annealing to a melted target duplex (black) and being extended by a DNA polymerase, creating two new duplexes (A).
3SR shows a target RNA (blue) annealing to a DNA primer (red) with a T7 RNA polymerase promoter sequence (orange), and extension by reverse transcriptase. The RNA is then degraded by the RNAse H activity of reverse transcriptase, allowing a second primer to anneal and to be extended. The now double stranded promoter can recruit T7 RNA polymerase and multiple RNA copies (blue) are produced, which can then each support extension of the red primer (B).
EXPAR occurs through the binding of a template (bottom strand, with a repeated segment in red) with a T7 promoter or nicking enzyme recognition sequence (orange) to the target oligonucleotide (black). The target is extended across the template by a DNA polymerase. The product is either cut and refilled, or T7 RNAP binds and generates RNA (blue). The RNA or released segment can then serve as a primer at the 3′ end of another template and the cycle repeats (C).
LAMP includes the interplay of inner (orange-blue and green-purple) as well as outer (orange and pink) primers extending from binding sites adjacent to the target sequence (black) via toe-hold exchange. The primers are designed so that a dumbbell template is generated, allowing loop primers (red/blue and purple/green) to bind and extend (D).
HDA uses helicase (green) and accessory proteins (orange) to open double stranded target DNA (black) so that primers (red) can bind and be extended by DNA polymerase, generating new double stranded duplexes, which are then again opened by helicases (E).

An assay that does not require energy-intensive temperature control would be simpler to perform as a PoC diagnostic, and the rise of isothermal amplification systems followed this realization. The first of such systems was Self-Sustained Sequence Replication (3SR),[13,14] which amplifies RNA in a sample by generating a DNA complement with a T7 RNA polymerase promoter sequence that will in turn generate many copies of the first RNA, which can then be copied by the initial primer again (Figure 1B). 3SR is not a particularly optimal assay in the field, however, due to the perishable nature of RNA. The more stable descendant of 3SR is EXPonential Amplification Reaction (EXPAR),[15] which one can design with either the original T7 promoter or a site for a more thermostable nicking enzyme (Figure 1C). The previous two techniques are primarily designed to detect small, single stranded oligonucleotides. Loop-mediated isothermal AMPlification (LAMP)[16] instead requires relatively long sequences: its target sequence must be flanked by a large enough number of bases for multiple different sets of primers to anneal. This technique is considered one of the most complicated to design, as it requires the interplay of four to six primers along a template strand to generate the amplicon (Figure 1D). Also, while LAMP does not require temperatures that would degrade RNA during the course of the reaction, it is performed at 65 °C to minimize non-specific binding and to help with the toehold exchange necessary for new primers to bind.[17] Helicase Dependent Amplification (HDA)[18,19] also uses elevated temperatures, despite its use of helicases to melt the double stranded duplex in a mimic of PCR without the need for thermocycling (Figure 1E). While these assays work well in clinical settings, it is not straightforward to maintain a constant temperature of 65 °C without advanced electronics, and many of the enzymes used in these assays, notably T7 RNA polymerase, are fragile. Pure PoC diagnostics must rely on

significantly more resilient techniques. Rolling Circle Amplification (RCA) is one such robust technique, in which a DNA polymerase generates single stranded amplicons from a primer (Figure 2). This very simple model has no unduly fragile enzymes nor any finicky toe-hold kinetics to take into account, and therefore can be performed at a wide range of temperatures, including the more accessible 37° C.

The RCA reaction relies on the ability of a polymerase lacking a 5′ to 3′ exonuclease domain to extend a primer on a single-stranded, circular DNA template, continuously displace the DNA from previous cycles, and generate amplicons of theoretically infinite length[20]. The formation of this circular template can be incorporated into the assay, as shown in Figure 2A, through the hybridization of the adjacent 3′ and 5′ ends of a linear precursor of the circular template, frequently described as a padlock probe due to its resemblance and its ability to 'lock' around a target sequence. Once circularized, amplification can be initiated through a primer so that the primer gets displaced as the polymerase circles around, generating single stranded amplicon comprised of multiple repeats of the template's complement (Figure 2B-C). Altering the polymerase used allows for variation in the temperature and amplification rate of the reaction, allowing for modulation of the technique for varied reaction conditions. As previously stated, the single stranded amplicon is noteworthy as it allows for additional functional elements to be inserted into the sequence of the amplicon, broadening the range of applications of the technique. It is this quality of RCA that makes the technique particularly interesting for PoC design. The signal output can be altered from a non-specific method such as DNA intercalating dyes to a much more specific technique such as the cleavage of a dye-labeled signal DNA. The single stranded amplicon can be designed to hybridize to the signal DNA

and upon hybridization the dye can be enzymatically cleaved from the DNA and quantified.[21]

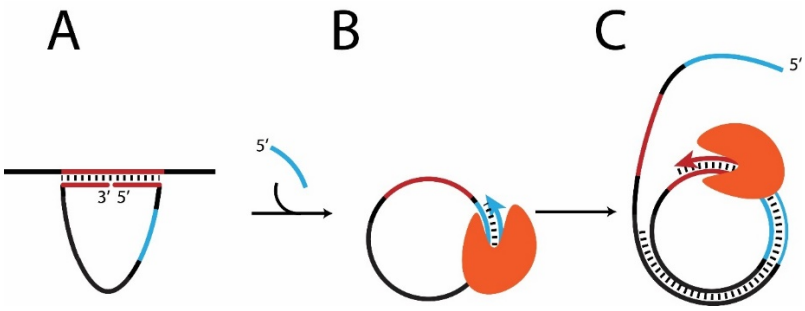

Figure 2: Scheme of the mechanism of RCA amplification: (A) target hybridization to the padlock template and subsequent ligation of the template into a circular DNA, (B) hybridization of a primer to the circular template, and (C) the amplification of the circular template by a DNA polymerase (orange) lacking 5′ to 3′ exonuclease activity.

Another advantage of RCA is that the only step absolutely required to initiate amplification is the binding of the primer to the circular template. This has allowed for different approaches to target recognition, including (i) the binding of a primer to a pre-circularized template[22] or (ii) using the primer as a splint to ligate a linear template into a circular one[20]. This simplicity in design requires few restrictions on what can be considered a primer, expanding the range of diagnostics that can be performed.

RCA's biggest disadvantage is that it is a linear amplification scheme; each target binding event only generates one amplicon, thus implying that it cannot reach the detection performance of PCR and other amplification methods that generate product at a nonlinear (e.g. exponential) rate. While the amplicon itself contains multiple copies of the original sequence, there is no possibility in the classic design to cycle the amplified product, which would result in signal generation at a nonlinear rate. The answer to this has come in many forms: (i) the addition of primers that can extend while hybridized to the amplicon,[22–25] using restriction enzymes to cut the amplicon into more primers,[26,27] and (ii) priming a

single padlock multiple times.[28,29] These techniques, however, require the incorporation of additional enzymes or oligonucleotides that add complexity to the reaction.

We propose instead to incorporate two circular templates into the reaction scheme and turn the prolific but linear amplification mechanism into an even more prolific nonlinear system (Figure 3). This would entail the RCA amplicon of the first circle generating a primer for a second round of RCA through the use of a self-cleaving DNAzyme sequence (Figure 3D). The in situ generated primer could then either hybridize another Template I, ligating and priming it allowing it to amplify to give additional primers (Figure 3E), or prime a second circle (Figure 3F) that contains signal-generation elements for quantification of the target (not shown). Multiple modes of signal generation are explored in this thesis, described at length in chapters 4 and 5.

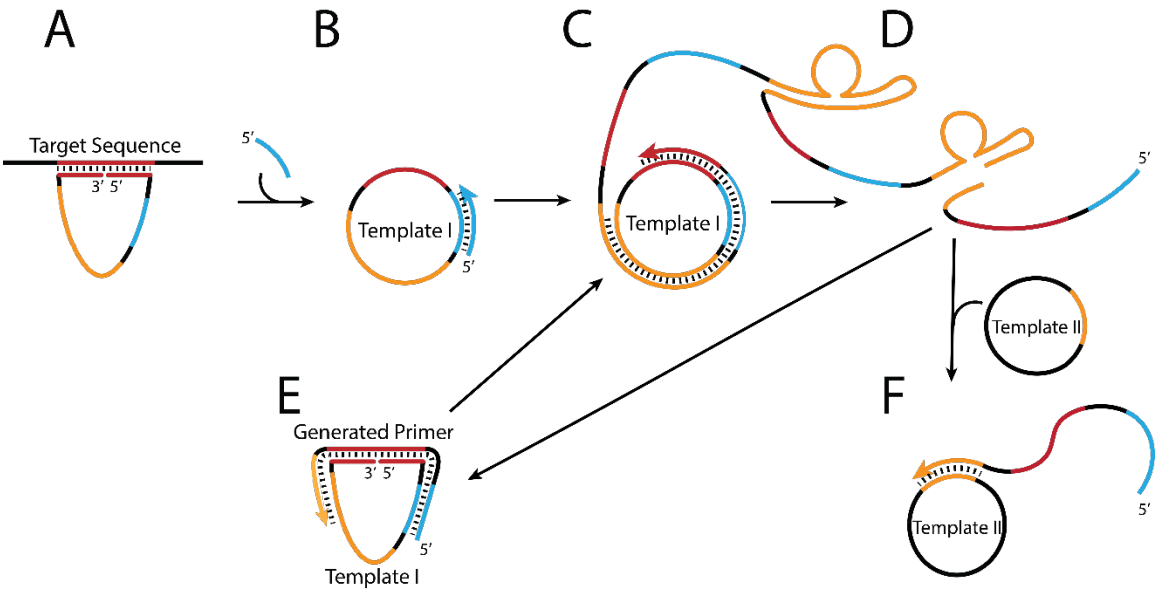

Figure 3: Hybridization of the linear Template I to the Target Sequence and ligation of the template ends (A), followed by priming of the template (B) and RCA amplification (C), generating a DNAzyme that self-cleaves in the presence of Cu^{2+} (D). The cleaved amplicon can then be hybridized to another Template I, allowing for the ligation of another circle and generating more primer for RCA (E) of either/both Template I or/and preformed Template II (F), shifting the reaction from linear to near-exponential amplification.

This bicyclic system is amenable to a wide range of target sequences, requiring only that they are single stranded in solution. As such, miRNA sequences and viral RNA (such as Zika virus RNA)[30,31] are key targets for this assay. Importantly, this assay is the first of its kind to be able to be performed in one pot, and in principle it even enables multi-sequence detection in a single reaction with a one-pot assay.

This dissertation explores DNAzymes that could be used to drive the nonlinear RCA and then narrows in on a promising contender and explores its use in various assays. **Chapter 2** is a review of the breadth of existing DNAzymes available and their catalytic cofactors, as well as some examples of their uses in published assays. **Chapter 3** encompasses an analysis of the DNAzymes that were tested for viability in our assay, with a discussion of their mechanisms of cleavage, cofactor requirements, and cleavage efficiencies in the context of being tethered to an amplification strategy. **Chapter 4** analyzes the complete bicyclic assay, first in stages then as a complete system. The limit of detection will be presented and limitations on the assay will be discussed, as well as the possibility of multiplexing the assay. **Chapter 5** presents the implementation of the assay in a low-complexity, low-cost system previously developed by the White lab – thermally activated phase change partitions. **Chapter 6** summarizes all of the work and presents the contributions to the field.

2
A Review of DNAzyme Candidates for Implementation in the Amplification System

2.1 Introduction

The importance of enzymes as biocatalysts is indisputable, as their catalytic turnover of substrates makes life on this planet possible. Until 1982, proteins were believed to be the only biological polymer capable of catalyzing reactions, but the publication of Cech's work on self-splicing RNA, named an RNAzyme by analogy to its protein cousins, changed the field forever.[32] They described an RNA self-cleaving intron that could process itself in the presence of mono- and divalent salts. Not only did this stimulate new models of the chemical makeup of early life, it opened avenues to cheaper, more highly controlled enzymatic manipulation of nucleic acids. This discovery was followed a decade later with the first catalytic DNA, a sequence that could cleave an RNA substrate in the presence of divalent cations as sole cofactor.[33] Subsequent advances in DNA synthesis technologies and the development of SELEX allowed for the discovery a multitude of catalytic DNAs, also known as DNAzymes, since Breaker's discovery.

DNAzymes have since garnered attention in the biosensing and therapeutic communities, as DNA has practical advantages compared to proteins or RNA. DNA is the cheapest of the three to manufacture,[34,35] and it has the longest shelf life as well as the best resistance to extreme conditions. Additionally DNA can remain active under a broad range of reaction conditions, including temperature, salt concentrations, and pH.[36]

While the catalytic activity of all three biopolymers require folding of a linear chain into a functional tertiary structure, DNA and RNA structure is more hierarchical than protein structure: nucleic acid secondary structure is stable independent of the tertiary arrangement.[37] This imparts nucleic acids' largest advantage as a tool for biotechnology: substrate recognition can be separated from catalytic activity. This has led to an ease of programmability of substrate recognition, allowing for rapid redesigns without losing functionality.

In trying to evolve catalytic biopolymers, the smaller number of nucleic acid monomers available and the ease of sequencing make DNA- and RNAzymes simpler to screen and identify than protein enzymes. Advances in DNA synthesis make it simple to perform directed evolution[38] towards binding a target analyte, or for any other purpose, because a large number of random sequences can be generated quickly and cheaply. Even brute-force selection approaches can be successful due to the large accessible sequence space. There are now DNAs capable of catalytically ligating,[39–41] phosphorylating,[42,43] acting as a peroxide,[44,45] as well as the cleavage of both RNA and DNA.

Previous reviews in this area include a global view of catalytic DNAs[46] as well as highly targeted reviews, such as those by Li and colleagues, in which they highlight the advances in both the discovery of DNAzymes[47] and their novel applications.[48] This chapter provides a comprehensive overview of the existing range of nucleic acid-cleaving DNAzymes and their uses as sensors for metals and biomolecules.

2.2 Oligonucleotide-cleaving DNAzymes

There is now a wide variety of DNAzymes, obtained largely from in vitro selection-amplification experiments. The DNAzymes discussed here are classified first by their cleavable substrate and subsequently by their catalytic cation, and additionally compiled in Table 1 (Page 35) for ease of choosing those with appropriate properties. For each DNAzyme discussed, the minimal sequence is also available in Appendix Table 2 for those who wish to elaborate on them.

2.2.1 RNA-Cleaving DNAzyme

The 2′ hydroxyl present on RNA allows for more facile cleavage by DNAzymes or other catalysts, leading to a larger library of RNA-cleaving DNAzymes than DNA-cleaving DNAzymes. Within the scope of RNA-cleaving DNAzymes, there are two clear classes: DNAzymes that can cleave substrates made exclusively of RNA (full RNA) and those that can cleave chimeric RNA-DNA sequences. This distinction is important when selecting DNAzymes for different applications, as a DNAzyme that requires an RNA-DNA chimera may not be useful for cleaving natural biopolymers for therapeutic techniques, whereas chimera are preferred in a sensing applications. The following is a showcase of DNAzymes that can cleave full RNA, single RNA bases in a DNA context, or both.

2.2.1.1 Full RNA Substrate Cleaving DNAzyme

In 1994, the first reported DNAzyme could catalytically cleave a DNA:RNA chimera on the 3′ side of the riboadenine in the substrate strand in the presence of Pb^{2+}.[33] The authors suggested that this sequence could be optimized to cleave full RNA substrates instead of the chimera they used, and three years later the 8-17 and 10-23 DNAzymes were developed (Figure 4).[49] These two DNAzymes, named for the batch and cycle of in vitro

selection from which they were isolated, could both cleave full RNA substrates. 8-17 was found to cleave best with Pb^{2+}, though some catalytic activity remains if Zn^{2+} or Mg^{2+} are substituted. 8-17 is also remarkable as it is a very short sequence, and later studies mapping the bases required to conserve catalytic activity identified 5 bases in the catalytic loop that are commonly found in many RNA-cleaving DNAzymes, highlighted in Figure 4 with a dashed outline.[50] Crystal structures of the 8-17 DNAzyme further reinforce the necessity for these highly conserved bases, with the GC and GA conserved bases interacting through hydrogen bonds in the catalytic core.[51] It is important to note that 8-17 is one of the few DNAzymes to have its structure elucidated, and in all cases throughout this chapter the secondary structure is proposed by the authors.

The conserved sequence of 8-17 is also found in 10-23, which cleaves in the presence of Mg^{2+}. Like 8-17, 10-23 is capable of cleaving both full RNA and chimeric substrates, but it has a preference for bases other than rA(C/U/T) flanking the cleavage site.[49] The sequences of 8-17 and 10-23 have been refined through mutation studies to isolate the bases necessary for catalysis, which allows us to identify both the 8-17 pattern within 10-23 and the additional six conserved bases in 10-23 that appear to be necessary for Mg^{2+} preference.[52] 10-23 has one of the fastest rates of cleavage of any RNA-cleaving DNAzyme while using a readily abundant cation, and thus 10-23 has risen to prominence in bioanalytical spheres.[53]

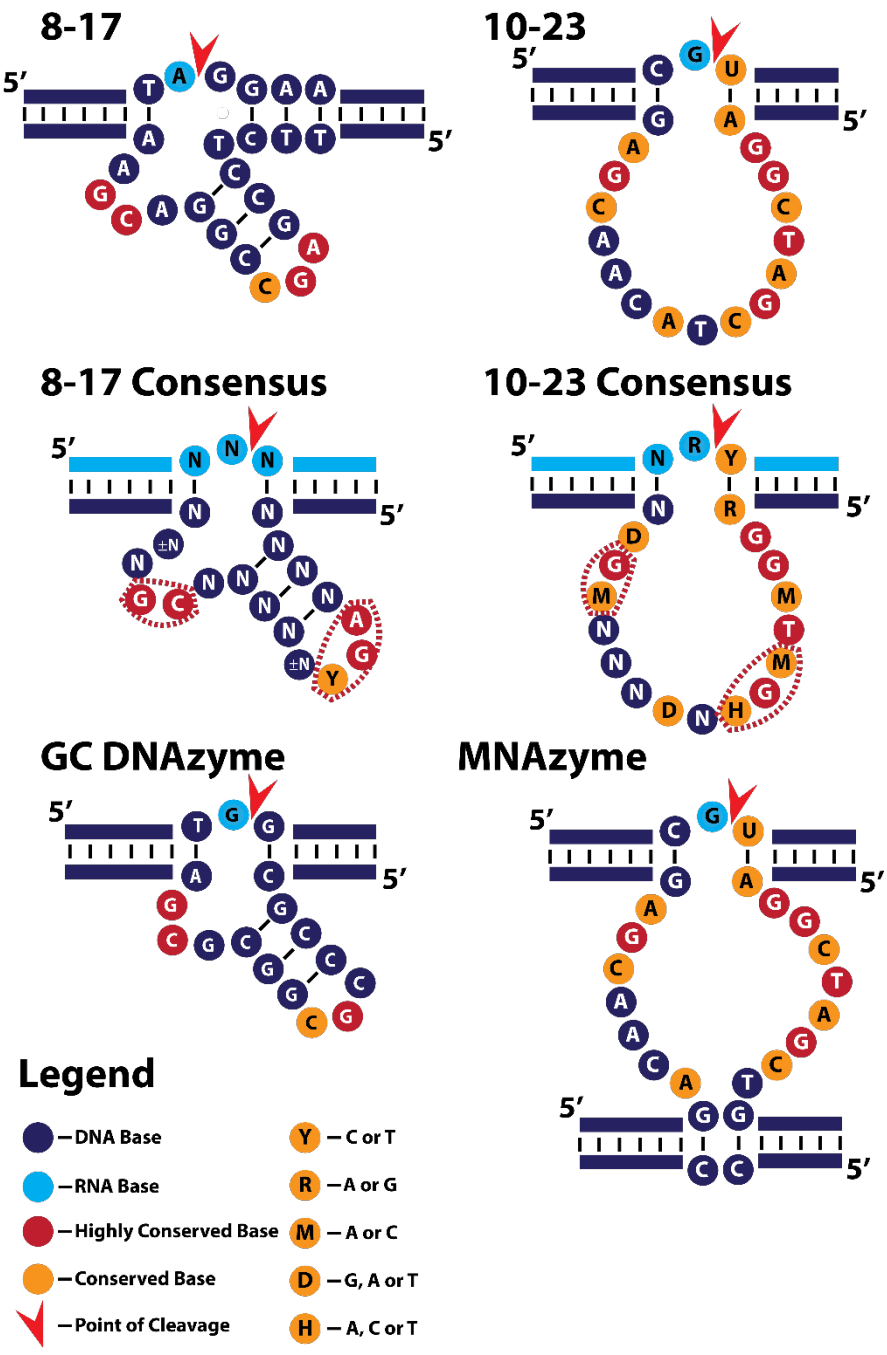

Figure 4: Sequences and structures of full-RNA cleaving DNAzymes: the Pb^{2+} dependent 8-17 and its consensus sequence, along with Mg^{2+} dependent 10-23 and its consensus sequence, determined through selective mutation studies. The consensus sequences are shown binding to a full-RNA substrate to demonstrate the ability of these DNAzymes to cleave both full-RNA and chimeras. The GC DNAzyme is a Mg^{2+}-dependent analogue of 8-17 constructed of only GC bases,[54] and the modified 10-23 known as MNAzyme.[55] Highly conserved bases (red) are required for catalytic activity, moderately conserved bases (orange) are believed to specify the catalytic cation. The dashed outlines indicate the conserved cataltic sequence of the 8-17, and the appearance of that same sequence in the 10-23 DNAzyme.

Additionally, Multi-component DNAzymes, or MNAzymes, have been derived from the 10-23 sequence.[56] These MNAzymes contain a cleaved 10-23 catalytic loop upon which a second set of binding arms are added, so that the loop can only be correctly structured if a 4th DNA bridges across the gap and 'closes' the loop. This allows for added specificity, as all four DNAs need to be present for the reaction to occur, but it does increase the complexity of the structure assembly. Polylysine-*g*-dextran has been shown to increase the cleavage activity of MNAzymes when included in the reaction buffer, potentially facilitating the assembly of the active complex through volume exclusion.[55]

The 8-17 structure is also found in several other published DNAzymes, though not all of them exhibit the same substrate specificity. The GC DNAzyme (Figure 4) is an example that can cleave full RNA substrates in the presence of both Mg^{2+} and Mn^{2+}, but it is much more active on chimeric substrates.[54] Additionally, several other DNAzymes that contain the 8-17 conserved sequence show no affinity for full RNA substrates, cleaving only chimerae. [57–59] These will be discussed in a subsequent section.

There are also several DNAzymes that do not have the 8-17 sequence that are capable of cleaving full RNA substrates, although they have a higher affinity for chimeric substrates. In 2008 the Li lab published the results of a screen for DNAzymes that cleave specifically at pyrimidine-pyrimidine junctions within chimeric sequences. These junctions were specifically chosen because 8-17 and its sequence analogues exhibit much slower cleavage kinetics with these target dinucleotides. Three of their hits, named S4, S9 and S21 (Figure 5), showed some level of catalytic activity on full RNA substrates.[60] All of these sequences exhibit catalytic activity in the presence of Mn^{2+}, though S4 shows an increase in activity with the addition of K^+ or Na^+.

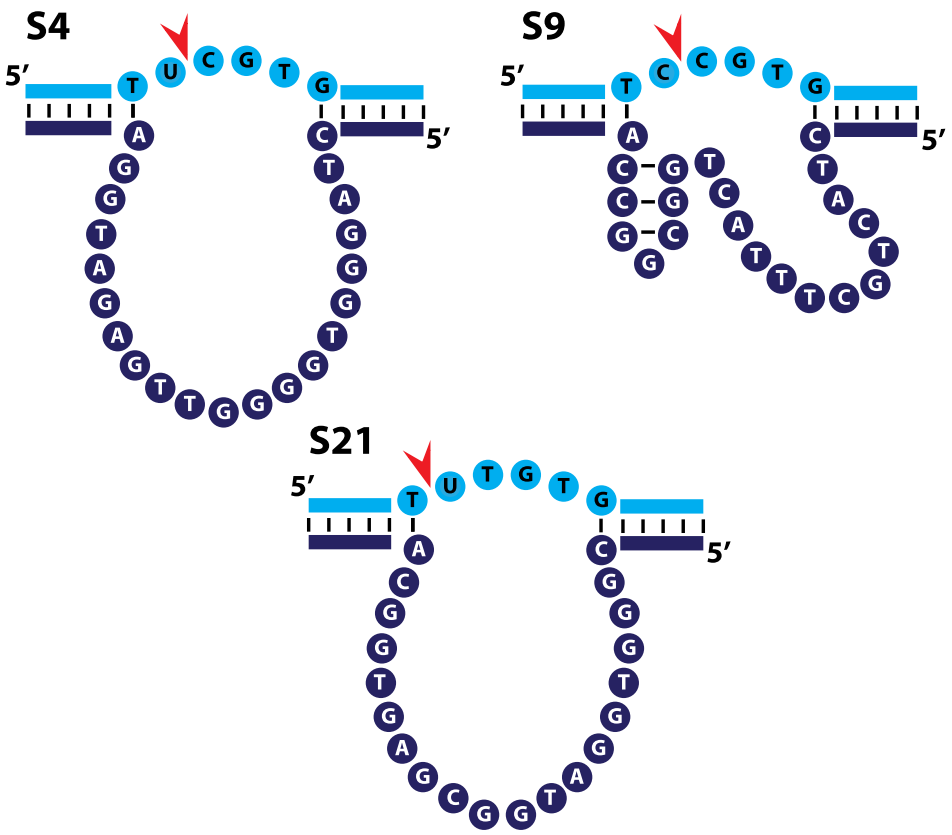

Figure 5: Sequences and structures of the full RNA substrate cleaving DNAzymes that do not belong to the 8-17 family: S4, S9 and S21. All require Mn^{2+}. The GUG sequence in each of the substrate strands is a remnant of the primers used to generate the SELEX pool, so it is not known if the sequence is strictly required for DNAzyme activity.

2.2.1.2 Chimera-cleaving DNAzymes

The largest category of DNAzymes are those which cleave RNA-DNA chimera. This is perhaps because they are much easier to work with than full RNA, especially when immobilized onto a surface as a cleavage target as during SELEX. Chimera are additionally chosen more often as they are likely to be more chemically stable than full RNA in biological media, while maintaining the chemical reactivity of RNA's 2′ hydroxyl. This has been of particular interest to the low-resource point-of-care community, for which reagent storage in ambient conditions is extremely important.

2.2.1.2.1 DNAzymes with Divalent Metal Ion dependence

Figure 6 illustrates several chimera-cleaving DNAzymes. As with the DNAzymes capable of cleaving full RNA sequences, many require divalent cations. E6, one of the chimera-cleaving DNAzymes that contain 8-17's conserved bases, cleaves in the presence of Mg^{2+}, with Na^{+} accelerating cleavage (the rate increases linearly with Na^{+} concentration above 0.1 M).[58] CT10.3.29, a DNAzyme designed to preferentially cleave the rC-T junction that 8-17 cannot, cleaves in the presence of Mg^{2+} and Mn^{2+}.[61] While it is not the fastest pyrimidine-pyrimidine cleaving DNAzyme, it is of particular interest due to the investigator's ability to control specificity simply by altering only the base opposite the 5′ nucleotide of the cleavage site dinucleotide, shown in orange in Figure 6. The M5 variant of CT10.3.29 shown in Figure 3 with a T in the position opposite the cleavage site, has a preference for rU-A/T and rA-A/T cleavage sites while the M4 variant with a G as the opposite base, prefers rC/T and rU-A/T. S15, a DNAzyme found in the same SELEX screen as the full-RNA DNAzymes discussed in Figure 5, also cleaves pyrimidine-pyrimidine chimerae in the presence of both Mn^{2+} and Mg^{2+}.[60]

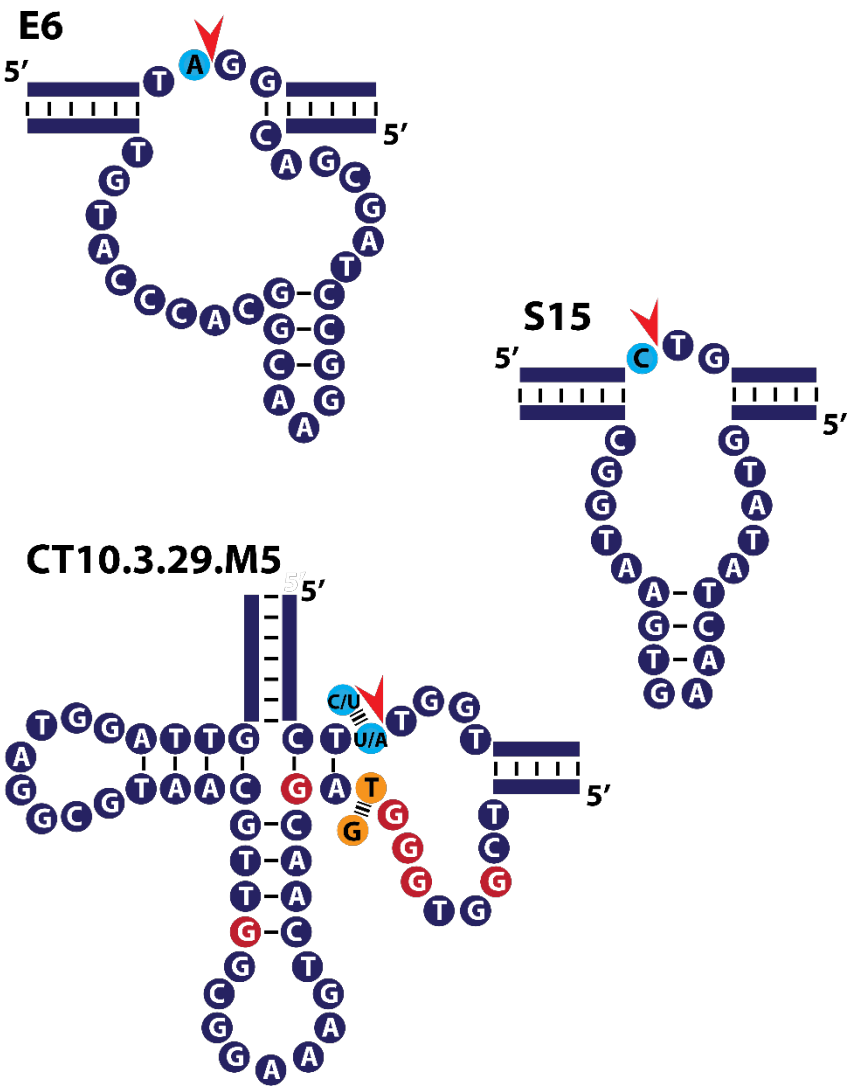

Figure 6: Shown are the sequences and structures of the magnesium- and manganese-dependent DNAzymes E6,[58] CT10.3.29M5[61] and S15.[60] Conserved bases for CT10.3.29.M5 are identified by comparing all hits within a selection pool for consensus. The changing the orange base to G (M4 variant) alters the sequence preference for the RNA base (light blue) at the cleavage site.

2.2.1.2.2 DNAzymes with Uncommon Metal Ion Dependence

Many RNA-cleaving DNAzymes were selected for use with divalent cations that are not ubiquitously found in buffers, several of which are described in Figure 7. These DNAzymes, such as Ag10c, which cleaves in the presence of Ag^{+},[62] can be used as sensors to detect the ions in solution, and field tests of contaminated water samples have led to an effort to develop DNAzymes for most heavy metals. Additionally, these DNAzymes have

been screened to be as selective for their cation as possible; while Ag10C has slight catalytic activity in the presence of Hg^{2+}, $E_{Hg}0T$[63] is much more sensitive to the mercuric ion. $E_{Hg}0T$ was derived from mutations to DNAzyme 39, which cleaves in the presence of UO_2^{2+}.[64] Despite being the first lead-dependent DNAzyme discovered, 8-17 is not very selective for lead, so a search for a more specific DNAzyme led to the isolation of GR5, which is responsive only to Pb^{2+}.[65] While there are DNA-cleaving DNAzymes that use copper ion as a cofactor, there are currently no identified Cu^{2+}-dependent RNA-cleaving sequences. There is, however, the PSCu10 DNAzyme, which contains a phosphorothioate bond to the 3′ of the RNA base, allowing for self-cleavage specifically in the presence of the thiophilic Cu^{2+} ion.[66] DEC22-18 is a DNAzyme that cleaves in the presence of Co^{2+}, though it can also use either Ni^{2+} or Mn^{2+}.[67] DEC22-18 is also of interest because the substrate strand can be cleaved between an internal fluorophore and quencher pair, allowing for fluorescence signaling for Co^{2+} allowing for the DNAzyme itself to perform as a FRET probe, and generating signal from the cleavage directly. This cleavage across a fluorogenic substrate can also been seen in several other DNAzymes, namely the Mg^{2+} cleaving MgZ[68] and Mg^{2+}, Mn^{2+}, Co^{2+}, or Ni^{2+} dependent 5J-A28.[69]

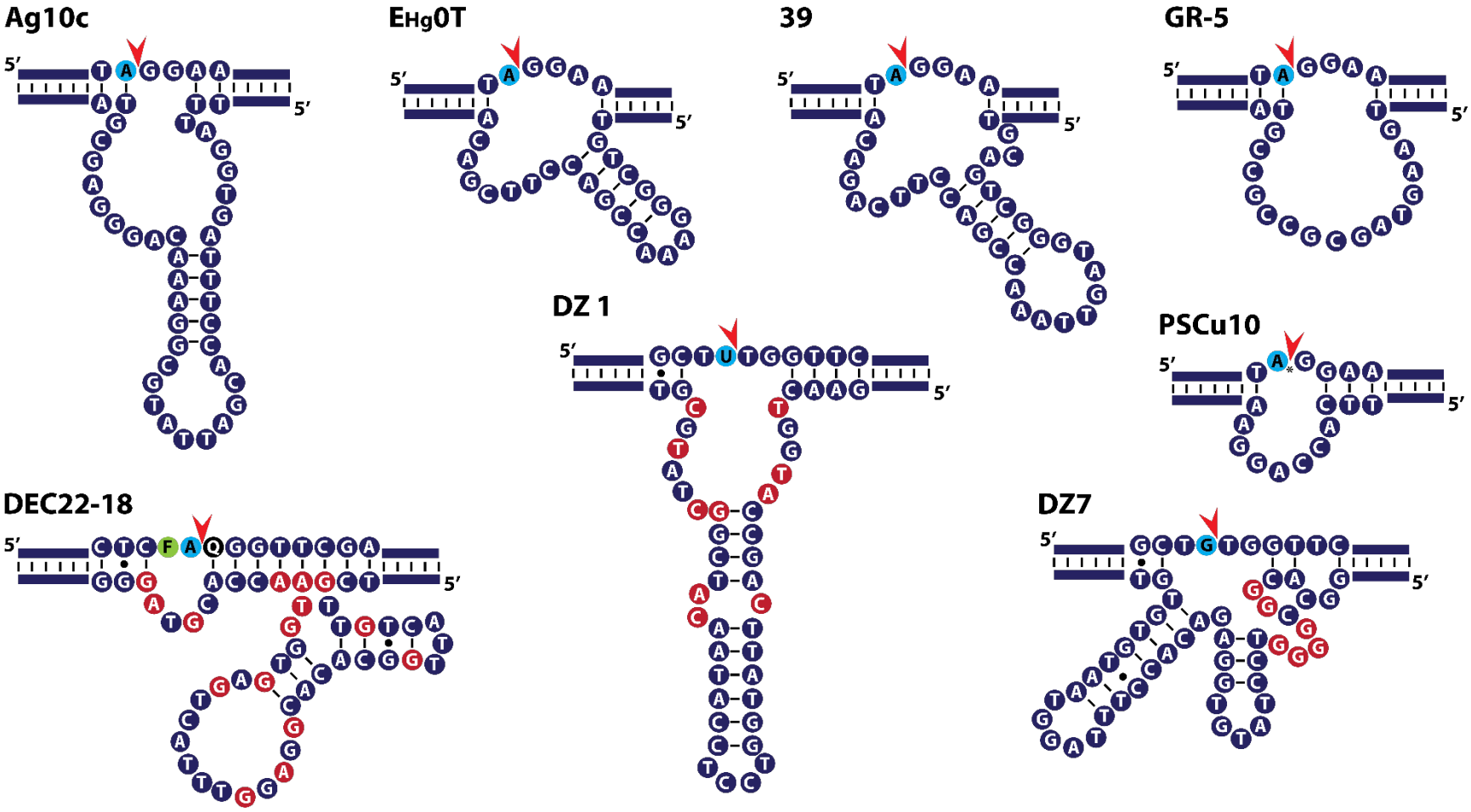

Figure 7: Sequences and structures of transition metal dependent chimeric substrate cleaving DNAzymes: the Ag^{2+} dependent Ag10c, [36] Hg^{2+} dependent E_{Hg}0T,[37] UO_2^{2+} dependent 39,[38] Pb^{2+} dependent GR-5,[39] and Co^{2+} dependent DEC22-18.[41] PSCu10 is a DNAzyme with a phosphorotioate linkage (indicated by an asterisk) that confers dependence on Cu^{2+} for self-cleavage.[40] DZ1 and DZ7 catalysis can be assisted by a range of metal ions (Mn, Ni, Co, Zn, Pb, Cd).[44] Conserved bases are identified by comparing all hits within a selection pool for consensus.

Achieving selectivity for one single metal ion is a common challenge in the development of metal-dependent DNAzymes, as can be seen through the lack of specificity for the catalytic ion exemplified by 5J-A28 or DZ1, the latter of which can catalyze cleavage in the presence of Mn^{2+}, Ni^{2+}, Co^{2+}, Zn^{2+}, Pb^{2+} or Cd^{2+}.[70] The catalytic activity of the DNAzyme varies with the different metal ions, as with the other DNAzymes identified in the same screen, but in all cases they are responsive to more than one ion, which could easily confound test results.

2.2.1.2.3 DNAzymes with Monovalent Ion Dependence

Rarer than the divalent cation dependent DNAzymes are those requiring monovalent cations only. That is not to say they are not available, as the DNAzyme G3 cleaves a riboadenosine on its substrate strand in the presence of either Na^+ or NH_4^+.[71] Additionally, EtNa, named after its two catalytic cofactors, cleaves in the presence of Na^+, with ethanol accelerating its activity when added up to 72 % v/v.[59] EtNa can also cleave in the presence of isopropanol, methanol or DMSO. NaA43 is another Na^+ cleaving DNAzyme, which contains the conserved 8-17 bases.[72] It was believed to bind exclusively sodium for some time, until the discovery of Ce13d, a Ce^{3+} dependent DNAzyme that was later found to contain the same catalytic core sequence as NaA43. Subsequent investigations demonstrated that NaA43 requires Na^+ and can be accelerated by Ce^{3+}, while Ce13d requires Ce^{3+} and can be accelerated by Na^+.[57]

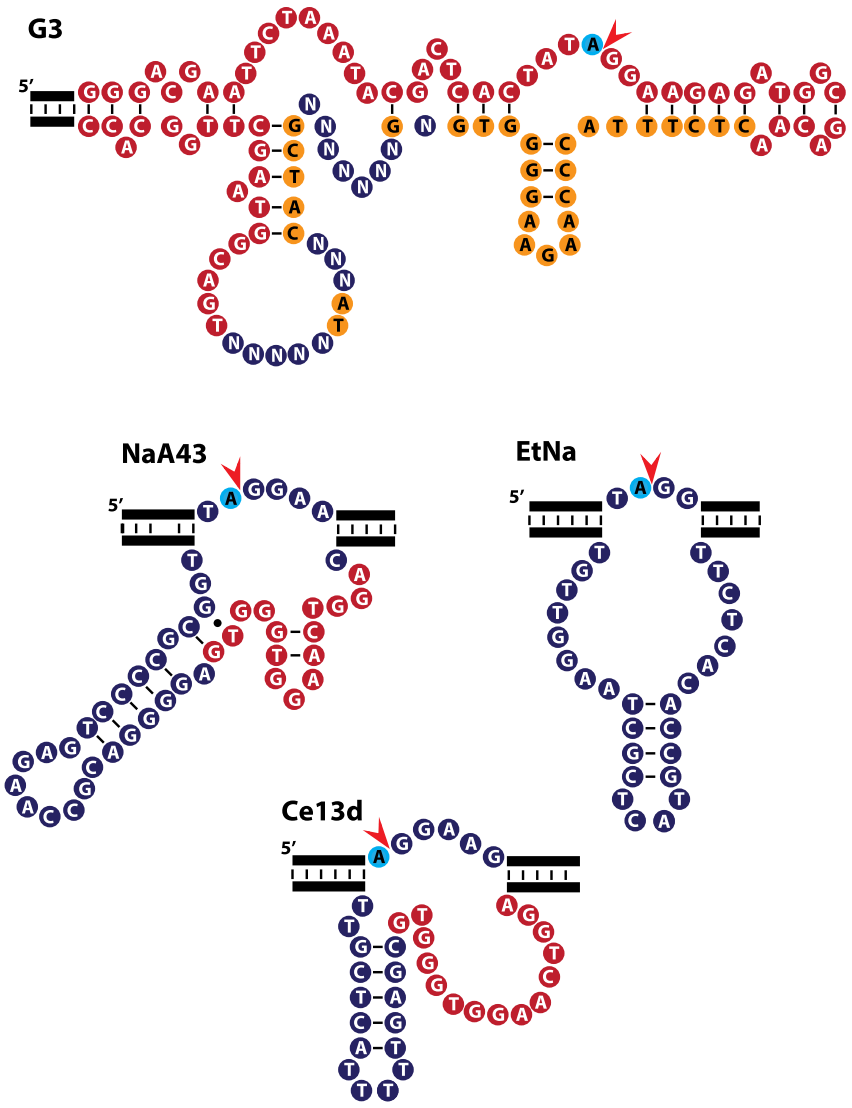

Figure 8: Sequences and structures of the monovalent ion chimeric substrate DNAzymes: the Na^+ or NH_4^+ dependent G3,[71] Na^+ dependent NaA43[72] and EtNa,[59] and Ce13d,[57] a variant of NaA43 that prefers $Ce3^+$ over Na^+. There is a strong but essentially accidental sequence homology to the substrates of the previously listed DNAzymes: TrAGGAA is in these sequences due to the selection conditions used in these various publications – it is the substrate sequence of 8-17. Due to the knowledge that 8-17 is dependent on divalent transition metal ions, most DNAzymes designed for ion specificity instead of cleavage sequence variety were screened against the 8-17 substrate.

2.2.1.2.4 DNAzymes with Activity at Low pH

With the exceptions of EtNa and Ag10C, which have both been found to cleave at a pH of 6.0, and 39, which cleaves at 5.5, every DNAzyme described so far cleaves at a pH of 7.0 to 7.5. This lack of variability in the pH motivated the directed evolution of DNAzymes that specifically allow for a broader range of assay conditions, shown in Figure 9. DZ15WS

and DZ27WS self-cleave only in a pH 4.0 - 4.5 sodium citrate buffer, and have been shown not to require divalent ions.[73] In fact, divalent cations reduce cleavage activity, with Cd^{2+} completely inhibiting cleavage of the DNAzymes. An additional study by the Li lab looking at pH specific cleavage led to the identification of DNAzymes that cleave only at pH values of 3.0, 3.8, 4.8 and 6.0 by DNAzymes correspondingly named pH3DZ1, pH4DZ1, pH5DZ1 and pH6DZ1 respectively.[74] These DNAzymes do not exhibit specificity towards one cation, though all of them showed cleavage in the presence of Mn^{2+} and Na^{+}. Interestingly pH3DZ1, pH4DZ1 and pH5DZ1 have no proposed secondary structures, presumably cleaving the substrate shown in Figure 9 through non-canonical interactions.

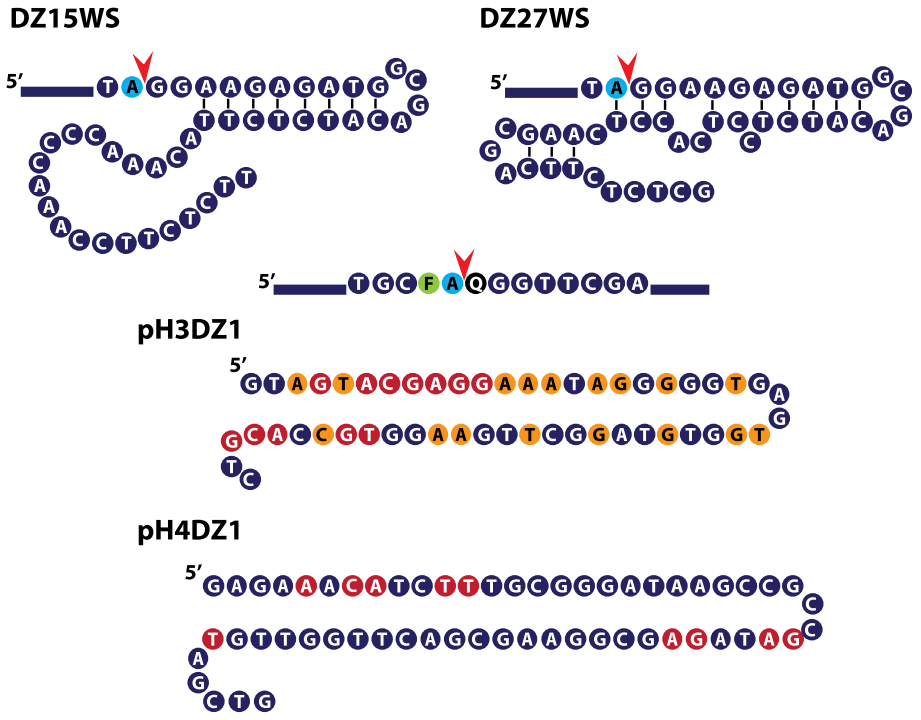

Figure 9: Sequences and structures of DNAzymes capable of cleavage in low pH conditions: pH 4 responsive DZ15W5,[73] pH 4.5 responsive DZ27WS,[73] pH 3 responsive pH3DZ1[75] and pH4 responsive pH4DZ1. [75] Conserved bases are identified by comparing all positive hits within a selection pool for consensus. pH5DZ1 and pH6DZ1 are not shown, however all sequences are available in Table 1.

2.2.2 DNA-Cleaving DNAzymes

DNAzymes capable of cleaving at a DNA nucleotide are significantly rarer than those that employ a 3′-OH. These DNAzymes, can be classified according to their varied cleavage mechanisms, or into subcategories according to the divalent cation used to enable catalytic activity. Continuing with the trend shown before, we will categorize them according to their cation, but a more thorough discussion of cleavage mechanism is provided in Chapter 3.

The first subclass was discovered in 1996 by the Breaker group when performing in vitro screening for DNAzymes active with Cu^{2+}.[76] This subclass is named Pistol-Like DNAzymes due to the characteristic shape of the drawing of the secondary structure, shown in Figure 10. These DNAzymes cleave themselves in the presence of micromolar Cu^{2+},[77] with some sequences having enhanced activity in the presence of both Cu^{2+} and hydrogen peroxide[76] or ascorbic acid.[78] The cleavage site for these DNAzymes is located in a Watson-Crick helix on the 'barrel' of the 'pistol,' and cleavage is possible with any barrel sequence as long as Watson-Crick base pairing is maintained.

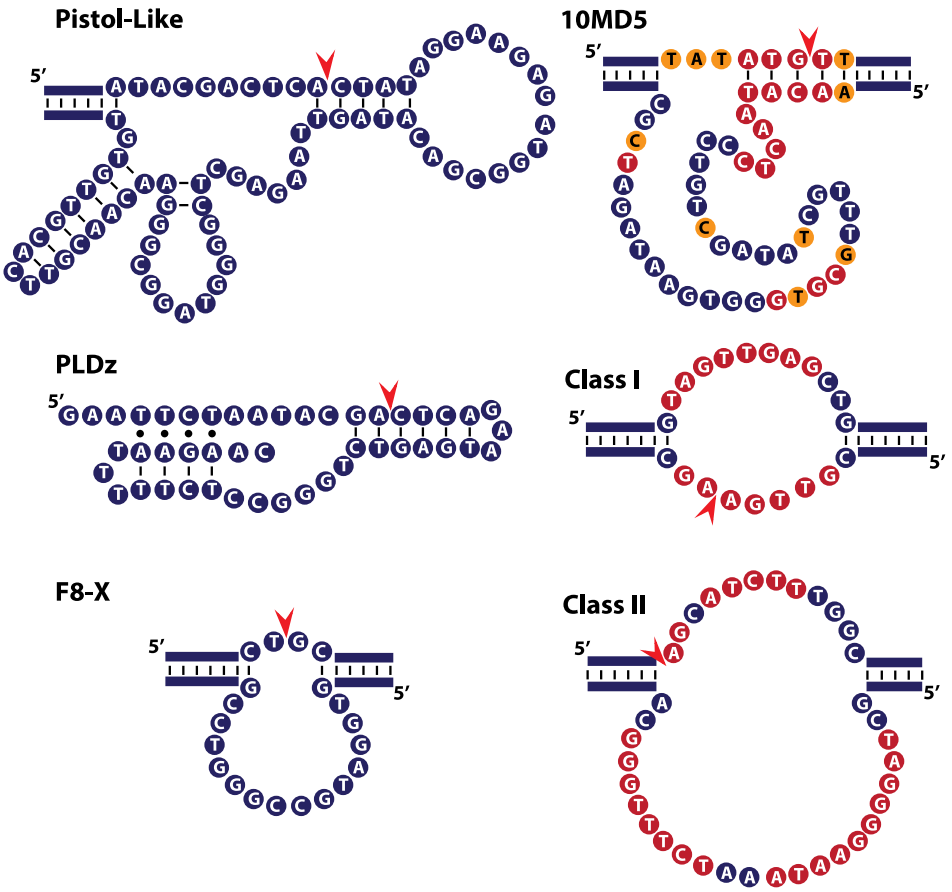

Figure 10: Sequences and structures of DNA-cleaving DNAzymes: the Cu^{2+} mediated Pistol-Like DNAzyme,[76] PLDz,[78] and F8-X,[79] as well as the Mn^{2+} and Zn^{2+} dependent 10MD5[80] and Zn^{2+} dependent Class I and II.[81] Conserved bases are identified by comparing all positive hits within a selection pool for consensus.

F8-X is a DNAzyme with a copper ion cofactor but it is structurally unrelated to the pistol-like DNAzyme family.[79] F8-X is particularly useful, as the cleavage site is between two variable binding arms, allowing for a copper-mediated DNAzyme that has no sequence restrictions. Just like the pistol-like DNAzyme, its activity can be enhanced by the presence of hydrogen peroxide, as well as DTT or Mn^{2+}.

Another subclass of DNA-cleaving DNAzymes was identified in 2009 by the Silverman lab.[82] This DNAzyme, called 10MD5, was found to cleave in the presence of either Mn^{2+} and Zn^{2+}, though either Cd^{2+} and Ca^{2+} can be substituted for Mn^{2+} with some decrease in

catalytic activity. The cleavage site in this class of DNAzymes is located in a Watson-Crick helix and requires the ATG^T sequence to cleave, but it will tolerate any sequence to the 3′ side of the cleavage site as long as Watson-Crick base pairing is maintained. 9NL27, a variant of 10MD5 that was identified when optimizing the sequence, varies by only 5 bases in the catalytic loop, shown in orange in Figure 10.[80] 9NL27 is notable as it requires only Zn^{2+} for catalysis, and selective mutation of the 5 bases showed that only the T16 to A and G19 to C changes are required for exclusive Zn^{2+}-dependent catalysis. The orange bases in the substrate, however are necessary to achieve cleavage by Zn^{2+}, further limiting the range of DNA analytes that can be cleaved.[83]

In 2013, the Breaker lab published two more DNA-cleaving DNAzymes dependent on Zn^{2+}.[81] In the selection subgroup they named Class I, they found a highly conserved sequence in the loop that correlated to catalytic activity. Notably, the cleavage site was located in the conserved sequence of that loop. This Class I DNAzyme is currently the fastest DNA-cleaving DNAzyme known, capable of nearly 90 % cleavage in 5 minutes. The Class II sequences had a similar structure and cation dependence, but with a cleavage site immediately outside the conserved sequence.

2.2.3 Allosteric DNAzymes

On occasion, a biosensor strategy needs to be more complex than a single cleavage step. DNAzymes can be used to perform multistep reactions just like their protein counterparts. Moreover, those multiple steps can be designed to mimic the if-then nature of allosteric enzymes. This has been done by incorporating the strictly conserved sequences of two cleaving DNAzymes into the same active loop, as shown by the DRc dual-activity enzyme, which combines the PLDz DNAzyme that cleaves in the presence of Cu^{2+} and ascorbic

acid, modified with the conserved bases of 8-17's catalytic core. The DRc DNAzyme, shown in Figure 11, is allosteric in that a switch in the cleavage mechanism and the specificity for DNA vs. RNA cleavage depends on the availability of a chimeric substrate.[84] An example of a more traditionally allosteric DNAzyme is the UO_2^{2+}-dependent 39 DNAzyme, whose cleavage activity additionally requires the binding of Hg^{2+} in the stem-loop to compensate for T-T mismatches that had been introduced in the catalytic core, generating a dual-sensor DNAzyme that reports on the simultaneous presence of uranium and mercury.[63]

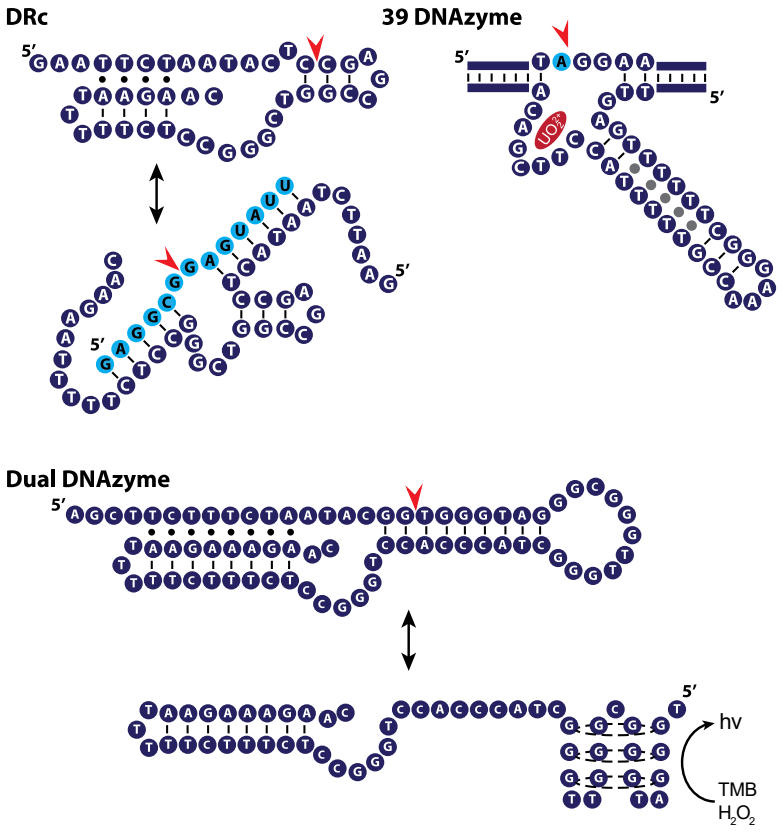

Figure 11: Sequences and structure representations of several allosteric DNAzymes. The 8-17 and pistol-like DNAzyme hybrid, DRc, that can cleave through either mechanisms depending on the available analyte.[84] The Dual DNAzyme undergoes pistol-like cleavage that allows for refolding to form a G-quadruplex for subsequent colorimetric signal generation through TMB.[85] Instead of introducing another DNAzyme's functionality, the addition of T-T mismatches to the DNAzyme 39 sequence led to a requirement for Hg^{2+} for cleavage, generating a DNAzyme that can detect the presence of either analyte: mercury and uranium.[63]

Colorimetric detection can also be introduced into the DNAzyme sequence, as in the case of the Dual DNAzyme, a pistol-like DNAzyme including a G-quadruplex sequence. Cleavage of the DNAzyme allows for formation of the quadruplex, into which hemin can intercalate and initiate the generation of a color change in solution.[86] The same concept has also been utilized when detecting a nucleic acid analyte, as in the case of a MNAzyme and G-quadruplex containing system that generates a color change upon formation of the MNAzyme complex.[85]

2.3 Emerging Sensing Applications for DNA-Catalyzed Cleavage

The simplicity and stability of DNAzymes has led to their implementation in a variety of assays, primarily for sensing or therapeutic purposes. These applications are driven by the thermal and buffer stability of the DNAzyme that allows for their substitution for enzymes or other fragile components in bioassays. The cleavage event is additionally dependent on both hybridization-mediated structure and the metal cofactor, generating two potential analytes for each DNAzyme to detect. The incorporation of modified bases such as fluorescent probes and quenchers, as in the case of the MgZ DNAzyme discussed previously, allows for the DNAzymes to act as single-step, real-time readouts that do not require complicated instrumentation to interpret.

As described in the allostery section above, the DNAzymes can be designed with additional DNA functionalities, such incorporating two different cleaving sequences, mixing both cleaving and other functional DNAzyme properties, or the addition of an aptamer-binding sequence to detect a small molecule target. These additional functions can allow for two-step assays to be performed in sequence, expanding the range of processes a single DNA sequence can perform, for instance an aptamer can require binding to the target

molecule to expose the self-cleaving DNAzyme sequence. DNAzymes can also feed into enzymatic assays, such as amplification strategies like polymerase chain reaction (PCR) for greater sensitivity, or horseradish peroxidase (HRP) for rapid signal generation.

In the following we present a showcase of the wide range of applications for DNAzymes in sensing. While the literature in this area is rapidly expanding, we have selected publications that highlight the advantages of DNAzymes and their potential for translation to PoC applications.

2.3.1 Ion Sensors

Heavy metals pose serious threats to human and environmental health, and as such many techniques have been developed to detect them. Due to the low permissible concentrations of lead (15 ppb) and mercury (2 ppb), the EPA suggests using Inductively Coupled Plasma-Optical Emission Spectroscopy (ICP-OES), a technique that is excellent for detecting trace quantities in a mixed sample, but entirely too expensive and immobile for field use.[87] At the other extreme there are several affordable tests that are commercially available for home use, but these tests cannot differentiate which metals they are detecting. In between these two extremes lie electrochemical sensors, such as the portable anodic stripping voltammetry (ASV) sensor that can detect Hg^{2+}, Pb^{2+}, and Cu^{2+} in a clean sample[88] or the carbon nanotube enhanced ASV assay capable of detecting trace quantities of lead and cadmium in processed water samples.[89] Most applicable to on-site testing is a surface-enhanced Raman spectroscopy (SERS) sensor capable of detecting metal ions in a complex organic mixture, removing the need to fully purify a sample before analysis.[90] These techniques, while accurate, are complex and expensive.

DNAzymes, with their cheap components and highly specific catalytic properties, provide a logical alternative for metal ion sensors, especially for field work. Ag10c, the DNAzyme dependent on silver, was designed with the intent to detect Ag^{+} contamination in lake water.[62] The $E_{Hg}0T$ enzymes were screened specifically for selectivity for only Hg^{2+} ions, with the aim of providing a sensitive mechanism for detecting trace mercury in water samples.[63] A straightforward fluorescence readout is easily obtained in real time due to the incorporation of a fluorophore and quencher on the substrate strand. Cleavage in the presence of Hg^{2+} separates the pair and generates a visible fluorescent signal. GR-5 was discovered as an optimization of the lead-catalyzed but promiscuous 8-17, for detection of Pb^{2+} on-site.[65] Similarly, PLDz DNAzymes were utilized as copper sensors to determine pollution levels in samples ranging from bottled water to sewage; a schematic of this assay is shown in Figure 12.[91] In all of these cases, the DNAzyme provides for a simpler mechanism of detection that can replace inherently complicated existing metal ion tests and allow for a cheaper, more portable assay.

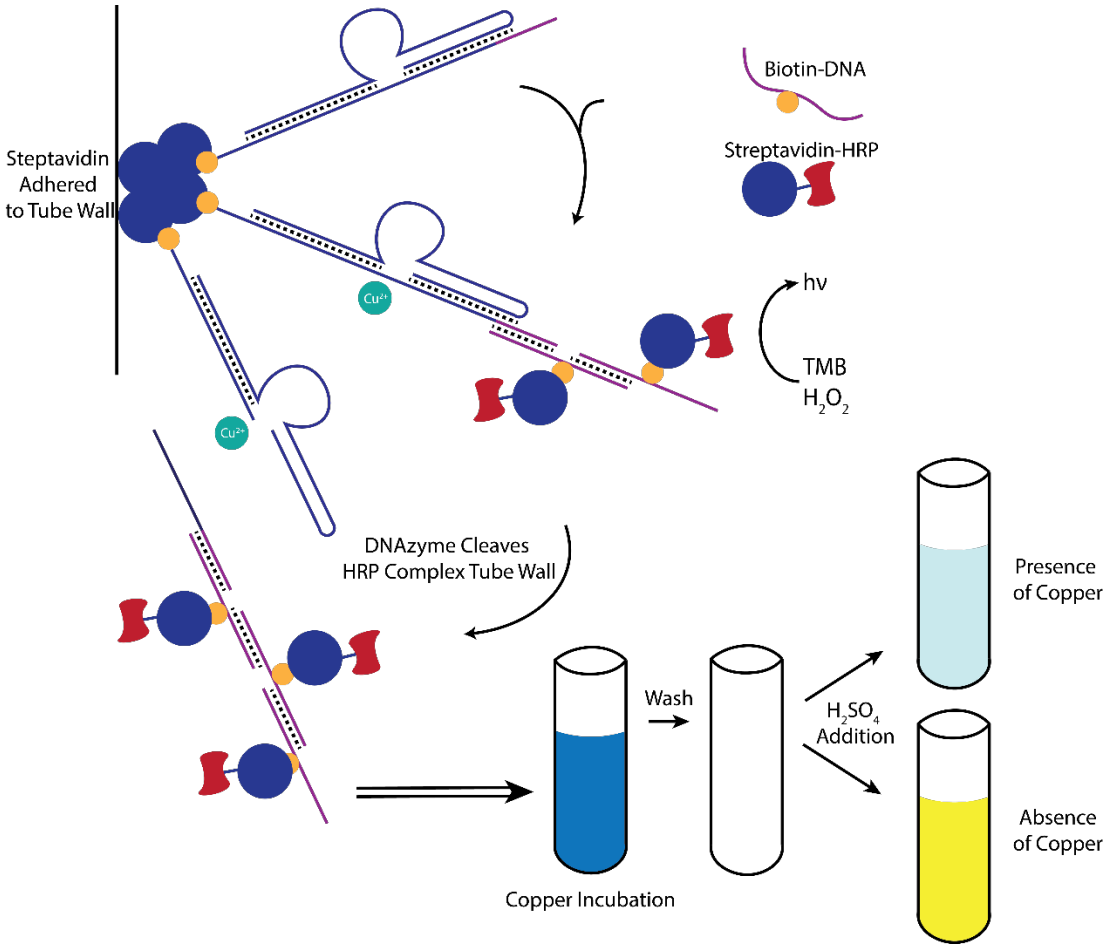

Figure 12: Utilization of an immobilized pistol-like DNAzyme to cleave HRP-conjugated streptavidin-biotin concatemers, allowing the HRP to be washed away upon copper ion mediated cleavage, and thus preventing the activation of the TMB and resulting in the absence of a colorimetric output.

The metal ions that enable DNAzyme cleavage can also be quantified in more complex environments. 17E, a variant of the DNAzyme 39 that can cleave in the presence of Ca^{2+} and Mg^{2+}, was screened in the presence of serum so that it would be functional in a cell.[92] This capability to detect the metal concentration in an non-invasive manner allows for real-time tracking of these analytes in a live cell. NaA43, a sodium-dependent DNAzyme, has been utilized as a Na^{+} tracker in cells using a photo-caging technique that blocks the catalytic 2′ hydroxyl from degradation in the cell until brief exposure to 365 nm light.[72]

This photolabile group allows for a delayed start to the imaging, generating a technique that can be initiated by an external stimuli at any time following the initial setup.

2.3.2 Biosensors

Conventional methods for the detection of biological analytes have so far been primarily either immunoassays such as the Enzyme-Linked ImmunoSorbent Assay, ELISA, for protein and small molecule biomarkers[93–95] or nucleic acid amplification techniques like the polymerase chain reaction (PCR) for nucleic acid sequence biomarkers.[96,97] ELISAs have numerous complicated manual steps. PCR generally requires multiple manual steps for preparation, and the reaction requires thermocycling, which has a significant energy and complexity requirement. These two techniques, while sensitive and specific, are difficult to use in low resource settings. While there have been some efforts to miniaturize thermocyclers so that they can be brought into the field[98] and to simplify ELISAs so that they can be performed by minimally trained staff,[8] they are still relatively complicated assays to perform away from the central lab.

DNAzymes can be incorporated into ELISAs to replace fragile enzymes, as in the assay shown in Figure 13. Here analyte detection has been performed through an antibody sandwich assay in which the secondary antibody is conjugated to PbS nanoparticles. The PbS particles will, when immobilized into the well by the presence of the analyte, generate Pb^{2+} ions upon HNO_2 treatment that will cleave an 8-17 DNAzyme and provide a signal in electrochemical assays, with the cleavage of the 8-17 substrate allowing the newly flexible complementary DNA to bring a ferrocene tag closer to the electrode surface.[99] This technique has also been used to separate the fluorophore from its quencher,[100] yielding a fluorescent signal that is significantly less instrument-intensive to analyze.

DNAzymes can also be used to detect specific cell types, as in the case of the DNAzymes RFD-CD1 and RFD-EC1 which can specifically cleave in only the presence of *C. difficile* and *E. coli*.[101] These DNAzymes contain the fluorophore and quencher motif seen in other DNAzymes, which was subsequently utilized in a paper-based printed *E. coli* sensor, allowing for the rapid and cheap production of these portable sensors.[102] Another sensor for breast cancer diagnosis has also utilized this technique, with the AAI2-5 DNAzyme capable of detecting the presence of a cytoplasmic protein from the MDA-MB-231 cell line, with a similar fluorophore-quencher signal generation.

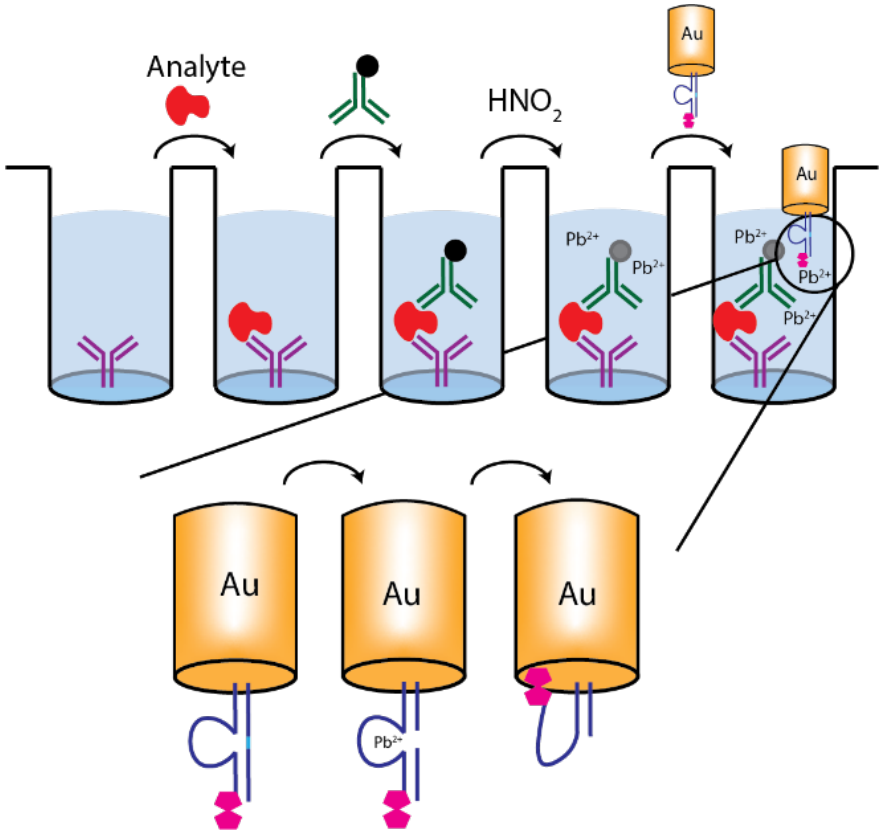

Figure 13: The utilization of the 8-17 DNAzyme as a lead-sensitive readout following a traditional ELISA. The lead ions generated in solution from the capture antibody's binding cleave the 8-17, allowing for a ferrocene molecule to come in contact with the gold electrode, generating a detectable electrical signal.[99]

The DNAzyme itself can also be used as the analyte, as in the case of MNAzymes. The target nucleotide sequence bridges across the MNAzyme arms, stabilizing the active DNAzyme enzyme conformation, which can then cleave a separate substrate strand.[56] This construct allows both for a lower background signal in the sensors and the ability to use the same expensive fluorophore and quencher labeled substrate strand in a different assay through simply changing the sequences of the two catalytic halves. This cost-cutting measure means that altering the target sequence entails synthesizing just three unmodified DNA sequences, with all the costly components retained and repurposed.

Additionally a DNAzyme can be used to generate an amplification cascade to increase the output of the initial detection signal, as in the case of the EC1 DNAzyme cleaving one of two concatenated DNA circles in the presence of *E. coli* and initiating rolling circle amplification (Figure 14).[103] The same concept can be seen in another scheme from the Liu group that utilizes the MgZ DNAzyme to generate primers for rolling circle amplification upon binding of a complementary target sequence.[104] In both strategies, the DNAzyme generates an overhang that phi29 DNA polymerase can shorten through its 3′→5′ exonuclease activity, allowing for subsequent amplification. This allows for a single binding event to generate many-fold its signal, thus lowering the limit of detection of the assay.

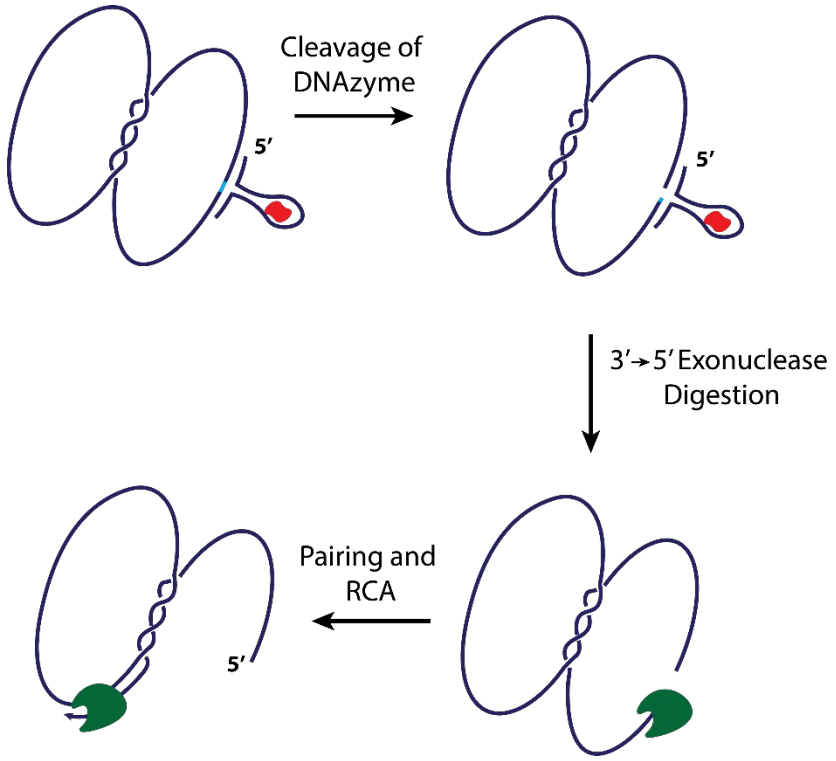

Figure 14: This assay demonstrates the use of a DNAzyme to generate a primer for Rolling Circle Amplification (RCA). The cleavage of the EC1 DNAzyme leaves a cyclic phosphate on the 3′ end. Upon end processing with PNK, the φ29 DNA polymerase (green) can excise back to a region that can pair with the other circle, and then it can extend the primer using the second concatenated circle as a template.[103]

2.4 Conclusion

The wide variety of conditions for DNAzyme self-cleavage, as well as their specific cleavage mechanisms, make an enormous difference in their utility, so a thorough account of the available literature on DNAzymes is necessary to make the appropriate choices for implementation in an assay. From this range of available DNAzymes, a select few have been incorporated into sensors for use in detecting ions, biological analytes, and nucleic acid sequences. This thesis focuses on the latter, demonstrating the design of a nucleic acid biosensor, testing four of the DNAzymes listed based on their speed and cleavage conditions.

The biosensor utilizes the DNAzyme as a bridge between two RCA cycles, having the DNAzyme cleave the first amplicon to provide primers for the second. This allows for an increase in the amplification output from a linear to a geometric scale. Additionally, the bicyclic RCA scheme has been designed with the intent to be one-pot, with no purification, heating steps or other manipulations outside of adding the target sample, significantly increasing the usability of these assays in low resource conditions. This will be discussed in more depth in the following chapters, and the assay discussed specifically in chapter 4.

Table 1: Compendium of DNAzyme properties

DNAzyme, reference	Substrate	Cleavage Site Preference	Required Cation	Small Molecule Promoter	Small Molecule Inhibitor
8-17[33]	RNA = Chim	All but rC^rT	$Pb^{2+} > Zn^{2+} > Mg^{2+}$		
10-23[49]	RNA = Chim	All but rA^rC or rA^T/rU	Mg^{2+}		
GC DNAzyme[54]	Chim > RNA	--	Mg^{2+} and Mn^{2+}		
S4[60]	Chim > RNA	NrU^C	Mn^{2+}	$K^+ = Na^+$	
S9[60]	Chim > RNA	NrC^C	Mn^{2+}		
S21[60]	Chim > RNA	NrU^T	Mn^{2+}		
EtNa[59]	Chimera	TrA^GG	Na^+	Ethanol	
G3[71]	Chimera	NrA^N	$Na^+ = NH_4^+$		
NaA43[72]	Chimera	TrA^GGAA*	Na^+	Ce^{3+}	
Ce13d[57]	Chimera	TrA^GGAA*	Ce^{3+}	Na^+	
E6[58]	Chimera	NrA^N	Mg^{2+}	Na^+	
CT10.3.29M[61]	Chimera*	NrU^N rU = rC* >> rA = rG	Mg^{2+} and Mn^{2+}		
S15[60]	Chimera	NrC^T	Mn^{2+}		
DZ1[70]	Chimera	NrU^N	$Mn^{2+} > Co^{2+} > Ni^{2+} > Zn^{2+} > Cd^{2+}$		
DZ7[70]	Chimera	NrG^N rG = rA = rU > rC	$Mn^{2+} > Co^{2+} > Pb^{2+}$		
Ag10C[62]	Chimera	TrA^GGAA*	$Ag^+ >> Hg^{2+}$		
E_{Hg}0T[63]	Chimera	TrA^GGAA*	Hg^{2+}		
39[64]	Chimera	TrA^GGAA*	UO_2^{2+}		
GR5[65]	Chimera	TrA^GGAA*	Pb^{2+}		
PSCu10 [66]	Chimera	TrA†^GG*	Cu^{2+}		
DEC22-18[67]	Chimera	FrA^Q	Co^{2+}		
MgZ[68]	Chimera*	FrA^Q	Mg^{2+}		
5J-A28[69]	Chimera	FrA^Q	Mg^{2+}, Mn^{2+}, Co^{2+}, Ni^{2+}		
DZ15[73]	Chimera*	NrA^N*	Na Citrate, pH 4-4.5	K^+	Cd^{2+}
DZ27[73]	Chimera*	NrA^N*	Na Citrate, pH4-4.5		Cd^{2+}
pH3DZ1[74]	Chimera*	NrA^N*		pH3	
pH4DZ1[74]	Chimera*	NrA^N*	$Mn^{2+} = Cd^{2+} > Ni^{2+}$	pH4	
pH5DZ1[74]	Chimera*	NrA^N*	--	pH 5, Mn^{2+}	
pH6DZ1	Chimera*	NrA^N*	Mn^{2+} and Ni^{2+}	pH 6.0	
Pistol-Like	DNA	--	Cu^{2+}	H_2O_2	
PLDz[78]	DNA	--	$Cu^{2+} > Co^{2+} > Mn^{2+}$	Ascorbic Acid	Fe^{2+}
F8-X[79]	DNA	CT^CG	Cu^{2+}	H_2O_2, Mn^{2+}, DTT	
10MD5[82]	DNA	ATG^T	Zn^{2+}	$Mn^{2+} > Cd^{2+} > Ca^{2+}$	
Class I[81]	DNA	GTTGA^AG	Zn^{2+}		
Class II[81]	DNA	N^AGNATCTT	Zn^{2+}		

*- only one variant tried, so others may be possible
^- cleavage site
F = Fluorophore (Fluorescein-dT), Q = Quencher (DABCYL-dT)
† - Phosphorothioate on the 3′ side of the cleavage site

3
Experimental evaluation of potential DNAzyme sequences for use in two-stage RCA

3.1 Introduction

While there are many DNAzymes presented in the literature,[46,48,105] a one-pot, two-stage RCA linked with a DNAzyme has a series of requirements that must be met for proper function of the assay. First and foremost, the DNAzyme must be capable of functioning in a buffer system common across all stages of the assay. It must not require a cofactor that severely impedes the function of the enzymes needed for RCA, namely an exonuclease-free DNA polymerase and T4 DNA Ligase. The DNAzyme should generate a 3′ end that is amenable to polymerase extension. Additionally, as this DNAzyme will be implemented in a biosensing assay, it must also have a hybridization region that is programmable and a tertiary structure that is stable in solution across a range of temperatures. It should ideally act isothermally, requiring no melt steps to function, so that the assay can be performed easily and without expensive temperature-ramping instrumentation.

This chapter is a summary of the experimental evaluation of the varied DNAzymes that I have investigated as a bridge for the two-stage RCA, with the benefits and drawbacks of each DNAzyme presented. The text of the chapter is organized by the four primary mechanisms by which DNAzymes cleave polynucleotides: one DNAzyme for each mechanism is discussed and analyzed for utility in the two-stage RCA.

To determine the viability of the DNAzymes assayed, each was tested for cleavage of the minimal sequence construct during incubation in a buffer found to be compatible with

the ligation, RCA and signal generation components of the reaction. The DNAzymes were tested for evidence of cleavage in the reaction conditions prior to being tested cleaving from the RCA amplicon. Finally, those that could cleave from an RCA amplicon were further tested for their ability to prime a subsequent amplification.

3.2 Different cleavage mechanisms of DNAzymes

The mechanism of RNA cleavage by DNA is virtually the same as cleavage by RNAzymes,[106] proceeding through promoting hydrolysis of the phosphodiester by the 2′-OH as shown in Figure 15A. The 2′ hydroxyl is deprotonated as the catalytic cation stabilizes the charge on the 3′ and 5′ oxygens, and a transesterification reaction occurs, resulting in a 2′,3′ cyclic phosphate and a 5′ hydroxyl after protonation.[107] The cyclic phosphate can be easily removed by polynucleotide kinase (PNK) or another phosphatase.[108]

DNA cleavage by DNAzymes, in contrast, requires a more complicated cleavage mechanism due to the lack of 2′ hydroxyl on the deoxyribose. There are thus many modes of cleavage, with the exact mechanism dependent on the individual DNAzyme. One model indicates that the cleavage generates a 3′ hydroxyl and a 5′ phosphate in the presence of a base (Figure 15B). Additionally, in some DNAzymes the mechanism involves the complete excision of a nucleoside, resulting in phosphates on the 3′ and 5′ ends of the remaining polynucleotide cleavage products, as shown in Figure 15C.[79] Another proposed mechanism suggests the DNA is cleaved across the ribose, generating a 5′ phosphate and a 3′ phosphoglycolate that can later be converted into a 3′ phosphate (Figure 15D).[78] The proposed mechanism is based on an analogous DNA cleaving system that is well characterized, the bleomycin-induced DNA scission.[109–111]

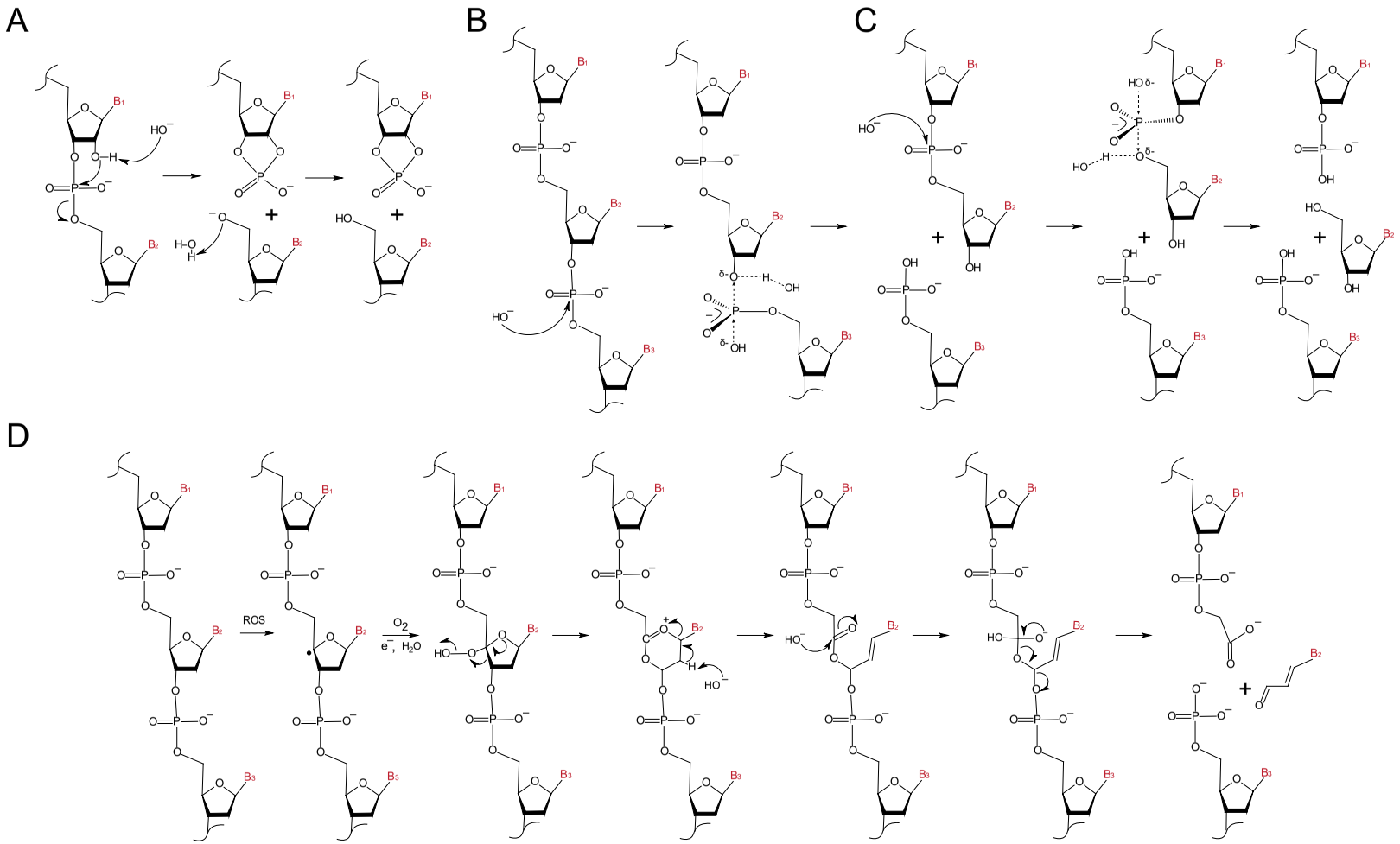

Figure 15: Mechanism of cleavage of an RNA base by DNA[92] (A) and several proposed mechanisms of cleavage of DNA by DNA. The hydrolysis of the 3′ phosphate (B),[98] the additional hydrolysis of the 5′ phosphate resulting in a base excision (C)[66] and cleaving across the nucleotide resulting in a phosphoglycolate (D).[65] The mechanism for (D) is infered from several sources, including bleomycin-induced DNA scission.[95–97]

In this chapter, DNAzymes utilizing each mechanism will be discussed, as each was tested for viability in the RCA assay. As illustrated in Figure 2 (Chapter 1), the DNAzyme is integrated into the RCA amplicon and then the cleaved product is used as a primer. This means that both the speed of cleavage and the resulting 3′ end are key to the functionality of the assay. Each of the listed DNAzymes will be discussed with these two factors in mind, with a special focus on being able to keep the reaction one-pot.

3.3 10-23: DNAzyme that cleaves chimeric DNA/RNA, leaving a 2′,3′ cyclic phosphate end

The only chimera DNAzyme tested for this project is the 10-23 DNAzyme isolated from HIV by the Joyce lab.[112] This DNAzyme is composed of two sequences, an enzymatic strand that folds into the catalytic structure and an RNA or RNA/DNA chimeric substrate that gets cleaved, which are shown in Figure 16A. As a chimera, the DNAzyme contains four RNA bases; two bases on each side of the cut site. It has been shown that cleavage is possible with only one RNA base, but there is increased cleavage efficiency with additional bases flanking the cut region.[113] The minimal sequence variant of this DNAzyme has been shown to cleave with only one RNA base in the substrate strand,[114] but the cleavage efficiency decreases dramatically. For our purposes, the loss in durability from the inclusion of more fragile RNA bases may be compensated for by the fact that 10-23 has the highest cleavage efficiency of the DNAzymes studied. Moreover, for a cofactor it requires only magnesium, a cation already present in the recommended reaction buffer for most enzymes. These two advantages make it a strong candidate for this assay.

3.3.1 Materials and Methods

Materials. Copper sulfate was purchased from Sigma. All DNAs were ordered from IDT (Coralville, IA, USA), with standard desalting. The oligonucleotides were resuspended in water (no EDTA was added due to cofactor fouling) to make 500 μM primary stocks and kept frozen at -20 °C except for removal to prepare new working 10 μM stocks. The concentration of the primary stock was evaluated by UV/Vis. As the DNAs were analyzed by denaturing PAGE, purity of the stocks was evaluated and working stocks were remade as necessary. The following sequences were used:

10-23 Enzyme 5′- GCACCCAGGCTAGCTACAACGACTCTCTCC-3′
10-23 Substrate 5′- GGAGAGArGrArUrGGGTGCG -3′
10-23 Substrate Ext 5′- TCGATGTGGAGAGArGrArUrGGGTGCGAGCTC -3′

Additional sequences are in Appendix Table A1. RCA enzymes were purchased from New England Biolabs (Ipswich, MA),

10-23 cleavage. Cleavage assays were performed in Reaction Buffer (10 mM Tris HCl, 50 mM NaCl, 10 mM $MgCl_2$, pH 7.9) in the presence of 0.1 μM 10-23 Enzyme and Substrate sequence. The reactions were performed at 25 °C for 15 minutes before denaturation and heat killing by addition of two volumes of 12 M Urea and heating at 95 °C for 5 minutes. In later assays, the Enzyme strand was replaced with 10-23 Circle I 3′ or 5′ end sequences which contain the Enzyme sequence.

10-23 RCA. Cleavage assays were performed in Reaction Buffer (10 mM Tris HCl, 50 mM NaCl, 10 mM $MgCl_2$, pH 7.9) with additional 1 mM ATP and 1 mM dNTPs in the presence of 0.1 μM of both 10-23 Circle I and Long Splint. 233 Unit/mL of T4 DNA Ligase

was added before incubation at 25 °C for 30 minutes. 33 Unit/mL of Klenow fragment DNA Polymerase (3′→5′ exo⁻) was added either subsequently or simultaneously as stated. Reactions were heat killed after addition of two volumes of 12 M Urea at 95 °C.

Interfering DNA Assay. 3 μM Interfering DNA was added to 1 μM each Circle I and Long Splint in reaction buffer with 1 mM ATP and 1 mM dNTPs. 233 Unit/mL T4 Ligase and 33 Unit/mL Klenow (3′→5′ exo⁻) was added and the reaction was run at 25 °C for 30 minutes. 3 μL 10-23 substrate was added to the reaction and kept at 25 °C for another 30 minutes before heat killing and running on a PAGE gel for analysis. The negative control is the identical reaction without the addition of the interfering DNA.

HinfI Digest. RCA was performed with 1 μM each Circle I and Long Splint in reaction buffer with 1 mM ATP and 1 mM dNTPs. 233 Unit/mL T4 Ligase and 33 Unit/mL Klenow (exo⁻) were added and the reaction was run at 25 °C for 30 minutes. 166 Unit/mL of *Haemophilus influenzae* (HinfI) restriction enzyme was added to the reaction and incubated at 37 °C for an hour before heat killing and analysis on a denaturing acrylamide gel.

3.3.2 Cleaving from a minimal sequence

The bimolecular assembly of the 10-23 DNAzyme is shown in Figure 16A, with the red arrow demonstrating the cleavage site. The k_{obs} , or apparent first-order rate constant for the cleavage of the unimolecular form of the DNAzyme, of ~10 min^{-1} of the 10-23 DNAzyme at pH 7.5,[112] as well as the use of Mg^{2+} as its cofactor, has led to near-100 % cleavage of the substrate strand within 5 minutes in the presence of just the reaction buffer, as shown by the appearance of the two cleavage bands of the 10-23 Substrate sequence in Figure 16B.

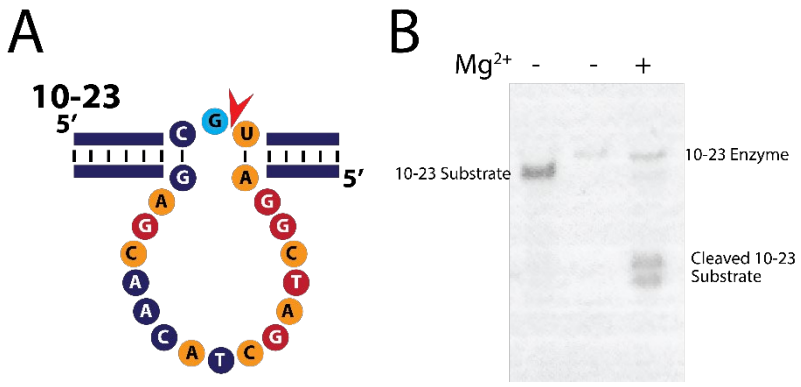

Figure 16: Structure of the 10-23 DNAzyme (A). Demonstration of 10-23 Substrate cleavage in the presence of the 10-23 Enzyme sequence and 10 mM $MgCl_2$ (B). Color-coding is as described in Figure 4.

3.3.3 Cleaving off the amplicon

Despite the rapid cleavage efficiency of the 10-23 DNAzyme, the structure of the DNAzyme is complicated to manage due to its bimolecular nature. Figure 17A demonstrates this by showcasing the cleavage of the 10-23 Substrate in the presence of either the 10-23 Enzyme sequence, or a truncated version of the circle's complement (Circle I 3′ end), or the RCA-generated Circle I Amplicon, all in otherwise identical conditions. The cleaved 10-23 Substrate bands at the bottom of the gel appear only with the shorter sequences: the 10-23 Enzyme or Circle I 3′ end. This suggests that formation of the DNAzyme's secondary structure is hindered within the more complicated Circle I RCA Amplicon, preventing any significant cleavage from occurring. Of note, the right-most lane of the gel in Figure 17A is only the 10-23 Substrate sequence at a higher concentration, showcasing the natural degradation that occurs at the site of the RNA bases, potentially hindering specificity.

Figure 17B follows from the conclusions of 17A to confirm that it is the conflicting secondary structures that are interfering with cleavage of the 10-23 Substrate and not some other component in the solution. The lane on the left shows the Substrate incubated with

the RCA Amplicon (1) and the lane on the right shows the same reaction with the 10-23 Enzyme sequence included in the reaction (2). The appearance of cleaved 10-23 Substrate products in lane (2) and, specifically, not in lane (1) implies that the lack of cleavage was largely due to secondary structure conflicts inhibiting either the binding of the Substrate strand to the amplicon, or the correct formation of the catalytic loop within the amplicon.

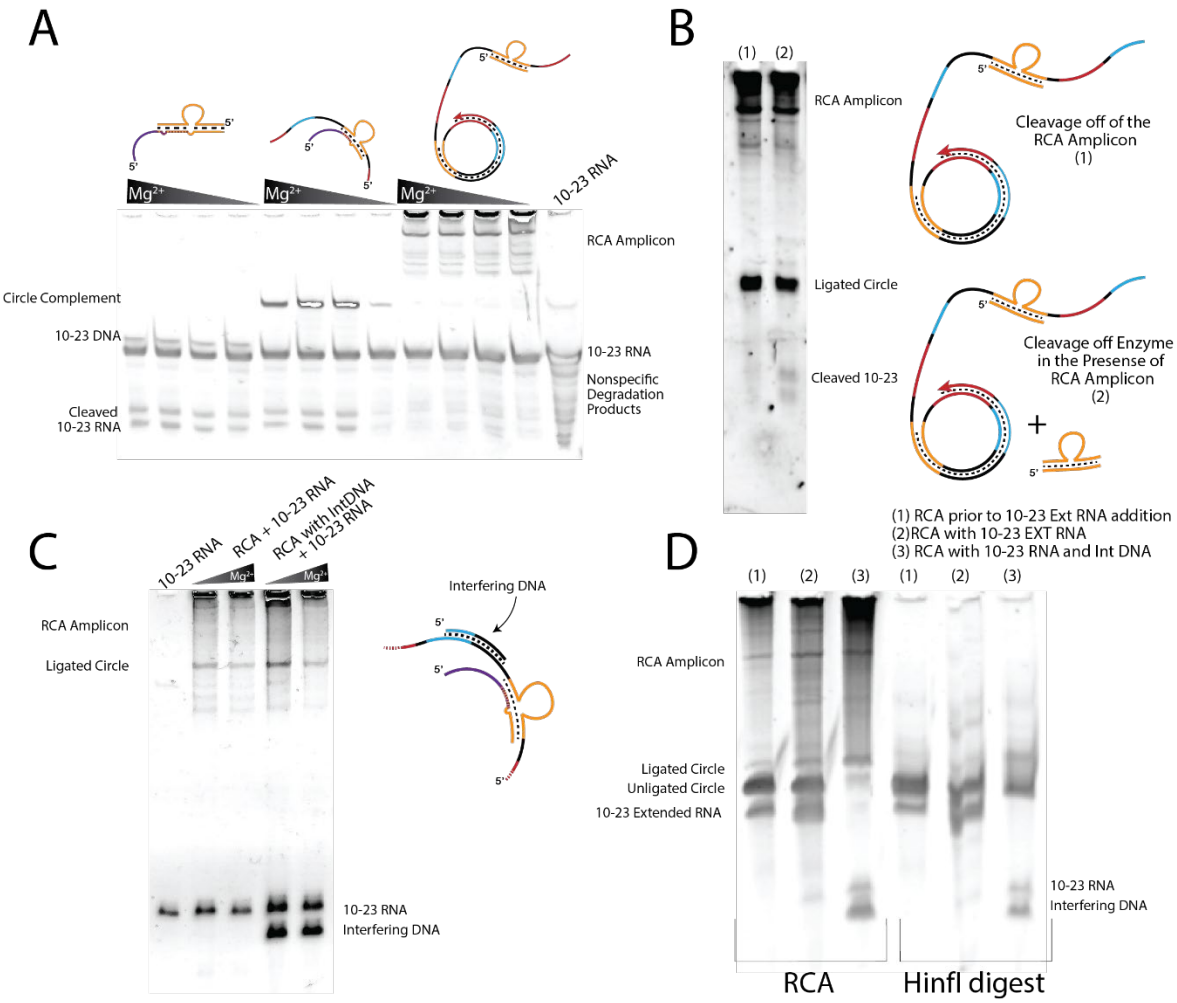

Figure 17: Testing the ability of the 10-23 extended substrate to be cleaved in the simple Enzyme-Substrate, Circle Complement-Substrate, and RCA Amplicon-Substrate design respectively. Mg^{2+} ranges from 10 to 40 mM across the reactions (A). Demonstrating that the 10-23 Substrate is capable of being cleaved in the RCA mixture (B). Employment of an interfering DNA to remove possible secondary structures blocking the cleavage of the 10-23 Substrate in the RCA Amplicon. Mg^{2+} concentration is 30 and 60 mM (C). Showing that the RCA Amplicon is accessible to the 10-23 Substrate by demonstrating cleavage with HinfI at one site within the Amplicon (D).

Since secondary structure formation was believed to be the greatest hinderance to cleavage, a sequence (named Interfering DNA) was designed to hybridize to the 3′ of the 10-23 Substrate binding site. The 3′ end was demonstrated in prior experiments to hinder Substrate cleavage more than the 5′ end when separated. The Interfering DNA, however, did not appear to increase cleavage efficiency as can be seen from both the sustained presence of the full 10-23 Substrate band and the lack of cleavage bands in Figure 17C.

The lack of effect of the Interfering DNA led to the belief that the RCA Amplicon was forming a densely packed entangled structure upon generation of the amplicon that was impenetrable to DNAs, excluding both the Interfering DNA and the 10-23 Substrate from hybridization and subsequent cleavage. A HinfI restriction site on the RCA Amplicon was utilized to test the accessibility of the Amplicon to an object much larger than the Substrate sequence. Figure 17D shows the reactions prior and after HinfI digestion, showing that the enzyme had access to the Amplicon DNA due to the cutting of nearly all the larger RCA products into fragments the length of the linear Circle I or shorter. This shows that it is truly the competing secondary structures that inhibit cleavage of the 10-23 Substrate.

3.3.4 Cleaved End Extension

The cleavage of the 10-23 DNAzyme, as reported earlier, generates a 3′ cyclic phosphate that needs to be cleaned up before extension is possible. It was initially believed that polymerases with 3′→5′ exonuclease domains like DNA Polymerase I (Klenow fragment) or BST Full might remove the terminal 3′ with the cyclic phosphate entirely, allowing one to skip the PNK cleanup step. Figure 18A shows tests with BST 3.0, which contains no exonuclease domain, and Klenow, demonstrating that the 10-23 Substrate gets converted into new products. The BST 3.0 polymerase, having no exonuclease domain, is

believed to amplify nonspecifically, especially as the products are of varying sizes that cannot be accounted for by the known hybridization structure of the complex. Klenow, on the other hand, appeared to make a discrete product that fell within the expected size of the extension product.

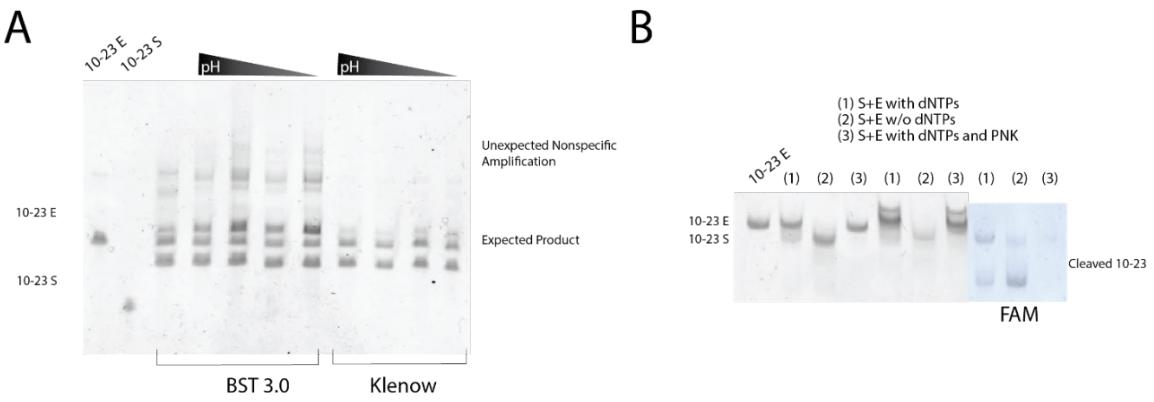

Figure 18: Extension of pre-cleaved 10-23 Substrate from the 10-23 Enzyme in reaction buffer at pH 8.8 to 7.0, with control lanes of the Enzyme and Substrate in isolation, and a pH 7.9 reaction to represent standard protocol (A). Incubation of pre-cleaved 10-23 Enzyme and Substrate with Klenow DNA polymerase (3′→5′ exo⁻) in the presence (1), and absence (2) or dNTPs and in the presence of dNTPs and PNK (3).

Figure 18B tested the extension of Klenow (3′→5′ exo⁻) by assaying the polymerase's activity on a cleaved Substrate with a 5′ FAM label, allowing for the visualization of the Substrate's incorporation. As can be seen in the (blue) FAM label view, FAM signal is only present at the size corresponding to the full and cleaved Substrate. Additionally, it appears that the PNK removal of the 3′ cyclic phosphate allowed for the Klenow to degrade the cleaved product, implying that the polymerase cannot process the cyclic phosphate. A PNK cleanup of the cyclic phosphate as well as the utilization of a polymerase without any exonuclease domains are required for this assay to be performed.

3.3.5 10-23 summary

While the cleavage of the 10-23 DNAzyme is extremely rapid in simple mixtures, the structural complexity imparted by the RCA Amplicon significantly diminished this benefit when it came to incorporation into the assay, especially as the PNK cleanup step is still necessary to generate the primer. Additionally, the fragility of the RNA bases and their degradation over time significantly impacts the specificity of the assay, as false-positives would foul the data.

3.4 1-R3: DNAzyme that cleaves DNA through hydrolysis, leaving a 3′ OH

The IR-3 DNAzyme, identified by the Breaker lab,[81] is a DNAzyme of particular interest because it cleaves both incredibility rapidly for a DNA-cleaving DNAzyme, with a rate constant (k_{obs}) of ~1 min^{-1}, and because it cleaves through a hydrolysis pathway. This is quite rare, or at least difficult to isolate for DNAzymes, but provides a wealth of benefits in our case because it obviates the need for a required cleanup of the 3′ end for subsequent extension. Additionally, the structure of the I-R3 DNAzyme is amenable to our later goals, as only 15 of the 44 bases are strictly required for catalytic function, allowing for the possibility to easily alter the sequences and multiplex without requiring a new DNAzyme construct, as shown in Figure 19A.

3.4.1 Materials and Methods

Materials. Zinc chloride was purchased from Sigma. All DNAs were ordered from IDT (Coralville, IA, USA), with standard desalting. The oligonucleotides were resuspended in water (no EDTA was added due to cofactor fouling) to make 500 μM primary stocks and kept frozen at -20 °C except for removal to prepare new working 10 μM stocks. The

concentration of the primary stock was evaluated by UV/Vis. As the DNAs were analyzed by denaturing PAGE, purity of the stocks was evaluated and working stocks were remade as necessary. The I-R3 sequence (5′-GTAACGTAGTTGAGCTGTCACAGAATGTGACGTTGAAGCGTTAC-3′) was used in all cases except when stated. Additional sequences are in Appendix Table A1. RCA enzymes were purchased from New England Biolabs (Ipswich, MA).

I-R3 cleavage. Cleavage assays were performed in Reaction Buffer (10 mM Tris HCl, 50 mM NaCl, 10 mM $MgCl_2$, pH 7.9) in the presence of 0.1 μM I-R3 sequence and 0 to 16 mM $ZnCl_2$. 0.1 mM ATP and 1 μM or 10 μM DTT (dithiothreitol) were added as indicated. The reactions were all performed at 25 °C for 30 minutes before heat killing by addition of two volumes of 12 M Urea and heating at 95 °C for 5 minutes.

I-R3 RCA. Cleavage assays were performed in Reaction Buffer (10 mM Tris HCl, 50 mM NaCl, 10 mM $MgCl_2$, pH 7.9) with additional 1 mM ATP and 1 mM dNTPs in the presence of 0.1 μM each I-R3 Circle I, Long Splint, and Primer I. 233 U/mL units of T4 DNA Ligase was added before incubation at 25 °C for 30 minutes. 33 U/mL Klenow fragment DNA polymerase (3′→5′ exo^-) Polymerase was added either subsequently or simultaneously as stated. Reactions were heat killed with two volumes 12 M Urea at 95 °C.

Gel Electrophoresis. Denaturing PAGE was used to analyze cleavage and RCA products. Reactions were run on a 12 % 19:1 acrylamide-bisacrylamide gel at 500 V for 15 minutes in a BioRad mini PROTEAN.

3.4.2 Cleaving in a minimal sequence

The I-R3 DNAzyme has a zinc-dependent cleavage mechanism, with 2 mM zinc chloride suggested by Breaker's publication.[81] Figure 19B demonstrates the cleavage efficiency of the DNAzyme through the appearance of the lower molecular weight I-R3 cleaved band, in the presence of 10 mM to 1 mM $ZnCl_2$ for 30 minutes. The addition of ATP, required for the ligation of the DNAzyme circle, was found to inhibit I-R3 cleavage, and a subsequent literature search discovered that zinc is capable of complexing with Tris and ATP in solution.[115] This effect was analyzed in Figure 19C, where the cleavage of I-R3 was tested at increasing concentrations of zinc chloride in the presence of constant 0.1 mM ATP, as would be required for the reaction conditions. 10 mM zinc chloride was found to be the minimum acceptable concentration required to overcome the inhibitory effects of ATP on cleavage, determined by the appearance of the cleaved I-R3 band. DTT was similarly found to have inhibitory effects on the reaction, as shown in Figure 19D, and there was found to be no permissible concentration for cleavage to occur: the cleavage band was only present in the absence of DTT, with even 1 μM DTT inhibiting cleavage completely.

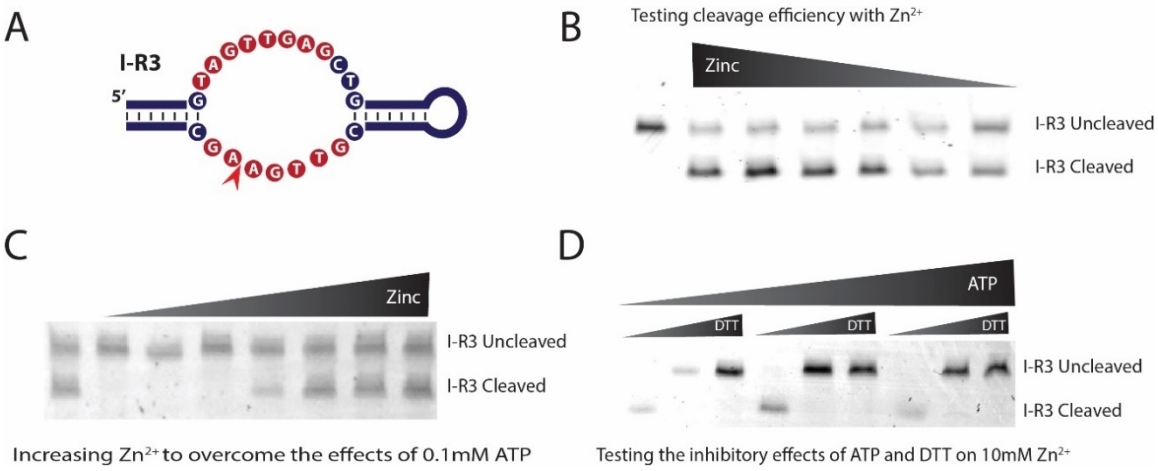

Figure 19: Structure of the I-R3 DNAzyme with conserved sequence shown in red and cleavage point shown with an arrow (A). I-R3 cleavage efficiency in the presence of 10-1 mM $ZnCl_2$ in Reaction Buffer at 25 °C for 30 min. I-R3 in the absence of any zinc is shown on left as a control (B). Increasing concentration (0 to 16 mM) of $ZnCl_2$ to overcome the sequestering effects of 0.1 mM ATP, with I-R3 in the presence of 10 mM $ZnCl_2$ and no ATP on the left as a control (C). Increasing DTT concentration (0 to 10 µM) to determine the inhibitory effect on available $ZnCl_2$ (D). Analysis of (B), (C) and (D) were done on denaturing PAGE.

3.4.3 Cleaving from the amplicon

As alluded to in the previous section, incorporation of the DNAzyme into the padlock probe scheme, shown in Figure 20A, was complicated due to zinc's characteristics. Not only does zinc complex with ATP, it precipitates into insoluble $Zn(OH)_2$ in even mildly basic conditions, as is required for the proper function of the polymerase and ligase selected for this assay. To perform the assay without precipitation, the zinc chloride stock was kept at pH 5, which lowered the reaction buffer's pH. The lower pH needed to accommodate for the zinc's solubility, and perhaps the presence of the zinc itself, generated an inhibitory effect on the polymerase as shown in the lack of amplification demonstrated in the zinc-containing lanes of Figure 20B. It was found that 2 mM Zinc allowed for the function of Klenow (exo^-) but was too low to overwhelm the inhibitory effect of ATP on cleavage.

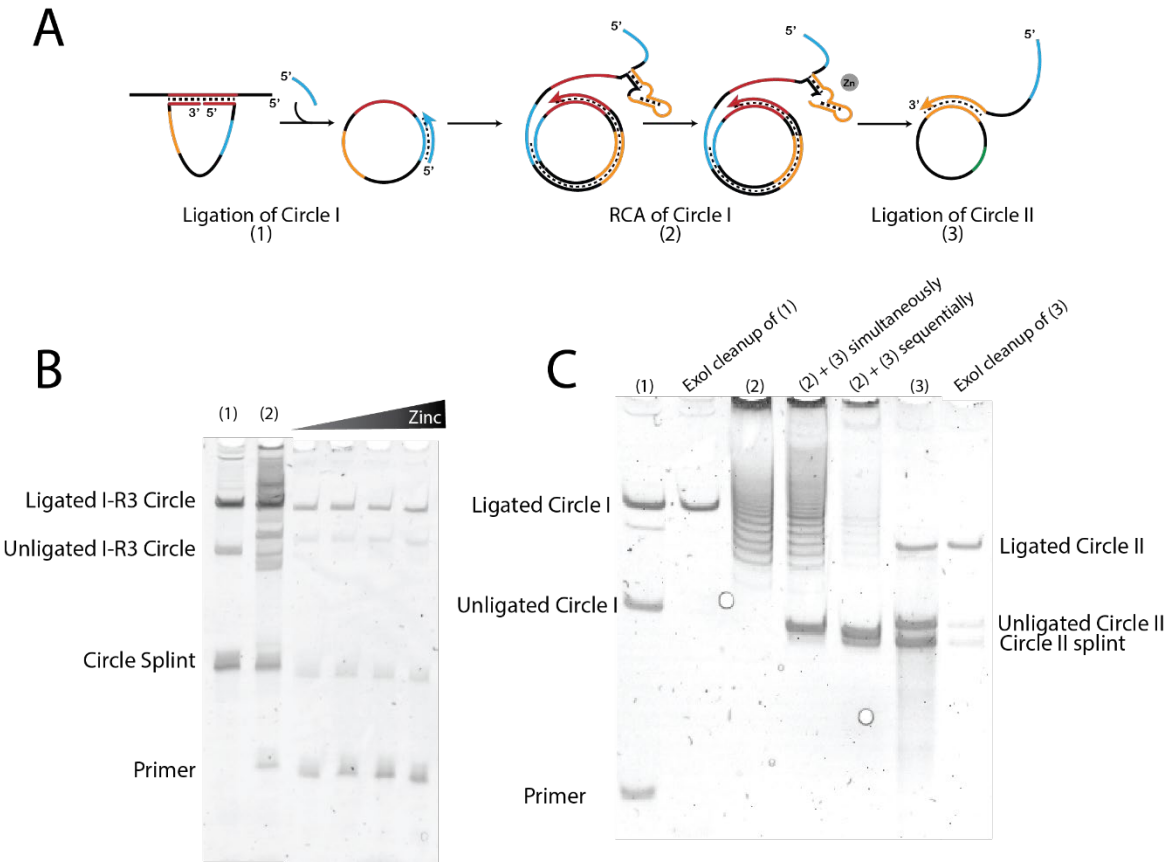

Figure 20: A schematic of the I-R3 DNAzyme in the bicyclic padlock system (A). A demonstration of the inhibitory effect of zinc on the polymerase, with the ligation and RCA in the absence of zinc on the left, followed by the increasing presence of $ZnCl_2$ (4 to 16 mM) during RCA (B). The effect of potential secondary structures competing with hybridization to the second circle, ligation of the first circle, Exonuclease I cleanup to demonstrate the presence of the circle, RCA in the absence of zinc, simultaneous or subsequent addition of the second circle to the RCA amplicon and ligation of the second circle and proof of the circle's presence (C). Analysis of (B) and (C) were done on denaturing PAGE.

The full reaction was performed with the I-R3 padlocks in the absence of zinc to demonstrate the system's ability to splint the second circle and allow for its ligation. It was discovered that the secondary structure of the I-R3 DNAzyme, while uncleaved, does not promote hybridization to a competing strand. This is shown through the absence of a ligated Circle II band in the 3rd and 4th lanes of the gel in Figure 20C, in which an RCA Amplicon containing the I-R3 sequence was allowed to cleave in the presence of zinc either simultaneously or prior to a small fraction being used to hybridize to and ligate Circle II. The 5th and 6th lanes are the controlled ligation of Circle II upon hybridization to a splint

whose sequence is contained within the amplicon, and its exonuclease digestion to reveal ligation products respectively.

It was also discovered that the zinc chloride stock precipitated into $Zn(OH)_2$ in all buffers except those of pH 3 or lower. New zinc chloride was purchased and generated the same result. Believing it to be an environmental factor associated with the lab space, the reactions were performed in a different building. When the same behavior was observed, it was decided that the finicky behavior of zinc was problematic for a point of care setting even if it could eventually be resolved. Since it has been demonstrated that I-R3 cannot use other cofactors to assist in cleavage, it was eliminated from further consideration.

3.4.4 I-R3 summary

Overall, the I-R3 DNAzyme initially appeared to be promising due to its rapid cleavage and unimolecular design, but the inhibition of polymerase activity by I-R3's Zn^{2+} cofactor, as well as the complicated buffering gymnastics necessary to keep the Zn^{2+} in solution, made I-R3 too unwieldy to use in the assay.

3.5 46mer Pistol-like: DNA-cleaving DNAzyme generating a phosphoglycolate 3′ end

The Pistol-like DNAzyme also comes from the Breaker lab, refined into this particular minimal 46-base sequence shown in Figure 21A.[77] While this DNAzyme is much slower to cleave, having a rate constant (k_{obs}) of 0.2 min^{-1},[77] it requires only 10 μM Cu^{2+} which is significantly easier to accommodate for in the reaction. This DNAzyme also has the advantage of being completely non-sequence specific in the portion of the sequence that would be used as a primer, as the triplex sequence encodes for the catalytic functionality

as shown in Figure 21A. The freedom to have any sequence in the cleaved helix implies this DNAzyme should have little trouble being altered for multiplexing.

3.5.1 Materials and Methods

Materials. Copper sulfate was purchased from Sigma. All DNAs were ordered from IDT (Coralville, IA, USA), with standard desalting. The oligonucleotides were resuspended in water (no EDTA added due to cofactor fouling) to 500 μM primary stocks and kept frozen at -20 °C except for removal to prepare new working 10 μM stocks. The concentration of the primary stock was evaluated by UV/Vis. As the DNAs were analyzed by denaturing PAGE, purity of the stocks was evaluated and working stocks were remade as necessary. The 46mer sequence (5′-AATTCTAATACGACTCAGAATGAGTCTGGGCCTCTTTTTAAGAAC-3′) was used in all cases except when stated. Additional sequences are in Appendix Table A1. RCA enzymes were purchased from New England Biolabs (Ipswich, MA). Poly-d-Lysine was provided by Prof. Kimberly Stroka's Lab, dextran and dialysis tubing was purchased from Sigma-Aldrich (Steinheim, Germany) and sodium cyanoborohydride was purchased from Acros (Geel, Belgium).

46mer cleavage. Cleavage assays were performed in Reaction Buffer (10 mM Tris HCl, 50 mM NaCl, 10 mM $MgCl_2$, pH 7.9) in the presence of 0.1 μM 46mer sequence and 0 to 1 mM $CuSO_4$. The reactions were performed at 25 °C for 30 minutes to 24 hours before heat killing with two parts 12 M Urea and heating at 95 °C for 5 minutes.

pDL-g-Dextran Synthesis. The pDL-g-dextran synthesis was adapted from Atsushi Maruyama et. al. [116]. 1 mL 100 mM poly-D-Lysine was incubated with 100 mg dextran

(MW 150,000) and 30 mg sodium cyanoborohydride in DMSO at 25 °C overnight. The products were then dialyzed with a MW 10,000 cutoff membrane in DI Water for 48 hours at room temperature before being lyophilized.

46mer RCA. Cleavage assays were performed in Reaction Buffer (10 mM Tris HCl, 50 mM NaCl, 10 mM $MgCl_2$, pH 7.9) with additional 1 mM ATP and 1 mM dNTPs in the presence of 0.1 μM both 46mer Circle I and Long Splint (splint with a poly-T tail to prevent extension). 233 U/mL units of T4 DNA Ligase was added before incubation at 25 °C for 30 minutes. 33 U/mL Klenow fragment DNA Polymerase (3′→5′ exo^-)and 0.1 μM Primer I was added either subsequently or simultaneously as stated.

Post-RCA Cleavage. Post-RCA cleavage was performed in 1 mM $CuSO_4$ with either 100 μM ammonium sulfate, 500 μM betaine, 1 % Glycerol or 0.1 % w/v pDL-g-dextran. Reactions were run at either 25 °C or 37 °C as stated and were heat killed after addition of two volumes 12 M Urea at 95 °C.

Gel Electrophoresis. Denaturing PAGE was used to analyze cleavage and RCA products. Reactions were run on a 12 % acrylamide, 19:1 acrylamide:bis gel at 500 V for 15 minutes in a BioRad mini PROTEAN.

3.5.2 Cleaving in a minimal sequence

The slow cleavage of the 46mer DNAzyme was first demonstrated in the simultaneous decrease in the full 46-mer band and the appearance of a lower molecular weight band representing the cleaved product in Figure 21B. Increasing the concentration of Cu^{2+} improves the cleavage efficiency marginally, but it does not significantly improve it, considering the timescale of the reaction.

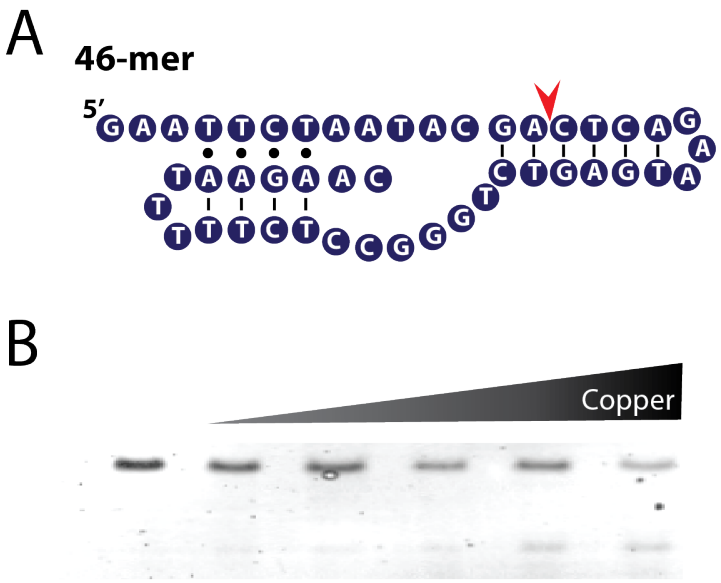

Figure 21: Structure of the 46mer pistol-like DNAzyme (A). Cleavage in the presence of 1 μM-1 mM $CuSO_4$ overnight (B).

3.5.3 Cleaving from the amplicon

The primary advantage of the 46mer DNAzyme is that it was the first to demonstrate replicable cleavage in the RCA amplicon, with the integration of the DNAzyme shown in Figure 22A. This cleavage was first seen with 1 mM $CuSO_4$ but can be significantly accelerated through the presence of additives that have been reported to ameliorate hybridization. The additives assayed are betaine[117], ammonium sulfate[118], glycerol, and pDL-g-Dextran[55]. Figure 22B shows the effect of the additives on the cleavage of an RCA amplicon, with betaine and ammonium sulfate showing clear cleavage, as discrete bands appear on the gel. Of note, there appears to be some banding in the reactions without Cu^{2+} (leftmost lanes). Trace cleavage in the absence of copper has been witnessed at very long timescales, and it appears that betaine and ammonium sulfate accelerate this behavior. This nonspecific behavior will not interfere with the reaction scheme, as specificity is imparted in the initial ligation, not the cleavage step.

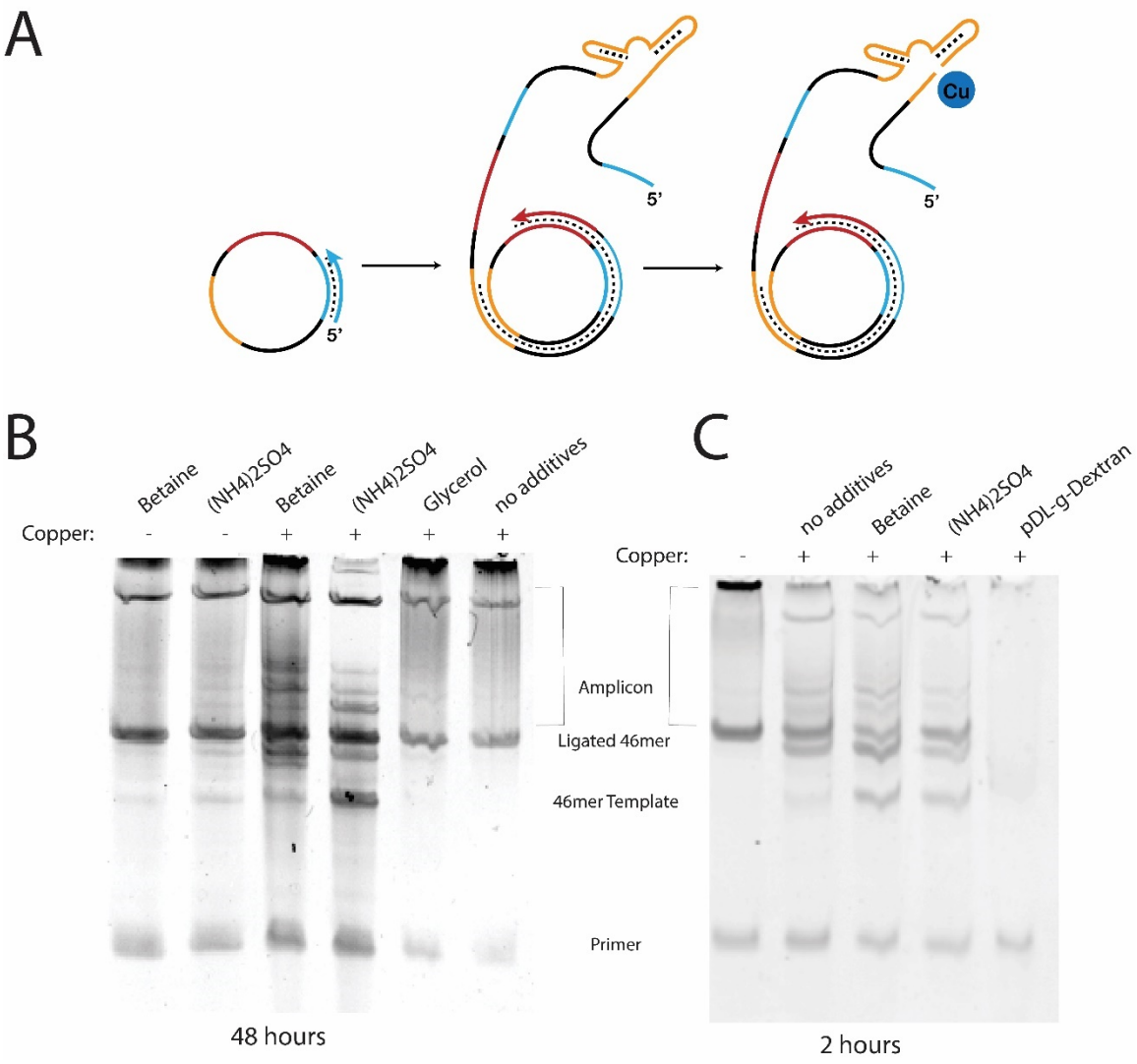

Figure 22: Scheme of the cleavage of the 46mer within the RCA amplicon (A). Off-amplicon cleavage of the 46mer DNAzyme post RCA in 1 mM $CuSO_4$ with either 100 µM ammonium sulfate, 500 µM betaine, or 1 % glycerol for 48 hours (B). Post-RCA cleavage of the 46mer DNAzyme in the amplicon in the same conditions during a 2 hour incubation (C).

As the 48 hours necessary for the previous reaction is excessive in a PoC setting, the reaction was tested again after 2 hours incubation at 37 °C to determine if the heat would make the competing secondary structures less stable and promote increased cleavage. As shown in Figure 22C, the increase in temperature did generate visible cleavage in the presence of copper ion alone (lane 2), demonstrated through the disappearance of the well-band and the appearance of lower molecular weight bands, which was only bolstered by

the presence of betaine and ammonium sulfate (lanes 3 and 4). pDL-g-dextran appears to complex with the DNA, as indicated by the lack of any DNA other than the primer in lane 5.

The 46-mer DNAzyme has shown to be able to cleave upon hybridizing to the amplicon, which is a significant step forward, but its utility is decreased because of its cleavage mechanism. The phosphoglycolate that is left on the 3′ end of the newly cleaved primer is reportedly capable of being removed by *E. coli* Exonuclease I,[119] leading to the idea that a polymerase with a 3′→5′ exonuclease domain might be able to remove it. However, tests with all polymerases in the lab showed that they were not capable of removing the phosphoglycolate. Additionally, the literature shows that T4 PNK is also incapable of cleaning up the 3′ end; instead, the cleanup is performed using specialized enzymes such as human tyrosyl-DNA phosphodiesterase (hTdp1),[120] PhosphoGlycolate Phosphatase (PGP),[121] and others that are not commercially available.

3.5.4 Pistol-like summary

This additional burden to using the 46mer product as a primer in addition to the slow cleavage time made the 46mer a viable backup DNAzyme, but disincentivizes its use in this particular assay.

3.6 F8-X: DNA-cleaving DNAzyme with both a 3′ and 5′ phosphate

The F8-X DNAzyme (Figure 23A) is the minimal sequence construct of F8, a DNAzyme with a k_{obs} of 0.14 hour^{-1}.[79] It is similar to the previously discussed Pistol-like 46-mer in its slow cleavage and its use of copper ion as a cofactor for cleavage, but the specific mechanism of cleavage is different. This particular DNAzyme undergoes base-

excision, resulting in a phosphate on both the 3′ and 5′ ends of the break. Converting 3′ phosphates into hydroxyl is a known behavior of T4 PNK, allowing for a very simple cleanup of the cleavage ends in preparation for extension.[108]

Additionally, while the three-dimensional structure of the DNAzyme is not known, the two-dimensional sequence arrangement is reminiscent of the 10-23 DNAzyme, as shown in the sequence diagram in Figure 23A, allowing for this sequence to be designed in both a uni- and bi-molecular construct depending on the needs of the assay.

3.6.1 Materials and Methods

Materials. Copper sulfate was purchased from Sigma. All DNAs were ordered from IDT (Coralville, IA, USA), with standard desalting. The oligonucleotides were resuspended in water (no EDTA added due to cofactor fouling) to 500 μM primary stocks and kept frozen at -20 °C except for removal to prepare new working 10 μM stocks. The concentration of the primary stock was evaluated by UV/Vis. As the DNAs were analyzed by denaturing PAGE, purity of the stocks was evaluated and working stocks were remade as necessary. The primary sequences used are listed below.

F8-X Full (5′-GAAAGTCTGCACACCGAATCGGTGTGTGGATGCCGGGTCCGACTTTCAGTGA-3′)

F8-X Substrate (5′-GAAAGTCTGCACACCGA-3′)

F8-X Enzyme (5′-TCGGTGTGTGGATGCCGGGTCCGACTTTCAGTGA-3′)

Additional sequences are in Appendix Table A1. RCA enzymes were purchased from New England Biolabs (Ipswich, MA).

F8-X cleavage. Cleavage assays were performed in Reaction Buffer (10 mM Tris HCl, 50 mM NaCl, 10 mM $MgCl_2$, pH 7.9) in the presence of 0.1 μM F8-X Full or 0.1 μM each F8-X Enzyme and Substrate sequence and 1 nM to 1 mM $CuSO_4$. The reactions were incubated at 25 °C for 30 minutes to 24 hours before addition of two volumes of 12 M Urea denaturant and heat killing at 95 °C for 5 minutes.

F8-X RCA. Cleavage assays were performed in Reaction Buffer (10 mM Tris HCl, 50 mM NaCl, 10 mM $MgCl_2$, pH 7.9) with additional 1 mM ATP and 1 mM dNTPs in the presence of 0.1 μM both F8-X Circle I and Short Splint. 233 Unit/mL of T4 DNA Ligase was added before incubation at 25 °C for 30 minutes. 33 Unit/mL Klenow fragment (3′→5′ exo$^-$) Polymerase was added either subsequently or simultaneously as stated. Reactions were heat killed after addition of two volumes of 12 M Urea at 95 °C.

Extension from Cleaved DNAzyme. Bimolecular F8-X cleaved as directed above was incubated with 1 mM ATP and 5 Units of T4 PNK or rSAP for 30 minutes at room temperature. 1mM dNTPs and 1 Unit of Klenow fragment (3′→5′ exo$^-$) was added and the reaction was held at room temperature for another 30 minutes before being heat killed at 95 °C for 5 minutes.

Gel Electrophoresis. Denaturing PAGE was used to analyze cleavage and RCA products. Reactions were run on a 12 % acrylamide (19:1) gel at 500 V for 15 minutes in a BioRad mini PROTEAN apparatus.

3.6.2 Cleaving in a minimal sequence

As stated previously, the F8-X DNAzyme was investigated as both a uni- and bi-molecular sequence, established through the presence or absence of the dashed loop in the

structure shown in Figure 23A. Cleavage of the bimolecular variant is shown in Figure 23B, as demonstrated by the appearance of the lower molecular weight cleavage band at higher Cu^{2+} concentrations.

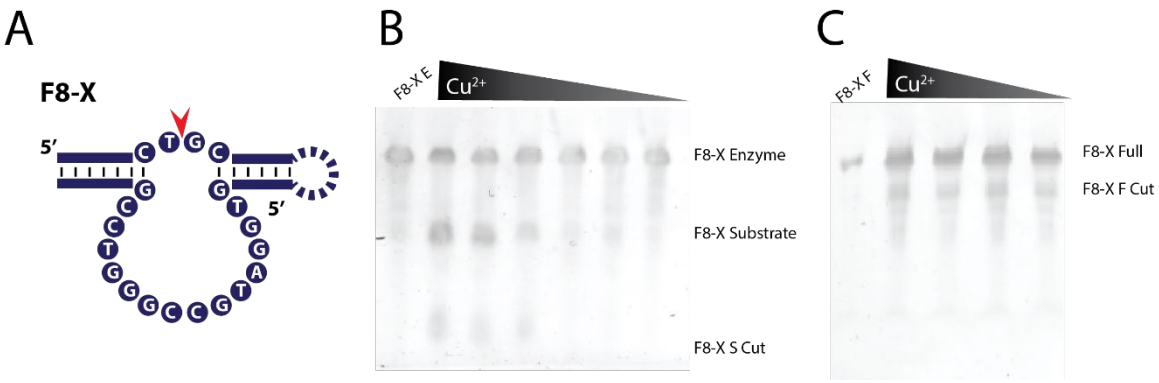

Figure 23: Structure of the F8-X DNAzyme Enzyme and Substrate sequences (without loop) and F8-X Full (with loop) (A). Cleavage of the F8-X Substrate sequence from the Enzyme strand in 1 mM to 1 nM copper sulfate (B). Cleavage of the F8-X Full sequence in 1 mM to 10 nM copper sulfate (C). Both are 1 hour incubations.

The unimolecular, or 'Full', form of the DNAzyme cleaves faster than the bimolecular version, as shown by the more intense cleavage band on the gel in Figure 23C, though both cleave much slower than I-R3 or 10-23. This likely due to local availability of the substrate, and thus quicker assembly kinetics allowing for the correct formation of the DNAzyme. The unimolecular form also tolerates lower concentrations of Cu^{2+}, which is optimal for enzyme activity in the assay.

3.6.3 Cleaving from the amplicon

Both forms of the F8-X DNAzyme were converted into circle templates, the bimolecular one containing the enzymatic sequence in the RCA Amplicon and the Substrate strand being present in solution, as shown in the schematic in Figure 24A. Trace cleavage, as seen from FAM signal, of the F8-X Substrate is possible when hybridized to the amplicon. Additionally, there is a visible shift in the band due to the removal of the 3′ phosphate, with

the ‘cut’ band on the gel in Figure 24A containing the phosphate, and the ‘trim’ band having it removed.

The unimolecular construct can also cleave in the amplicon, as demonstrated by the banding in Figure 24B, representative of the amplicon being cut at regular intervals by the DNAzyme.

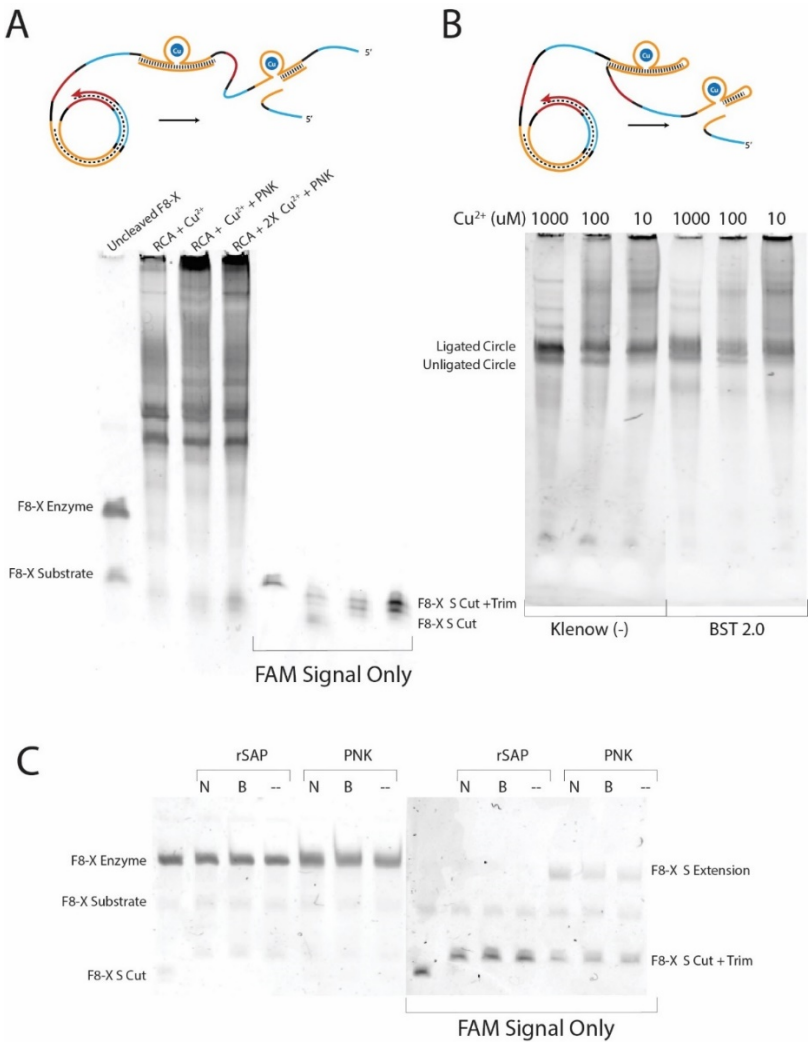

Figure 24: Demonstration of bimolecular F8-X cleavage from the RCA Amplicon via visualization of the 5′ FAM labeled Substrate strand. Reactions were performed in either 0.1 or 0.2 mM copper sulfate and in the presence or absence of PNK as labeled (A). Demonstration of unimolecular F8-X cleavage in the presence of 10-1000 µM Cu^{2+} from amplicons generated by Klenow (exo^{-}) or BST 2.0 DNA polymerases (B). Testing the 3′ phosphate cleanup by Shrimp Alkaline Phosphatase (rSAP) and PNK and visualizing extension via the

5′ FAM label. Reactions were performed in standard reaction buffer (--) or in the presence of 100 μM ammonium sulfate (N) or 500 μM betaine ("B"); (panel C).

The 5′ FAM labeled Substrate was also cleaved in the presence of the Enzyme sequence and then processed with either T4 PNK or Shrimp Alkaline Phosphatase (rSAP) to remove the 3′ phosphate before extension with Klenow (exo$^-$). The appearance of a FAM signal at the same height as the F8-X Enzyme band in Figure 24C indicates that the cleaved Substrate was extended.

3.6.4. F8-X summary

This ability to cleave from both the bi- and uni-molecular variants as well as the simple 3′ end cleanup via PNK makes F8-X the optimal DNAzyme to employ in the bicyclic assay. The unimolecular variant, with its quicker cleavage and lower required copper ion cofactor concentration can be used to generate the primer in the first stage of the assay, while the bimolecular variant can be used to introduce the signal generation component through a fluorescently labeled Substrate strand. The use of F8-X in the bicyclic assay will be covered in Chapter 4.

3.7 Conclusion

The rapid cleavage of the RNA hydrolysis mechanism employed by the 10-23 DNAzyme posed significant advantages in terms of the duration of the assay but showed some disadvantages in terms of durability of the component sequences. The I-R3 DNAzyme, which uses base-catalyzed cleavage resulting in an extension-ready 3′ hydroxide, initially appeared to be optimal, but the cofactor proved to be prohibitive. The complex cleavage resulting in a phosphoglycolate in the Pistol-like DNAzyme requires a highly specialized enzyme to clean up the 3′ end, so despite the DNAzyme's cleavage in

complex mixtures, it was discarded from consideration. Finally, the DNAzyme that excised a base to generate a 3′ and 5′ phosphate, F8-X, proved to be amenable to all the requirements of the assay, despite its need for PNK cleanup prior to extension. Thus, F8-X was selected for investigation in the bicyclic RCA presented throughout the remainder of this dissertation.

4
Bicyclic RCA: Rapid amplification and real-time readout with a two-stage RCA system

4.1 Introduction

Despite its many advantages as an isothermal amplification assay and its comparatively simple design, the utility of RCA is reduced by its linear amplification mechanism. There have been many techniques to increase the amplicon output. Of note are branched RCA[122,123] and its descendant, hyperbranched RCA,[28] as well as multi-primed RCA[29] and nicking-amplified RCA.[26,124,125] While these strategies are excellent for increasing the amount of amplicon generated, they all either increase the risk of non-specific signal generation, as any amplification of the linear padlock can cause significant false positive problems. Additionally, these strategies all turn the structurally plastic ssDNA amplicon into a double stranded helix, eliminating the possibility of introducing functional DNA structures into the amplicon.

This thesis proposes a modified version of nicking-amplified RCA, but instead of using a traditional nicking enzyme, the amplicon is converted into a primer, or potentially many primers molecules, for the circular template through self-cleavage of a DNAzyme segment (Figure 25). Additionally, this generated primer would be able to bind and amplify from not only the first circular template, but also a second circle, so that the RCA amplifies at nonlinear levels while also generating a signal that can be easily visualized, as can be seen in Figure 25.

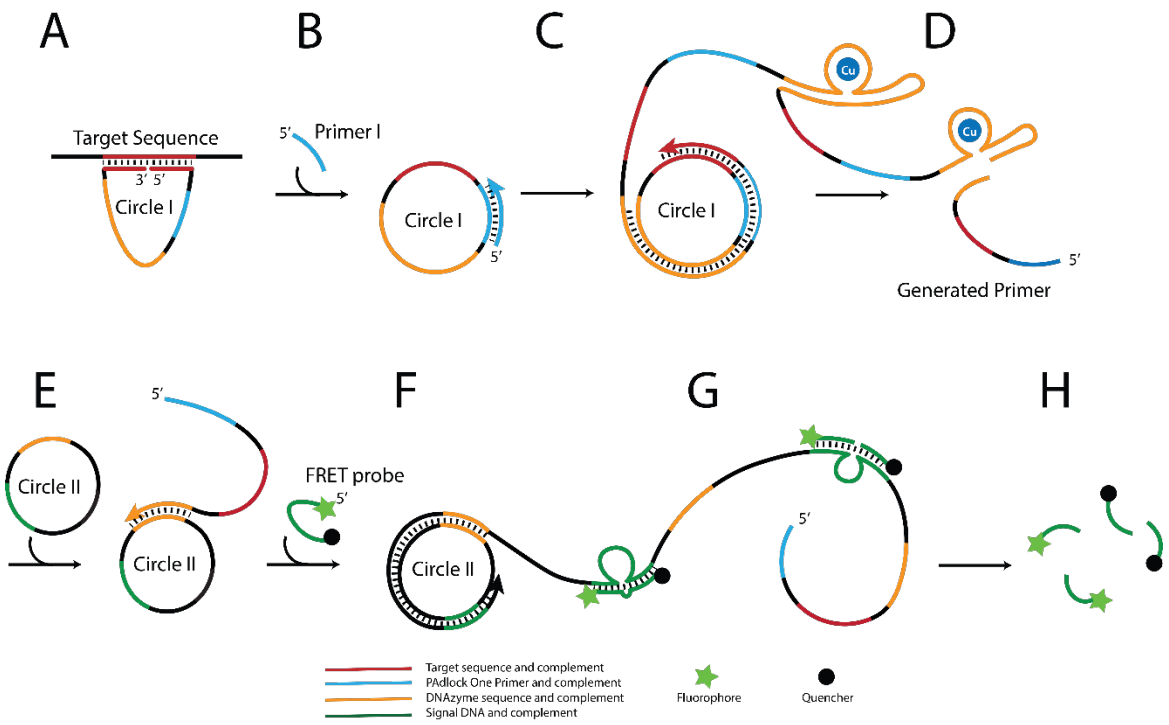

Figure 25: The scheme representing the bicyclic reaction, starting with ligation of the padlock probe hybridized to a target DNA or RNA sequence (A), priming of the newly circularized Template I (B) and RCA (C) that generates an in-amplicon DNAzyme capable of cleavage in the presence of low concentrations of copper ion (D). This newly cleaved amplicon has its 3′ phosphate removed by T4 PNK and is used as a primer for a pre-circularized Template II (E), initiating a second round of RCA (F) and generating an amplicon that contains the enzymatic portion of the same DNAzyme, allowing for the fluorophore-quencher FRET probe DNA to bind to the amplicon (G) and to be cleaved, generating a fluorescent readout (H) or allowing for separation of a small labeled fragment.

This assay is designed for one-pot performance, allowing for signal generation without buffer exchange or purification steps. This is novel and challenging due to the complexity inherent in the individual steps, which is increased when they are combined, especially when introducing a transition metal ion to the RCA reaction, as the metals often inhibit enzymatic activity.[126] Prior studies have attempted to create multi-step one pot RCA detection strategies, however they demonstrate the reaction in discrete stages with extensive sample manipulation.[104] This reaction was validated at every step to demonstrate that F8-X, the most optimal DNAzyme described in Chapter 3, performed as intended. The

full reaction was additionally tracked over time using a FRET probe to show the real-time signaling capabilities of the assay.

4.2 Materials and Methods

Materials. All DNAs were purchased from IDT (Coralville, IA, USA), with standard desalting except for Template I, which was HPLC Purified. The oligonucleotides were resuspended in water (no EDTA added due to cofactor fouling) to make 500 μM primary stocks and kept frozen at -20 °C except for removal to prepare new working 10 μM stocks. The concentration of the primary stock was evaluated by UV/Vis. As the DNAs were analyzed by denaturing PAGE, purity of the stocks was evaluated and working stocks were remade as necessary. The following sequences were used:

F8-X Full 5′-
CGAATTAGAAAGTCTGCACACCGAATCGGTGTGTGGATGCCGGGTCCGACTTTCAGTGA-3′

Template I 5′-
/5Phos/TTGGTATGTTCACAGGCACGGACCCGGCATCCAGACTTTCTATTAGAAAGTCAGTGCCTGTGACTTTGTT-3′

Template II 5′-
GACTTTCTAATTCGTCGAATGCTTTTTTTTCCCAACCCGCCCTACCCATTTTGACTTTCTAATTCG-3′

Additional sequences (F8-X precut primer, Template I splint, Template II splint, Template II G Version I, Template II G Version II, Template II G Version III, Template II F8-X, F8-X Substrate Ext, FRET Probe) are in Appendix Table A1.

RCA enzymes (T4 Ligase, Klenow (exo$^-$), T4 PNK) were purchased from New England Biolabs (Ipswich, MA). Copper sulfate was purchased from Sigma.

Methods and Procedures

F8-X cleavage. Cleavage was performed in Reaction Buffer (10 mM Tris HCl, 50 mM NaCl, 10 mM $MgCl_2$, pH 7.9) in the presence of 0.1 μM F8-X Full or 0.1 μM each F8-X Enzyme and Substrate sequence and 1 μM $CuSO_4$ (refer to Chapter 3 for F8-X DNAzyme description). The 30 μL reactions were performed at 25 °C for 30 minutes to 24 hours before 3′ PNK cleanup was performed by adding ATP to 1 mM and 166 Unit/mL of T4 PNK for 30 minutes at room temperature.

Template I Cleavage. RCA of Template I was performed in Reaction Buffer (10 mM Tris HCl, 50 mM NaCl, 10 mM $MgCl_2$, pH 7.9) with 0.1 μM Template I and 0.1 μM Target Sequence and 1 mM ATP and 1 mM dNTPs. RCA was initiated by adding 233 Unit/mL of T4 DNA Ligase and 33 Unit/mL Klenow fragment (3′→5′ exo^-) and the reaction was incubated at room temperature for 30 minutes. At the 30 minute mark, 1 μM $CuSO_4$ was added and the reaction mixture was kept at room temperature for another hour. 3′ end cleanup was then performed by adding 166 Unit/mL of T4 PNK for 30 minutes at room temperature.

RCA of Template II. RCA was performed in Reaction Buffer (10 mM Tris HCl, 50 mM NaCl, 10 mM $MgCl_2$, pH 7.9) with additional 1 mM ATP and 1 mM dNTPs in the presence of 0.1 μM Template II and a complementary sequence to close the circle for ligation (Template II Splint). 233 Unit/mL of T4 DNA Ligase and 166 Unit/mL of T4 PNK was added before incubation at 25 °C for 30 minutes. Various primers were introduced along with 33 Unit/mL Klenow fragment (3′→5′ exo^-) polymerase to initiate RCA. Reactions were heat-killed at 95 °C for 5 minutes.

Pre-ligated Template II Preparation. 1 μM each Template II and Template II Splint were incubated at 25 °C for 30 minutes in reaction buffer with 1 mM ATP, 233 Unit/mL of T4 DNA Ligase and 166 Unit/mL of T4 PNK. The reaction was then heat killed at 95 °C for 5 minutes before being brought back to room temperature, and 100 Unit/mL of Exonuclease I and 200 Unit/L of Exonuclease III were then added. The reaction was incubated at 37 °C for 1 hour before heat killing at 95 °C for 10 minutes.

Full Reaction. The reaction is performed with 1 μM Template I, 1 μM Template I Primer, and 100 nM pre-ligated Template II in reaction buffer with 1 mM ATP, 1 mM dNTPs and 100 μM $CuSO_4$, followed by addition of 233 Unit/mL of T4 DNA Ligase, 166 Unit/mL of T4 PNK and 33 Unit/mL of Klenow (exo^-) and varied concentration of the Target Sequence. The reaction is incubated at 37 °C for 1 hour to overnight before heat killing and analysis by denaturing PAGE.

Gel Electrophoresis. Except when otherwise stated, denaturing PAGE was used to analyze cleavage and RCA products. Reactions were denatured in 8M Urea for 10 minutes at 95 °C before being run on a denaturing 12 % 19:1 acrylamide:bis gel at 500 V for 15 minutes in a BioRad mini PROTEAN apparatus. All gels were 0.75 mm thick, 70 mm by 100 mm.

Divided Reaction Real-Time Fluorescent Readout. The Template I was ligated in the presence of three different concentrations of Target as well as the absence of Target, and RCA was performed with 33 Unit/mL of Klenow (exo^-) and 100 μM $CuSO_4$ overnight before being added to 100 nM ligated Circle II, 3 μM FRET Probe, 166 Unit/mL of T4 PNK and 33 Unit/mL of Klenow (exo^-). A positive control was run with the addition of

the synthetic primer instead of the Template I reaction mixture. The second stage RCA reaction was run at 35 °C for 60 minutes, with real time monitoring of fluorescence, using excitation at 495 nm, emission at 520 nm, measurements taken every 2.5 minutes.

Complete Reaction Real-Time Fluorescent Readout. 100 nM Template I and varying concentrations of Target were added to 100 nM ligated Template II, 3 μM FRET Probe and 100 μM $CuSO_4$ in the reaction buffer. 233 Unit/mL of T4 DNA Ligase, 166 Unit/mL of T4 PNK and 33 Unit/mL of Klenow (exo^-) were added to the 30uL reaction at the start of the run. The negative control (blank) is the absence of Target. The reaction was run at 35 °C for 60 minutes, with real time monitoring of fluorescence by a Tecan Spark ® Multimode Microplate Reader, using excitation at 495 nm, emission at 520 nm, measurements taken every 2.5 minutes.

4.3 Results and Discussion

Utilizing the F8-X DNAzyme, found to be the most compatible for this project in Chapter 3, the bicyclic reaction was adapted to generate a fluorescent readout without external manipulation of the reaction vessel. This required first testing to ensure that the entire reaction can occur specifically upon the presence of the Target sequence, and that each component of the reaction can function in a single buffer system before moving to quantifying and improving the limit of detection.

4.3.1 Specificity of RCA Amplification

It is imperative in this assay that any signal generation only occur in the presence of the target. To this end, the RCA reactions were tested to ensure that without ligation of Template I, or without the generation of the primer from the Template I amplicon, the

reaction does not proceed towards DNAzyme cleavage. In Figure 26, the linear Template I DNA was subjected to the ligation and RCA procedure in the presence or absence of the Target Sequence. Lane 2 showcases the banding expected from ligation of a padlock probe, as ligation can either ligate the 5′ and 3′ ends of the same sequence together to form a unimolecular circle, or it can ligate two or more Template I strands together to form linear multimers or higher order circles. In the absence of the Target Sequence, the Template I sequence is ligated into a circle extremely rarely. When these mixtures undergo RCA, if the Target Sequence is present, a clear amplicon smear is visible, demonstrating productive RCA. In the absence of the Target Sequence, the absence of any amplicon smearing confirms lack of RCA, indicating that the Template I sequence was not ligated into a circle: the only activity shown is due to dimer extension within the Template I sequence.

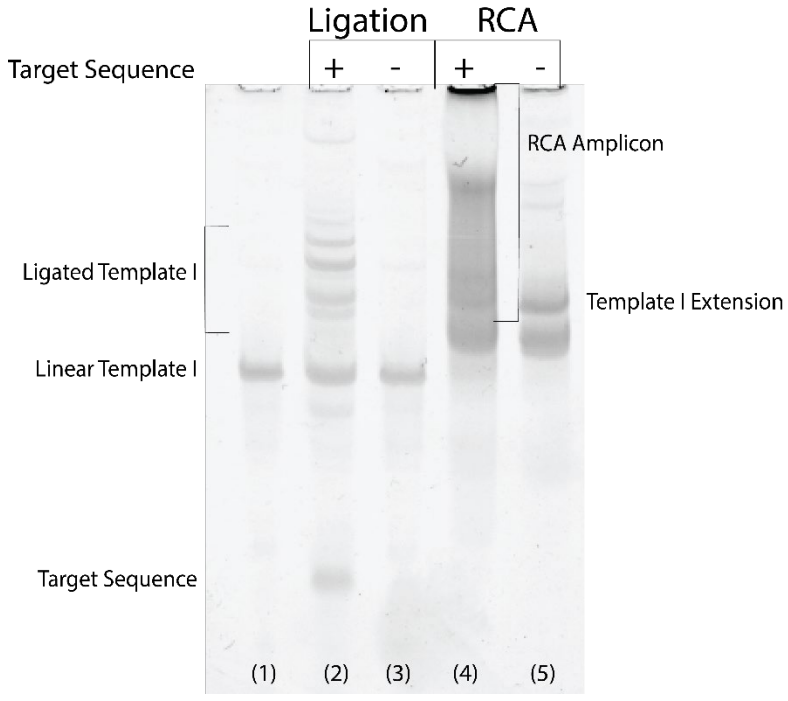

Figure 26: Ligation and RCA reactions amplifying Template I in the presence and absence of the Target Sequence. Lane (1) is the linear Template I DNA alone as a control. Subsequent lanes are the ligation of Template I in the presence (2) or absence (3) of the Target Sequence, and the RCA reaction of the two ligation reactions respectively (4,5). This was analyzed on a PAGE gel as specified in methods.

To develop the second stage of the bicyclic RCA, multiple variants of pre-ligated and purified Template II were tested for specific amplification by performing RCA with or without the primer that would be generated by cleavage of the amplicon of Template I. These variants contain different G-quadruplex sequences, as described in Chapter 5, and thus have different amplification efficiencies due to varying efficiencies for the polymerase reading through their cytosine repeats. As demonstrated in Figure 27A, the RCA reaction without the primer generated some slight extension products, likely the splint amplifying on the linear Template I sequence, but no large RCA amplicons are in those lanes, as can be seen in the lanes with the primer. Additionally, Figure 27B shows that the intensity of the RCA Amplicon smear is correlated directly to the quantity of primer added, further indicating that RCA is dependent on the presence of the primer, and will not occur otherwise.

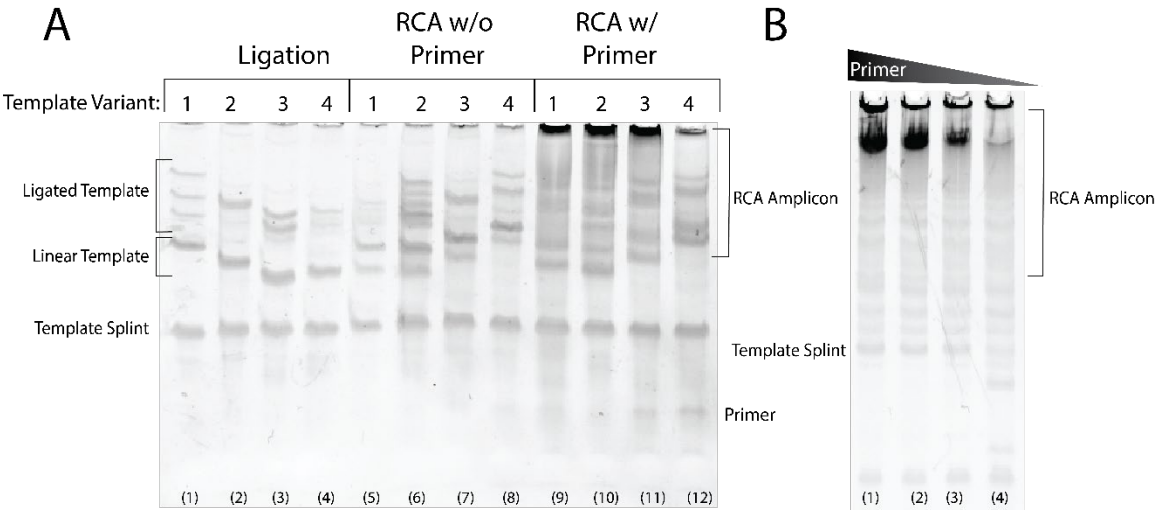

Figure 27: Testing the processivity of RCA using 4 different variants of the Template II (Circle II F8X and Circle II G Version I, II and III). The ligated circles are shown in the four lanes at the far left, followed by the RCA reaction in either the absence or presence of a primer, showing that the long amplicon forms only when the primer is present (A). The dependence on the primer is additionally emphasized by showing the dependence of the amount of RCA amplicon formed upon initial primer concentration, as demonstrated through RCA reactions run with 1 µM to 1 nM copper ion-cleaved F8-X and a constant 0.1 µM ligated Template II (B).

4.3.2 Template I to Template II transition

Having demonstrated that the two RCA reactions can each proceed independently, we then investigated whether the F8-X DNAzyme within the amplicon produced by the first RCA can serve as a primer for the second RCA. The priming capability of F8-X was compared against a primer of the same sequence as the resulting cleavage primer, only without the 3′ phosphate. The RCA priming of both are compared in Figure 28A, in which the DNAzyme and the control are tested on Template II. The appearance of comparable RCA products regardless of primer in the case of Template II shows that the removal by T4 PNK of the 3′ phosphate that remains after F8-X's cleavage allows the DNAzyme to extend in the same way as a standard primer.

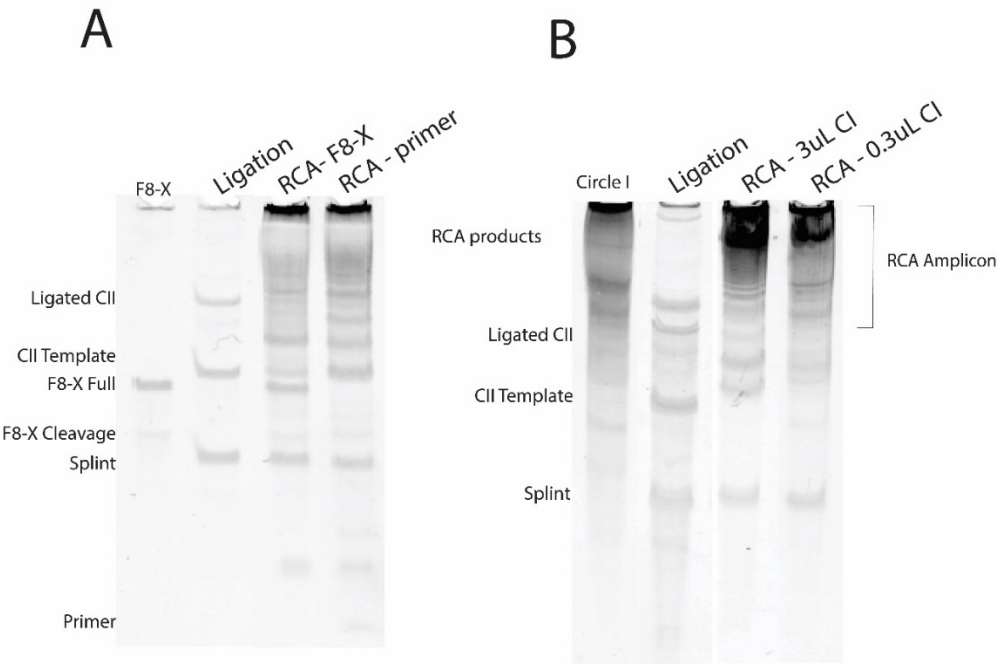

Figure 28: Extension of two variants of Template II by a precut F8-X primer that has a functional 3′ end (primer) and the cleaved and T4 PNK cleaned F8-X DNAzyme (F8-X) (A). Extension of variants of Template II from cleaved and cleaned Template I, with two concentrations of starting primer shown (B).

In Figure 28B, Circle I's amplicon is used as a primer for three variants of Circle II. The RCA product from Circle I was added as either 10 % or 1 % of the reaction volume to

demonstrate that the output RCA was from Circle II, and not traces from Circle I. All three variants tested generated significant amounts of Circle II Amplicon with the larger concertation of Circle I primer oversaturating the gel. At the lower concentration, variant II, which performs better overall, generated more amplicon than the other, whose smearing is likely from Circle I and not any significant amount from Circle II.

4.3.3 Cleavage of bimolecular F8-X

The real-time read-out of the bicyclic RCA reaction utilizes the change in fluorescence when an F8-X DNAzyme in the product of Circle II self-cleaves. Unlike the F8-X in the Circle I amplicon, the F8-X in Circle II is formed by two molecules instead of one (see Figure 25). The cleavage of the DNAzyme is slow but even more so when separated into two sequences, as the assembly of the DNAzyme is no longer dominated by an elevated local concentration. Figure 29 shows this cleavage in action through the use of a FRET probe version of the F8-X Substrate sequence. This sequence has a FAM label on the 3′ end and a Black Hole Quencher 1 on the 5′. While the BHQ-1 does not quench the FAM's fluorescence completely, it does decrease it up to 40 % according to the literature.[127] The reason to avoid a more optimal quenching configuration is to reduce the chances that the already fragile DNAzyme configuration could be further hindered by a quencher near the cut site.

Regardless, the cleavage of the bimolecular DNAzyme frees the FAM label from the effect of the quencher, increasing the fluorescence measured at 520 nm (excitation at 495 nm), as can be seen in Figure 29A after an overnight reaction. Visualization of the fluorescence from the acrylamide gel, either from the DNA itself through a FAM filter prior to staining (29B) or after SYBr gold staining (29C) show that the minimal sequence

DNAzyme as well as the full template complement both cleaved the FRET probe. While there is no cleavage visible in the ligated Template I reaction, there is still an increase in fluorescence, perhaps indicating that the FRET probe is hybridizing to the amplicon, separating the FAM label and the quencher, but not cleaving efficiently.

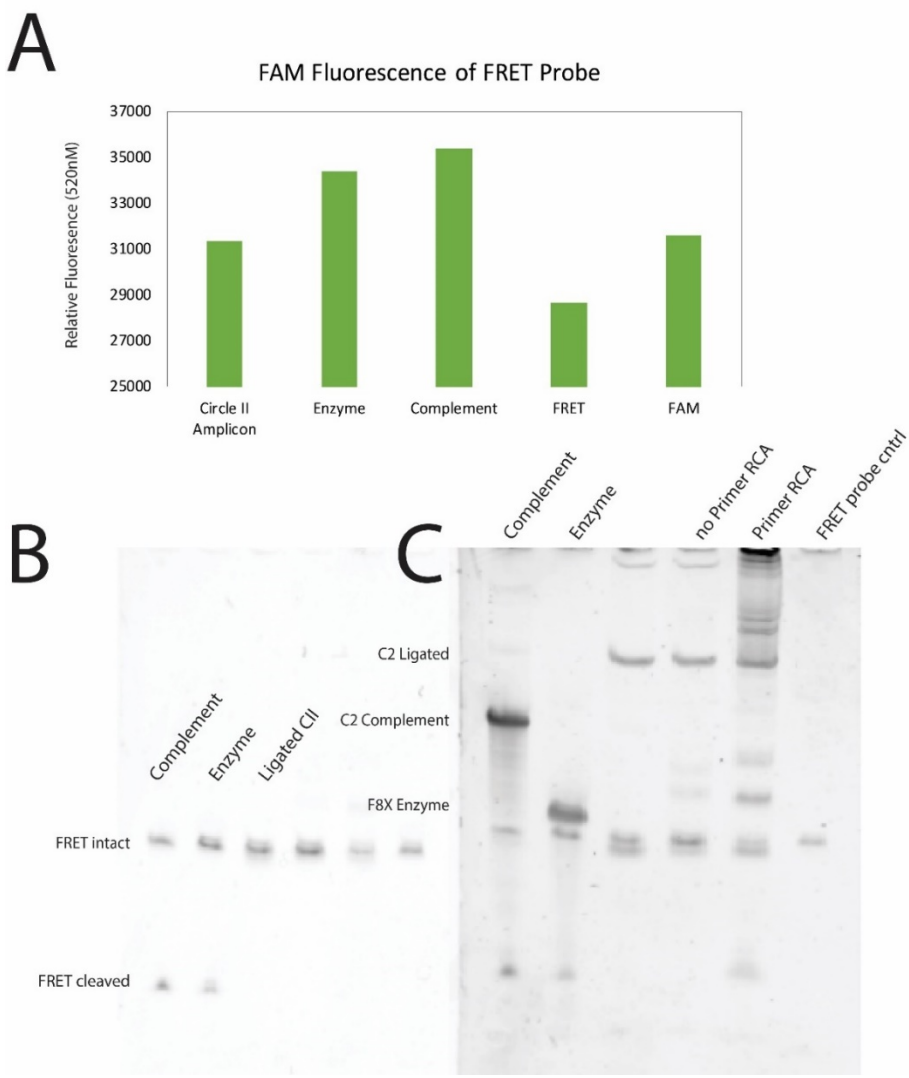

Figure 29: FAM fluorescence signal from the FRET probe in the presence of various DNAs and 10 μM $CuSO_4$. The DNAs are the RCA Amplicon of Circle II, the minimal sequence Enzyme moiety of the F8-X DNAzyme, and an artificial Circle II complement. The FRET probe alone is shown as the lower bound for fluorescence, and an unquenched FAM sequence is a positive control (A). The denaturing PAGE gel of the reaction with a FAM only (B) and SYBR-stained view (C), showing the cleavage products in the presence of the complement and the enzyme sequence.

While there is no strong cleavage signal in the RCA lane as there is with the positive control, as anticipated with bimolecular DNAzyme cleavage, there is still an increased FAM signal when assayed in the plate reader (Figure 29A). This is perhaps due to the design of the probe, as it is 26 bases (2.5 helical turns) long, allowing for approximately 88 Å distance between the FAM label and quencher disregarding their linker lengths. The Förster radius for FAM-BHQ1 has not been reported, but based on FRET quenching efficiencies of FAM-BHQ1 (88 %) and Cy3-BHQ2 (97 %) measured in the same system[128] and the 50-52 Å Förster radius of Cy3-BHQ2,[129] the Förster radius for FAM-BHQ1 is about 39 Å, so an 88Å separation along the helix axis as well as the placement of the two dyes on opposite sides of the helix should place them well beyond FRET quenching distance.

This fluorescence change in the presence of the RCA amplicon is demonstrated in Figure 30, where RCA is performed on Template II using varying concentrations of primer. The sharp increase in FAM fluorescence upon initiation of the reaction, which occurs faster than cleavage of the F8-X can be visualized, indicates that hybridization to the amplicon separates the FAM label from BHQ-1 quencher prior to cleavage, and the difference is detectable.

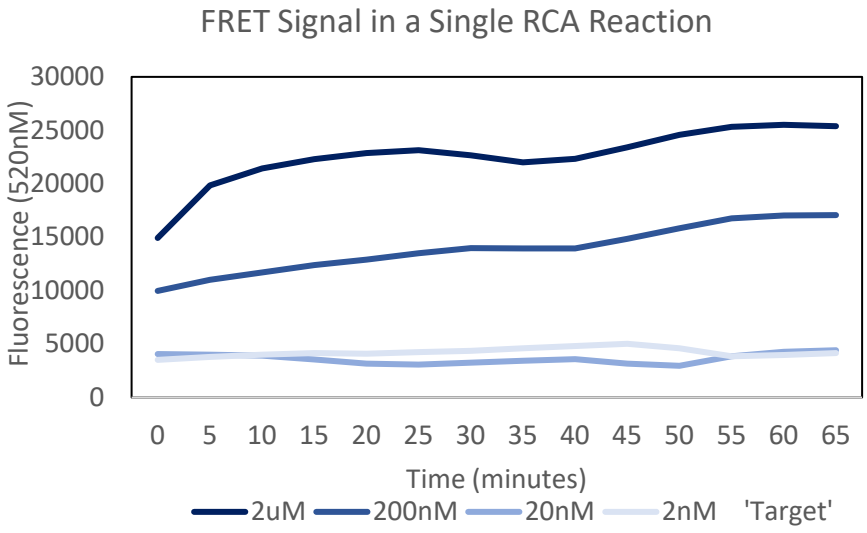

Figure 30: Time course of FAM signal during RCA of Template II, demonstrating the signal generation from the FRET probe as it hybridizes to the RCA amplicon. 'Target' is the Template II splint acting as a target for this assay.

This validation of the signaling mode, with additional confirmation through PAGE analysis of the amplification reactions, leaves only performing the full reaction, demonstrated in the following section.

4.3.4 One-Pot Reaction

To demonstrate the whole reaction, Circle I RCA was performed in the presence of 10 μM $CuSO_4$ and incubated at room temperature overnight before being added in various concentrations to a pre-ligated Circle II and FRET probe mixture along with PNK and Klenow (exo^-). While the traces seen in Figure 31 are not representative of concentration, the FRET probe is still under active development as it was discovered that the primer sequence does not bind efficiently to the circle, even when using a synthetic primer shown in purple. In the graph, it can be seen that the concentration of target in the initial reaction correlates to the amount of FAM signal that is emitted by the FRET probe when the

quencher is cleaved off, adding to that ability to quantify the starting concentrations that was shown in Figure 30.

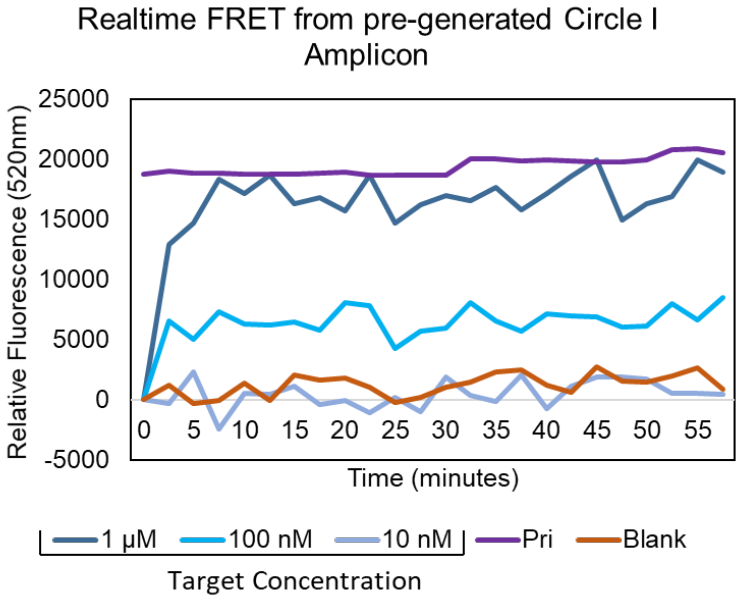

Figure 31: Realtime FRET of the bicyclic assay initiated by a pre-ligated Circle I RCA amplicon. Fluorescence is background subtracted by setting the reading at $t_0 = 0$ for all runs.

The full reaction was then performed, with all the components mixed into a single well, excluding enzymes that were added upon the start of the run. The resulting traces, shown in Figure 32, show that the reaction is prone to unfolding of the FRET probe early, though there is a promising steady increase in signal at the higher concentration. A more fully optimized FRET probe would likely result in cleaner data, and is a follow up experiment to be performed.

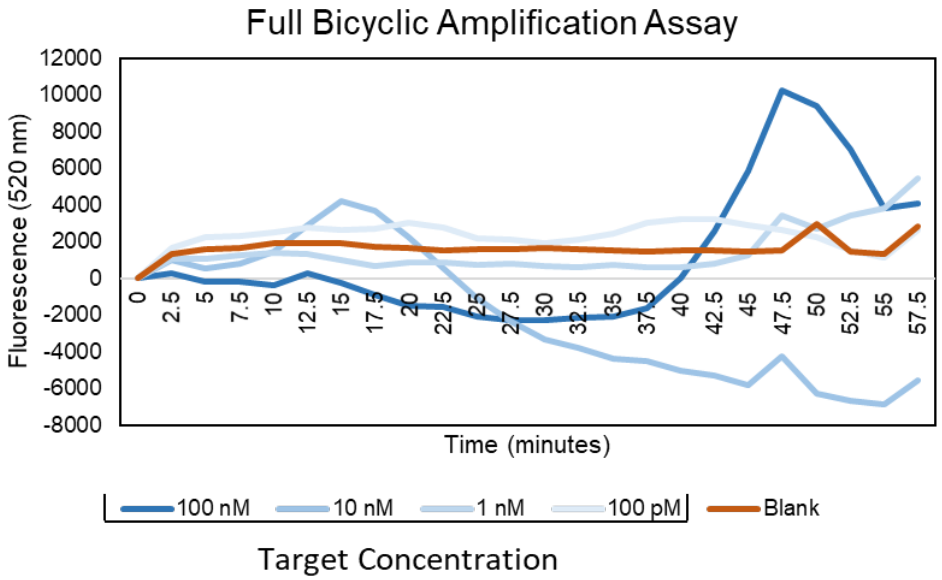

Figure 32: Full bicyclic RCA reaction performed in real time with a range of Target concentrations. Fluorescence is background subtracted by setting the reading at $t_0 = 0$ for all runs.

4.4 Conclusion

As this chapters shows, the copper-activated F8-X DNAzyme can be integrated into an RCA amplicon and used to prime a secondary RCA extension, bringing the linear amplification of RCA into the polynomial realm. Additionally, F8-X can be used as a FRET reporter, with a fluorescence increase upon hybridization and cleavage. However, cleavage with copper ion is a slow event, and PNK is not stable at 37 °C for very long, so a one-pot reaction is not yet achievable. Instead an addition of PNK after the 12 hour mark allows the reaction to proceed. Further development of this assay would help bring the timeframe into the clinical 8-hour range, as well as help improve the performance of the assay through lower background signal so that a smaller limit of detection can be achieved.

5
Integration of the Bicyclic RCA into a Phase Change Platform for PoC Applications

5.1 Introduction

When untrained users will be asked to perform diagnostic tests without supervision, it is necessary to remove as much of the complexity as possible. In our case, complexity comes from the need to have active enzymes in the reaction, which would require pipetting steps. Additionally, the intervening step of adding PNK after the Circle I RCA and cleavage is a manipulation that would require a trained hand. In this chapter we demonstrate the use of wax layers to enable automated reagent addition and mixing via thermal actuation, thus obviating the need for the user's intervention. The system also allows for the use of a more intuitive and potentially instrument-free colorimetric mode for naked eye evaluation.

G-quadruplexes are structures of stacked guanidine quartets upon which hemin can stack, allowing for the catalytic oxidation of colorimetric substrates such as 2,2′-azino-bis(3-ethylbenzothiazoline-6-sulfonic acid) (ABTS) and 3,3′,5,5′-tetramethylbenzidine (TMB) upon the addition of hydrogen peroxide.[130] G-quadruplexes are intriguing for PoC DNA amplification assays because they enable colorimetric readout and because they can be directly produced as a product of the amplification. The use of these elements has been growing in recent years, with examples of G-quadruplexes synthesized through the EXPonential Amplification Reaction (EXPAR)[131,132], Strand Displacement Amplification (SDA),[133,134] and RCA.[135–137] However, the hydrogen peroxide requirement has proven problematic: if H_2O_2 is present from the start of the reaction, it degrades the sample through

oxidatively damaging the DNA,[138] and destroys the enzymes. This leads to a requirement for manual addition of a measured amount of hydrogen peroxide after the amplification, which is antithetical to the goal of ease-of-use. Here we present a solution that precisely and automatically adds and mixes all the reagents needed for RCA with subsequent G-quadruplex based colorimetric readout.

Our lab previously developed a phase-change controlled reactor in which meltable wax layers initially sequester reagents and then upon thermal activation (heating) permit sequential mixing of reaction layers.[8] The wax layers are comprised of different pure alkanes so that each layer melts sharply at a specific melting temperature. The layers are arranged in order of melting temperature so that they 'release' sequentially as their environment heats. This allows for the step-wise mixing of different stages of the bicyclic reaction and the integration of signal output systems that would otherwise hinder the amplification reaction. Notably, this enables the incorporation of a G-quadruplex into the bicyclic system, as it is possible to partition the hydrogen peroxide and have it be added at the appropriate step without manual intervention. It also allows for the separation of the enzymes necessary in the reaction to safeguard them against denaturation during storage.

The design of the bicyclic RCA system within the thermally-actuated phase change reactor is presented in Figure 33. The separation of the reagents uses pure alkanes that melt at discrete temperatures, in this case octadecane (C18, $C_{18}H_{38}$ – m.p. 32 °C), eicosane (C20, $C_{20}H_{42}$ – m.p. 42 °C), docosane (C22, $C_{22}H_{46}$ – m.p. 48 °C) and tetracosane (C24, $C_{24}H_{50}$ – m.p. 54 °C) were used. A total of eight wax layers (two of each alkane) and nine reagent layers are used for the full bicyclic RCA reaction.

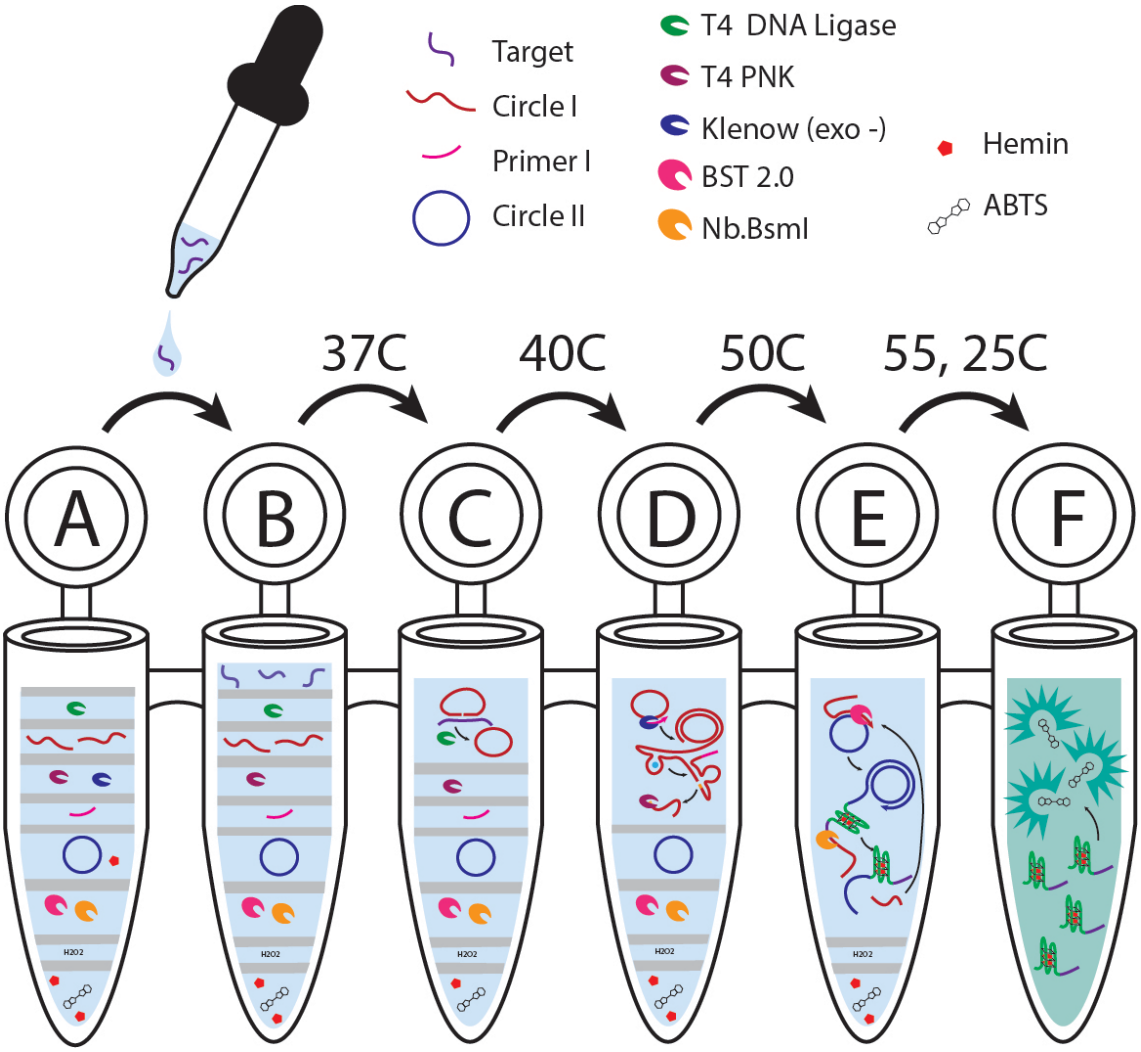

Figure 33: Scheme of the phase-change partitioned bicyclic RCA assay. This scheme demonstrates the partitioned reagents prior to addition of the target sequence, separated by pure alkanes represented by grey bands (A). The reaction is initiated through the addition of the target sample (B) and subsequent heating to 37 °C, melting the octadecane layer allowing mixing of the target with the linear Circle I precursor and T4 DNA ligase (C). The ligation occurs as the temperature ramps up to 40 °C, allowing the eicosane layers to melt and revealing Klenow (exo$^-$) and the Circle I primer to initiate RCA and T4 PNK to clean up the 3′ end of the in situ generated primers (D). The transition to 50 °C melts the docosane layer, revealing Circle II and BST 2.0, kicking off the second round of RCA, in which the amplicon is a G-quadruplex sequence. Hemin in this RCA mixture stabilizes the G-quadruplexes as they form, and Nb.BsmI allows for nicking of the amplicon to increase the G-quadruplex color output (E). Finally, heating to 55 °C melts the tetracosane layers, revealing the ABTS, additional hemin and the hydrogen peroxide. The reaction is then removed from the heating element and the colorimetric output develops for 30 minutes before analysis (F).

This chapter shows the implementation of the G-quadruplex generating RCA system with colorimetric readout, modifications that were undertaken to allow these reactions to occur at higher temperatures, and optimization of the colorimetric output and subsequent

demonstration of the full system. Specifically, the thermal stability of the components was tested to ensure that the reaction that was demonstrated at 37 °C in Chapter 4 can still occur at 55 °C, as well as ensuring that the colorimetric output is not hindered by the alkanes and remains specific to the presence of the target.

5.2 Materials and Methods

Materials. All DNAs were purchased from IDT (Coralville, IA, USA), with standard desalting except for Template I, which was HPLC Purified. The oligonucleotides were resuspended in water (no EDTA added due to cofactor fouling) to 500 μM primary stocks and kept frozen at -20 °C except for removal to prepare new working 10 μM stocks. The concentration of the primary stock was evaluated by UV/Vis. As the DNAs were analyzed by denaturing PAGE, purity of the stocks was evaluated and working stocks were remade as necessary. The following G-quadruplex sequences were used to determine assay viability at high temperature:

CatG4: 5′-TGGGTAGGGCGGGTTGGGAAA-3′

c-myc: 5′- GAGGGTGGGGAGGGTGGGGAG-3′

G5A5G5: 5′-AGGGGGAAAAAGGGGGA-3′

G5T5G5: 5′-TGGGGGTTTTTGGGGGT-3′

G4A4G4: 5′-AGGGGAAAAGGGGA-3′

G4T4G4: 5′-TGGGGTTTTGGGGT-3′

The following sequences were used to perform RCA with a G-quadruplex readout. The first 28 nt are common to all three.

Circle II G5

5′-GACTTTCTAATTCGTCGAATGCTTTTTTCCCCCTTTTTCCCCCTTTTTGACTTTCTAATTCG-3′

Circle II G4
5′-GACTTTCTAATTCGTCGAATGCTTTTTTCCCCTTTTCCCCTTTTTGACTTTCTAATTCG-3′

Circle II CatG4
5′-GACTTTCTAATTCGTCGAATGCTTTTTT
TTCCCAACCCGCCCTACCCATTTTGACTTTCTAATTCG-3′

Additional sequences are in Appendix Table A1. RCA enzymes were purchased from New England Biolabs (Ipswich, MA).

G-quadruplex Colorimetric Output Analysis. 200 nM G-quadruplex was incubated in Reaction Buffer (10 mM Tris HCl, 50 mM NaCl, 10 mM $MgCl_2$, pH 7.9) with 2 mM ABTS, 6 μM Hemin, and 300 μM H_2O_2 for 15 minutes at the temperature specified. Assays where the pH was changed were accomplished through the use of Tris stocks at the designated pH in the reaction buffer, with Tris adjusted to the appropriate pH with HCl. 100 μM ammonium sulfate was added to the reactions where indicated.

G-quadruplex Generation from a Template. 100 nM Circle II G5 was incubated in Reaction Buffer of appropriate pH with 1 mM ATP and 1 mM dNTPs. 120 Unit/mL of BST 2.0 and 166 Unit/mL of Nb.BsmI. were added to the reaction mixture, which was held at the indicated temperature for 30 minutes before heat killing with addition of two volumes of 12 M Urea at 95 °C for 5 minutes.

Gel Electrophoresis. Denaturing PAGE was used to analyze cleavage and RCA products. Reactions were run on a 12 % 40:1 acrylamide:bisacrylamide gel with 8 M Urea at 500 V for 15 minutes in a BioRad mini PROTEAN.

G-quadruplex Generation from RCA. 10 nM each linear Circle II CatG4 precursor and Circle II splint were incubated in Reaction Buffer with 1 mM ATP and 1 mM dNTPs for 30 minutes with 166 Unit/mL T4 PNK and 233 Unit/mL of T4 Ligase at 25 °C. Reactions

were then supplemented with 120 Unit/mL of BST 2.0 and 166 Unit/mL of Nb.BsmI and moved to a 55 °C water bath for a second 30 min incubation. Reactions were then heat killed at 95 °C for 5 minutes before either analysis by PAGE or adding 2 mM ABTS, 10 µM Hemin, and 300 µM H_2O_2 with visual observation for 15 minutes. Quantification of the absorbance change due to ABTS oxidation was done on a Tecan Spark® Multimode Microplate Reader, taking an absorbance scan from 390 nm to 550 nm so that the absorbance peak could be verified, with the absorbance at 420 nm used for quantification of ABTS oxidation.

Alkane Phase-Change Layer Assembly. 100 % octadecane, eicosane, dodecane, and tetracosane were melted in a sand bath at 250 °C. 30 µL of 10 µM Hemin and 2 mM ABTS in Reaction Buffer (pH 7.0) was added to the bottom of an 0.6 µL Eppendorf tube before careful addition of 25 µL tetracosane. After the wax layer solidified, 4 µL of 2 mM H_2O_2 was added in the center of the wax, followed by another 25 µL of tetracosane. Then 10 µL of 0.1 µM pre-ligated circle II and 1 mM dNTPs in reaction buffer was added, followed by 35 µL of docosane, then 400 Unit/mL BST 2.0 and 500 Unit/mL of Nb.BsmI in 5 µL glycerol, and another 35 µL of docosane. Then 10 µL of 10 µM $CuSO_4$, 1 mM dNTPs and 1 µM Circle I primer in the reaction buffer was added, followed by two additions of 20 µL octadecane to fully isolate the layer, allowing the layer to solidify between additions. Tubes were then placed in an ice bath to ensure complete wax solidification. Then, 500 Unit/mL T4 PNK and 700 Unit/mL of Klenow (exo^-) were added in 5 µL glycerol, followed by two more sequential additions of 20 µL eicosane. Finally, 10 µL of 1 µM linear Circle I precursor and 1 mM ATP in reaction buffer were added, followed by two additions of 20 µL of octadecane, 5 µL containing 7 Units of T4 Ligase, and two more additions of 20 µL

octadecane. The complete stack of reagents and alkanes amounts to 400 µL and requires approximately 20 minutes to assemble by hand. It can be seen in Figures 33 and 39.

Bicyclic RCA System in Phase-Change Layers. 10 µL of 1 µM to 1 nM Target sequence in Reaction Buffer was added to the top layer of wax, and the tube was placed in a water bath at 30 °C. The temperature was ramped up manually at approximately 0.5 °C per minute until the water bath reached 55 °C over the course of an hour. The reaction was then removed from the water bath and allowed to cool to room temperature while the ABTS color developed.

Organic Solvent Enhanced Imaging. 30 µL of 10 µM Hemin and 2 mM ABTS in the reaction buffer (pH 7.0)), with the addition of 20 % v/v of each pure solvent (methanol, ethanol, isopropanol, acetonitrile). Tetracosane was then added, followed by 4 µL of 2 mM H_2O_2, and either 1 µM CatG4 in the reaction buffer or the reaction buffer alone as a blank.

Organic Solvent RCA in Layers. Either 1 µM or 100 nM Target was added to 1 µM Circle I in the reaction buffer with 133 Unit/mL of T4 DNA Ligase, 33 Unit/mL of Klenow (exo -) and 100 µM $CuSO_4$. The reaction was left overnight to cleave, before 166 Unit/mL of T4 PNK was added and incubated for 30 minutes to remove the 3′ phosphate at room temperature. 30 µL of 10 µM Hemin and 2 mM ABTS in the reaction buffer (pH 7.0) and 20 % v/v acetonitrile or methanol was added to the bottom of the tube before careful addition of 25 µL tetracosane. After the wax layer solidified, 4 µL of 2 mM H_2O_2 was added in the center of the wax, followed by another 25 µL tetracosane. 10 µL of 0.1 µM pre-ligated circle II, 1 mM dNTPs in reaction buffer were added, followed by 35 µL of docosane, 400 Unit/mL BST 2.0 and 500 Unit/mL of Nb.BsmI in 5 µL, and another 35 µL

of docosane. The pre-prepared Circle I reactions, as well as a positive control consisting of the synthetic primer to Circle II and a negative control of no DNA, were added to the top of the layered assembly, with hemin included in the RCA mixture when indicated. The layers were melted sequentially in a water bath ramping from 40 °C to 55 °C over the course of an hour. The layers were allowed to solidify at room temperature before the aqueous layer was extracted for imaging on a microplate reader. An absorbance scan from 390 to 500 nm was performed on each well, and the absorbance at 420 nm was baseline subtracted by that at 550 nm to produce the value shown.

5.3 Results and Discussion

Adapting the bicyclic RCA reaction to the phase change system required substantial optimization. It was necessary to demonstrate that both the amplification and the readout could be adapted to the temperatures needed to melt the max layers, and that the hemin and other components would not be degraded.

5.3.1 Selecting G-quadruplexes for High Temperature Use

Due to their ability to bind hemin in a reactive conformation, G-quadruplexes enable a colorimetric readout, but the stability of the quadruplex to buffer and temperature changes varies based on its sequence. To ensure optimal colorimetric signal generation in the phase-change platform, several G-quadruplexes were tested at a range of temperatures to ensure that they were capable of forming under the reaction conditions. We assayed several "traditional" G-quadruplexes: 22AG,[139] CatG4,[140] and c-myc,[141] each of which has 3 stacked guanine tetrads, as well as quadruplexes with 4 (G4A4G4, G4T4G4)[142] and 5 tetrads (G5A5G5, G5T5G5).[143] In Figure 34A, the colorimetric readouts from three different G-quadruplexes (with increasing stability) are shown at 65, 55 and 37 °C and in

the presence of ammonium sulfate. Only G5A5G5, a quadruplex modified from a publication that aimed to create a G-quadruplex that can function at up to 95 °C,[143] was capable of visibly oxidizing ABTS at 65 °C. While the number of guanine tetrads do not have an implicit correlation with thermal stability, there is a signaling advantage to having a larger number of tetrads stacked to protect against denaturation. At lower temperatures, however, CatG4 is the G-quadruplex that generated the most oxidation, and was held as a second choice when performing further studies.

The reaction is buffered by Tris, which has a significant shift in its pKa when heated.[144] Thus, it is necessary to understand the impact of pH on the colorimetric signal from G-quadruplexes. The G-quadruplexes were tested at a range of pH from 7.0 to 9.5 and the colorimetric output was quantified, as shown in Figure 34B. While the pH-responsive behavior of the G-quadruplexes depends on their specific topology, our results corroborate prior studies[145,146] stating that a pH range between 6.0 and 7.6 is optimal for colorimetric output. Based on the known drift in pH for Tris buffers (Appendix Table 3), pH 8.8 to 7.6 at 25°C would be in that optimal range at 65 °C.

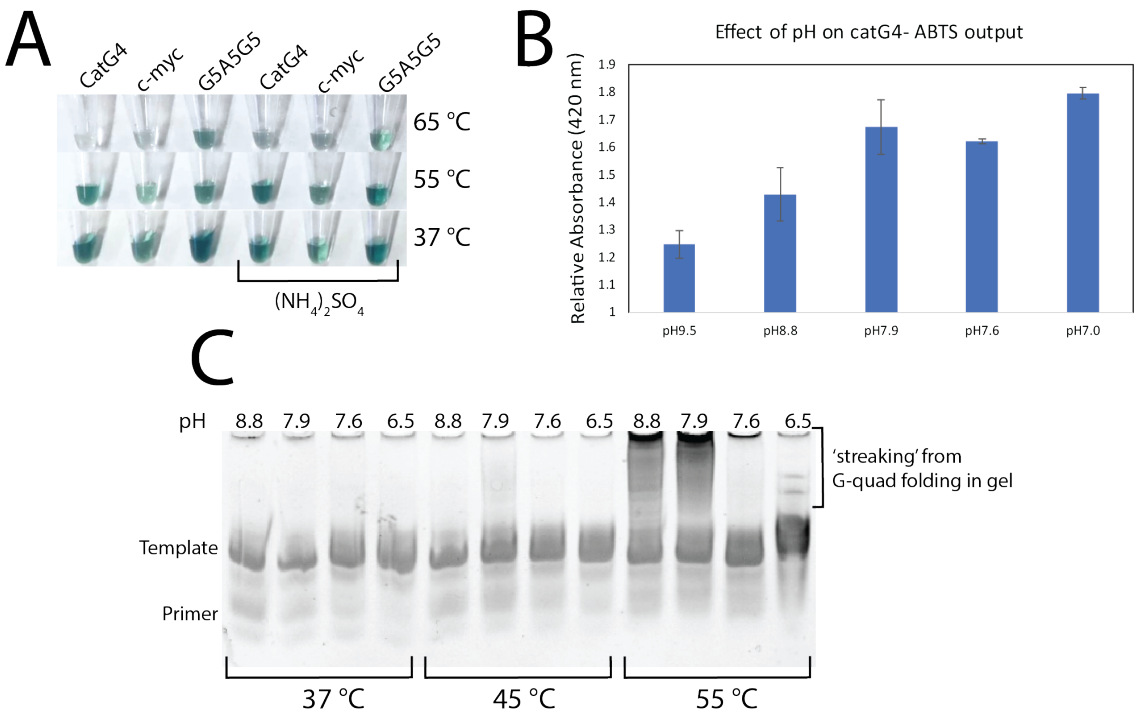

Figure 34: Testing various known G-quadruplexes in standard (pH 7.9) buffer at 65, 55 and 37 °C to determine thermal limits for their use (A). Testing CatG4 at pH 9.5 to 7.0 at 25 °C to determine optimal pH for colorimetric analysis (B). Generation of the G5A5G5 G-quadruplex from a linear template using BST 2.0 Polymerase at pH 8.8-6.5, incubated during the synthesis at 37, 45, or 55 °C before analysis with PAGE (C).

The optimal pH ranges determined from Figure 34B were then used to test the formation of the G5A5G5 G-quadruplex from a linear template (unligated RCA template with Template II splint as the primer) to ensure that the amplification mechanism operates properly in these conditions. It is important to consider that BST 2.0, the polymerase employed for extension in this case, is recommended to be used at 65 °C, with only 10-15 % efficiency at 37 °C and less than 50 % at 45 °C. Even so, a trend can be seen in Figure 33C, with pH 8.8 and 7.9 being strongly favored over the lower pH solutions near the BST 2.0 recommended reaction temperature. 65 °C was not assessed in this case because of the poor colorimetric output at that temperature.

5.3.2 G-quadruplex Generation from RCA

Having demonstrated that the G-quadruplex could be formed from the linear template, we proceeded to perform RCA on the circularized Circle II template, as shown in Figure 35A. Additionally, the RCA amplicon was nicked with Nb.BsmI during RCA due to concerns that the complex structure of the amplicon might not favor the G-quadruplex formation and existing literature indicating that G-quadruplex colorimetric output is greatly increased when isolated from the amplicon.[135] The nicking-RCA reaction was remarkably productive, generating so much DNA that the sample became cloudy in the tube and the amount of DNA product exceeded the loading capacity of the gel (Figure 34A, nicking lanes). The same reactions were run again for a shorter period of time, starting with a lower template concentration, and split in half so that they could be analyzed by both PAGE and colorimetric output, as shown in Figure 35B. All the reactions generated RCA amplicons, and the nicking enzyme reactions showed bands at higher mobility indicative of Nb.BsmI cleavage of the amplicon to release the G-quadruplex. Looking at the colorimetric outputs, the reactions without the nicking enzyme do not show significant output, possibly implying that the long amplicon makes formation of the G-quadruplex less favored. Of the reactions with the nicking enzyme, only the circle generating CatG4 has a colorimetric output, perhaps due to the design of the circle, as G5 and G4 both encode for only half of the G-quadruplex structure, while CatG4 has the entire structure in the template. The non-G-quadruplex control, NG, which is simply the Circle I template, showed RCA amplicon as predicted, and it has a slight color output consistent with background color found when hemin, ABTS, and hydrogen peroxide are mixed in solution.

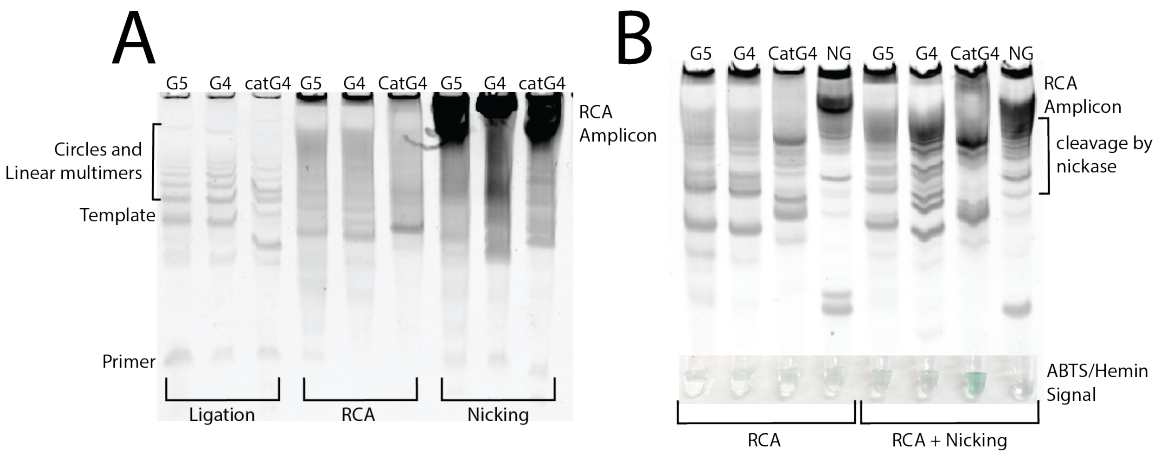

Figure 35: Ligation of an RCA template containing the complement to either G5A5G5, G4T4G4 or CatG4 and subsequent RCA at 55 °C for 2 hours in the absence or presence of Nb.BsmI, a nicking enzyme (A). RCA of the same templates, with the addition of a template (NG) that does not contain a G-quadruplex, in the presence and absence of Nb.BsmI. The outputs were analyzed after 30 minutes by denaturing PAGE and colorimetric output through complexing with Hemin and ABTS (B).

The poor colorimetric output of all RCA amplification reactions except that of CatG4, shown below the gel on Figure 35B, despite the intense bands visible in the gel, lead to the conclusion that the longer G-quadruplexes are not being generated efficiently, presumably due to competing secondary structure formed in the context of the amplicon or simply because large C tracts in the Template are complicated for the polymerase to extend through. To assist with the formation of the intended structures, 10 or 20 μM Hemin was added to the RCA mixture to potentially stabilize the G-quadruplexes that were formed. Both the PAGE gel of the RCA amplification reactions and the absorbance traces are shown in Figure 36A, demonstrating that while Hemin does have a mild inhibitory effect on the RCA, it increases absorbance output at 420 nm, so on balance it improves the assay. This increase is likely to be the result of the increased hemin concentration, as can be seen with the no DNA control that contains 10 μM Hemin and no G-quadruplex. The color is easy to differentiate by eye between the negative control and all samples containing G-quadruplexes, therefore it was deemed an acceptable background increase

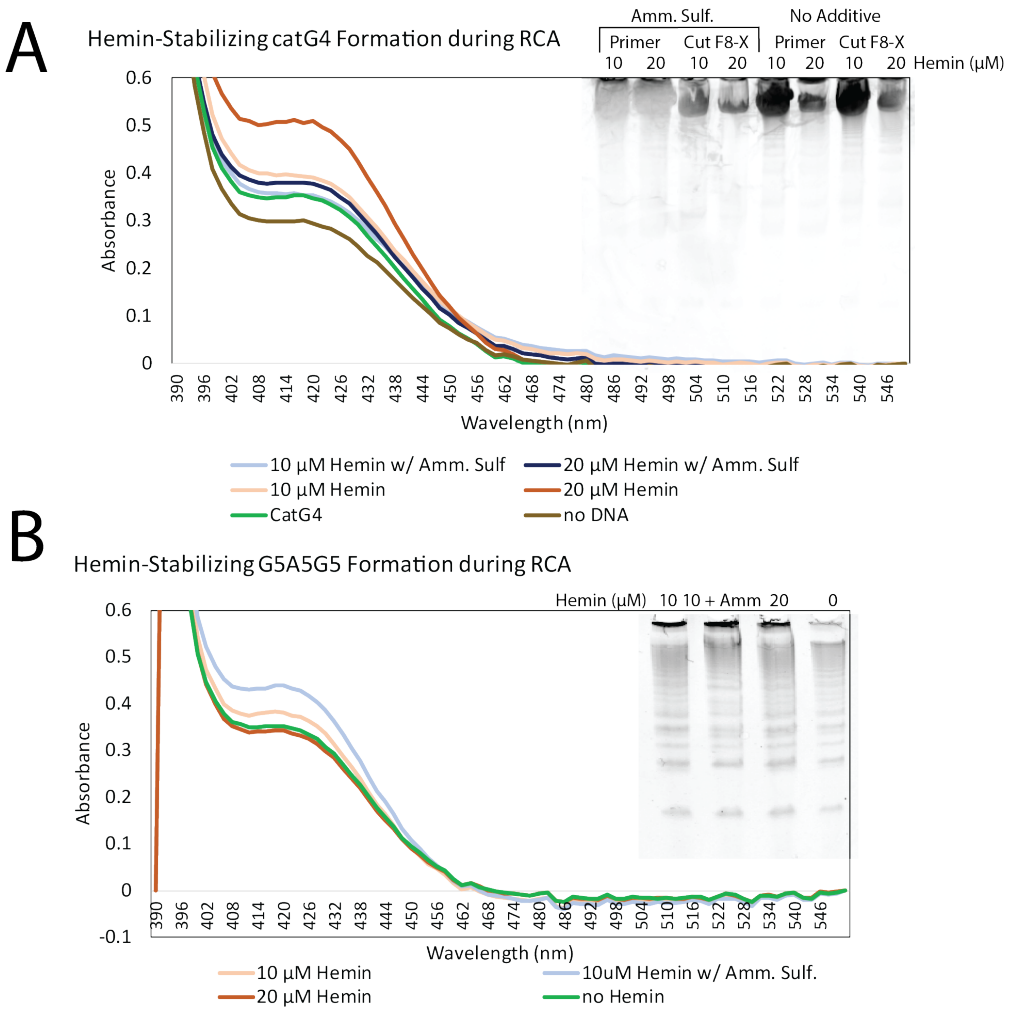

Figure 36: Stabilizing the formation of the G-quadruplexes on the amplicon using 10-20 μM hemin, with or without 10 mM ammonium sulfate, in the RCA mixture, followed by additional hemin during the colorimetric assay. RCA was performed with a primer ordered from IDT (primer) or a primer created through F8-X cleavage (cut F8-X). Only the cleaved primers are shown in the colorimetric traces (A). The addition of 10 μM hemin, 10 μM hemin and 10 mM ammonium sulfate, 20 μM hemin or the base RCA mixture to a Circle II variant that generates the G5A5G5 sequence instead of CatG4, with both absorbance scan and PAGE gel of the resulting RCA amplicon (B).

The stabilizing effect of hemin was additionally tested on a variant of Circle II whose G-quadruplex, G5A5G5 had not generated a significant amount of colorimetric signal after RCA. In Figure 36B the ABTS signal shows that the presence of hemin and ammonium sulfate increased color generation, but the PAGE gel shown as an insert in Figure 36B shows that this increase in color is due to an increased RCA output from those reaction.

One possible reason for this is that the DMSO in which the hemin stock is diluted is at a final concentration of 0.1 % in the RCA reaction, and DMSO is known to improve amplification across GC rich sequences, which is characteristic of this circle variant.[118]

The G-quadruplex generation is also demonstrated from in situ DNAzyme-generated primers, not just the synthetic primers, as in Figure 37. RCA of Circle I was incubated in 10 µM $CuSO_4$ overnight before 15 µL aliquots of the reaction were added to pre-ligated Circle II and incubated at 55 °C for half an hour. The colorimetric output of the reaction shows a clear absorbance dependence on concentration of Circle I Amplicon, though at a higher limit of detection than would be preferred.

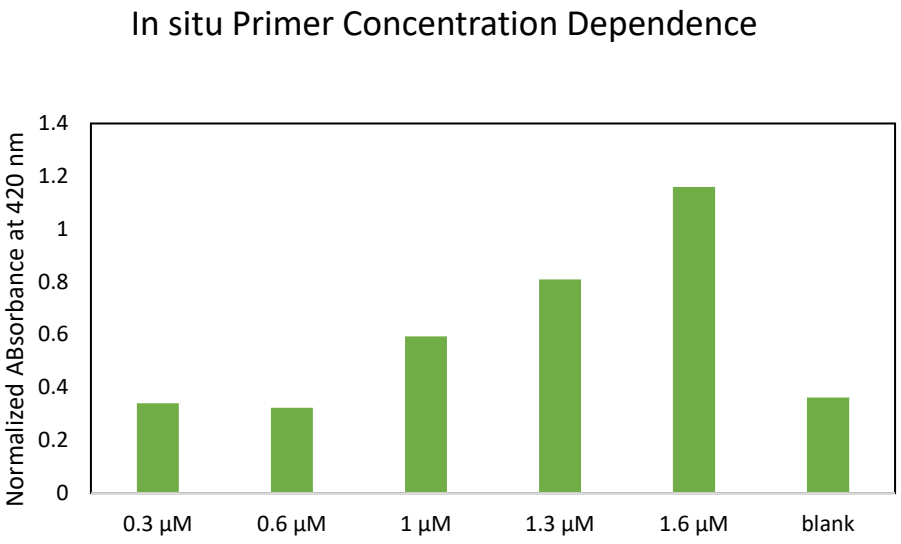

Figure 37: Concentration scale of in situ generated primer initializing Circle II RCA, visualized through endpoint ABTS absorbance. The absorbance at 420 nm is background subtracted against its baseline at 550 nm.

5.3.3 Colorimetric output optimization

As the absorbance scans in the previous section show, the background of the ABTS signal is significantly higher in the full RCA reaction. To determine the culprits for this

increase in the noise, each component of the reaction was isolated and tested in the presence or absence of a G-quadruplex, in this case 0.5 μM CatG4. As Figure 38A shows, there is a very large difference in the presence and absence of the G-quadruplex in only the reaction buffer, as was shown in the initial tests. When the necessary RCA compounds are added, as in the case of (All), there is very little difference between presence and absence, necessitating additive to regain that difference. This lack of colorimetric output could be in part due to the presence of ATP, which appears to kill any colorimetric output when added to the G-quadruplex, in a way that is comparable to the negative control (no H_2O_2). This is to be expected, as ATP is known to help protect DNA from oxidative damage by hydrogen peroxide, though this has also been reported to help amplify the colorimetric signal over long incubations.[130] dNTP and $CuSO_4$, which are also included in the RCA reaction mix (All), both exhibit an increased difference between the absence and presence of the G-quadruplex.

KCl,[147,148] ammonium sulfate[149,150] and betaine[151] are all compounds recommended to help stabilize G-quadruplexes in solution, and while ammonium sulfate and betaine do not have a marked increase in signal, KCl appears to significantly enhance the signal output. Additionally, ammonium sulfate has demonstrated the ability to stabilize non-G-quadruplex DNA and increase the signal background (not shown).

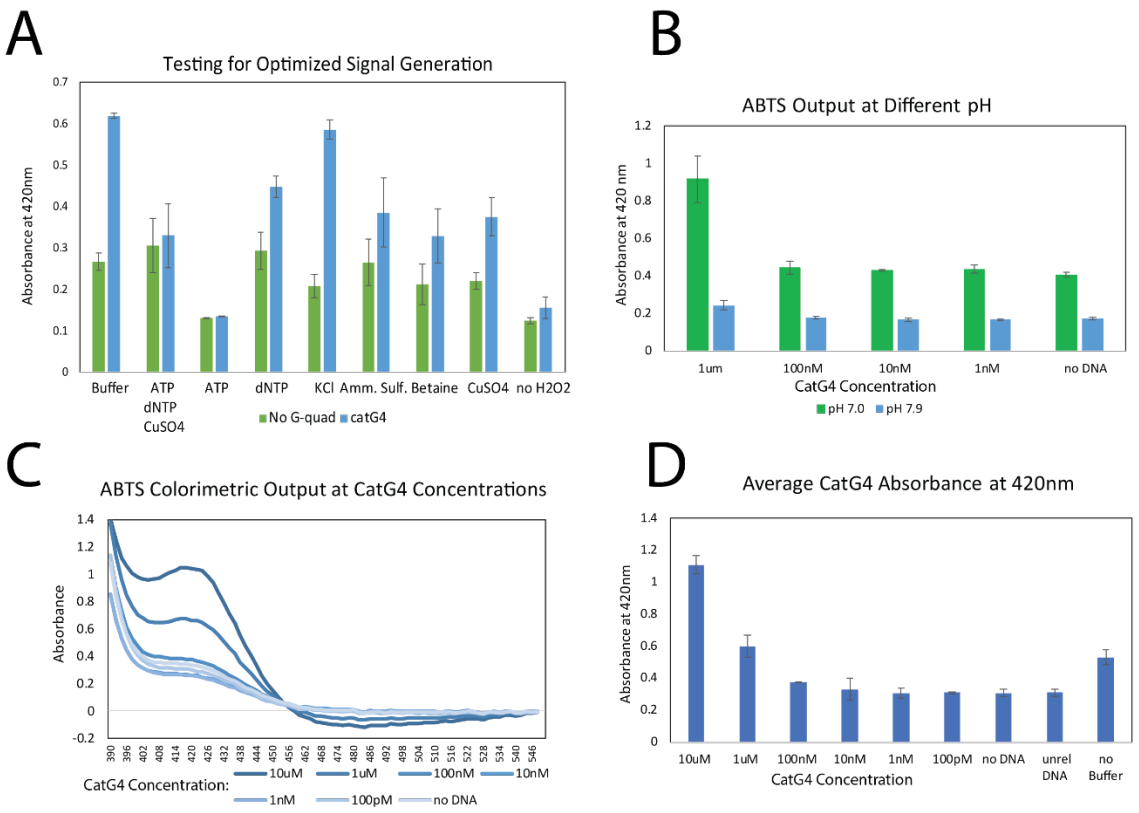

Figure 38: (A) Several compounds were tested for their G-quadruplex stabilizing and background reducing qualities, with the background subtracted absorbance at 420 nm shown. All G-quadruplex samples have 10 µM CatG4 in reaction buffer. (B) Changing to a pH 7.0 assay buffer from the pH 7.9 reaction buffer increases the colorimetric output of the G-quadruplexes. (C) Demonstrating the quantitation and limit of detection of the ABTS-hemin colorimetric output. The full absorbance scan of the colorimetric output is shown, baseline adjusted to zero absorbance at 550 nm. (D) The absorbance at 420 nm of an extended CatG4 concentration range is shown separately, demonstrating the background intrinsic to the reaction. Of note is the no buffer control showcasing that the buffer, and particularly KCl, is instrumental in decreasing the background absorption.

While the pH changes discussed earlier are important for the performance of the enzymes in the reaction, the alkane layers allow for the introduction of a separate buffer system exclusively for colorimetric quantitation. Figure 38B demonstrates the difference that simply changing from a pH 7.9 to a pH 7.0 reaction buffer, keeping everything else the same, generates. It is clear, however, that the background is also increased with this change, as 100 nM CatG4 and below all register at or near the blank. To more fully test the limits of quantification, the colorimetric output of a broader range of concentrations of

CatG4, 1 μM to 100 pM, was tested (Figure 38C and D). The significant background interference from the uncatalyzed reaction of ABTS and hydrogen peroxide is still present, but consistent.

5.3.4 RCA in layers

The assembly of the reaction inside the alkane layers requires two considerations, the first of which is the order of addition of the components. The key factor in this reaction is that it will be sitting without any agitation in a slowly warming water bath, so components must be layered in an order that allows for appropriate passive mixing. This relies largely on the fact that the alkanes used have lower densities than the aqueous phase, ranging from 0.77 to 0.79 g/cm^3. Therefore, upon melting, the alkane will migrate to the top of the liquid region, causing the aqueous reaction components to drop down and mix with the newly exposed layer. Additionally, the volumes of some of the aqueous layers are very small; enzymes in particular are kept in a minimum volume (maximum concentration) to minimize the extent of denaturation. The enzyme layer is thus placed above the larger reagent sections so that it released more effectively into the reaction mixture, especially due to its glycerol content. The arrangement of the layers is shown in Figure 39A.

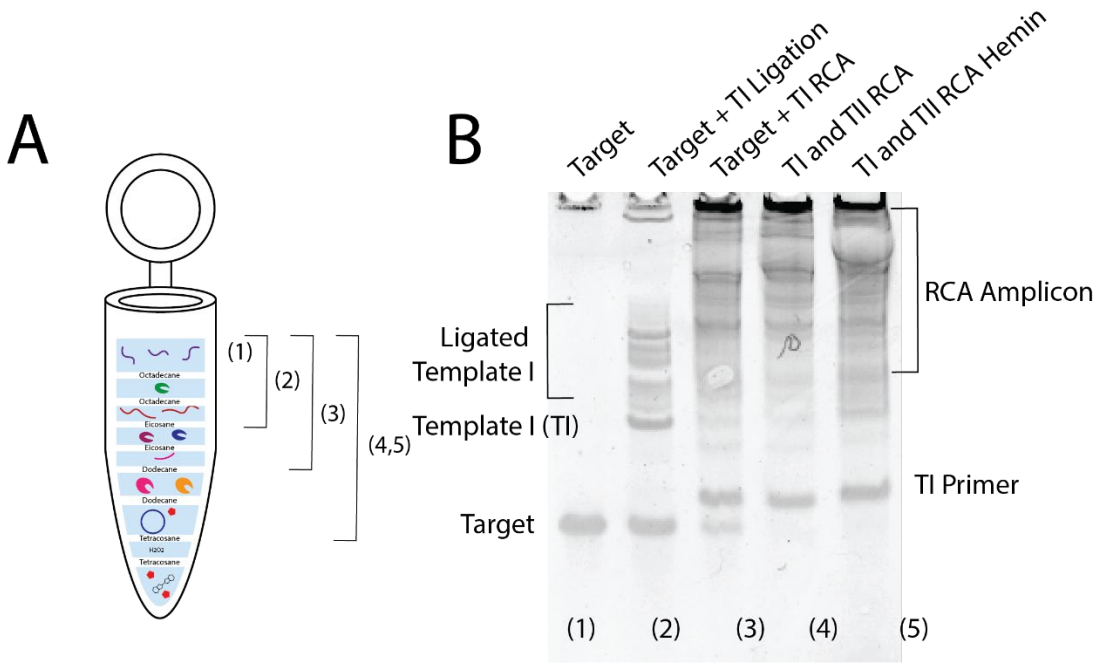

Figure 39: The order of layer assembly with the different wax layers identified (A) and a demonstration of the sequential melt layers on PAGE gel (B). Numbers on the gel correlate to the different stages of assembly indicated in (A).

In Figure 39B, successful stepwise RCA upon sequential melting of the layers is demonstrated. The reaction was performed with layers built in an Eppendorf tube that was then placed in a 30 °C water bath and slowly heated to 55 °C over the course of an hour. For example, the ligation of Template I (2) would only have the first 3 layers built in the tube, (3) would have the first 5 layers assembled, and the aqueous layer would be collected upon the reaction reaching 42 °C and 48 °C respectively. The samples were analyzed by PAGE, starting with the target DNA alone (1), followed by the Template I ligation step (2), its RCA amplification using Klenow (exo$^-$), that is 100 % active at the melting temperature of eicosane, and the formation of primers for the amplification of Template II (3). A second cycle of RCA is then performed in (4-5) with BST 2.0 as the polymerase, as it is optimally active at 50-55 °C and thus can form the G-quadruplexes for later quantitation. The increasing volume of each subsequent reaction, as well as the presence

of an active polymerase and nicking enzyme simultaneously, makes the 3rd and 4th/5th stage reactions appear comparable, despite the additional RCA cycle.

When the oxidation of ABTS was assayed in these layer reactions, there was a very faint color formation as compared to control reactions (not shown). It was theorized that the heating during the reaction causes decomposition of the hydrogen peroxide prior to its exposure to the hemin/G-quadruplex catalyst. Increasing the concentration of hydrogen peroxide tenfold was tested without effect, shown in Figure 40A. Upon extraction of the colorimetric mixture for quantification, it was noticed that the lower 2-3 millimeters of alkanes were saturated green with ABTS, indicating that a fraction was lost to the discretization medium. The ABTS and hemin concentrations were increased 2- and 3-fold respectively, resulting in increased absorbances across the board (Figure 40B), including in the negative control that is just buffer and an unrelated DNA. The increased ABTS colorimetric output in the RCA and G-quadruplex assays eclipse that of the negative control in the presence of 40 and 60 μM Hemin, with the difference in the RCA and CatG4 being due to the need to assemble the G-quadruplex in the complex system. The 40 μM hemin and 12 mM ABTS concentration was selected to move forward as it had the greatest difference between negative and positive absorbances, as reducing the background is paramount to this assay.

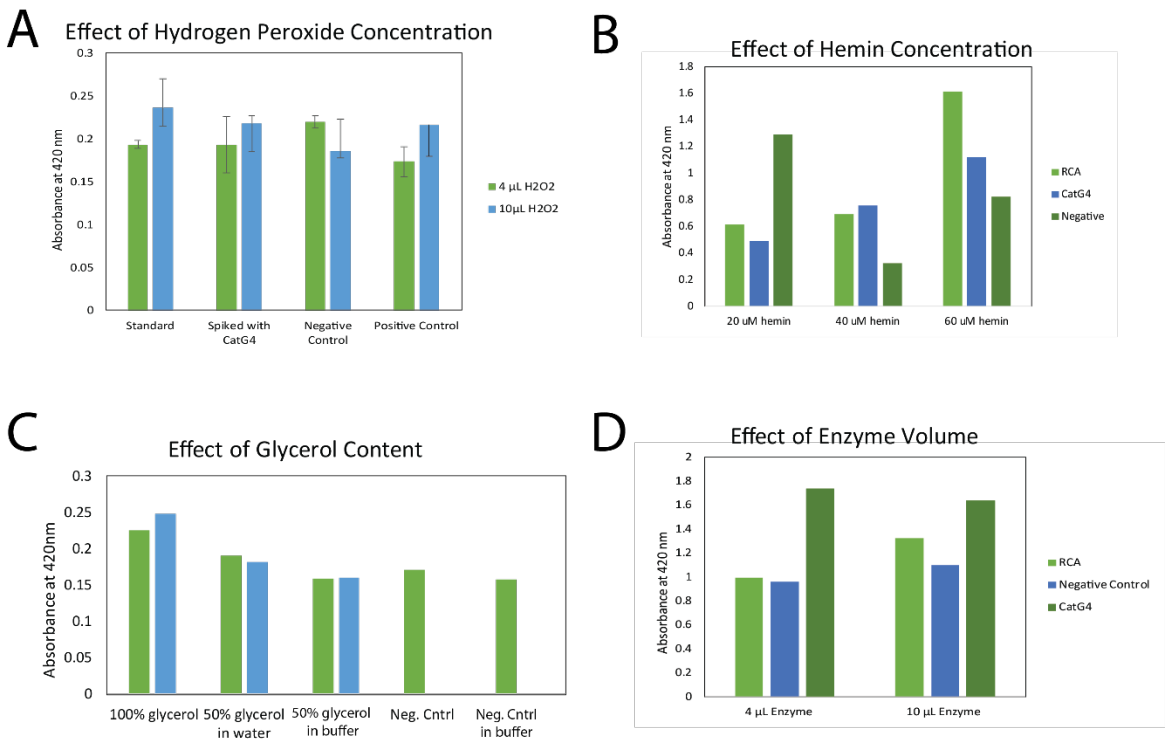

Figure 40: Optimization of the hydrogen peroxide addition by depositing 4 or 10 µL of 2 mM hydrogen peroxide in water (A). 20-60 µM of hemin and 4-10 mM of ABTS were tested to increase the output difference between negative and G-quadruplex positive samples (B), as well as varying the enzyme solution' glycerol composition (C), and either depositing 4 or 10 µL of the 100 % glycerol enzyme solution (D) in the layered reaction.

During the addition of the enzymes to the layers during assembly, they are deposited on cool wax to minimize denaturation, but it is impossible to avoid the subsequent addition of hot wax to seal the enzyme layer. There is extensive literature on how to prevent heat shock to enzymes, and it has been shown repeatedly that increased glycerol content helps prevent heat shock[152–154] while also reducing protein aggregation at high concentration.[155] Due to the high temperature and small volume the enzymes are subjected to in this assay, 50 % and 100 % glycerol were used to stabilize the enzymes during addition. In Figure 40C, the second half of the bicyclic reaction was run with the BST 2.0 and Nb.BsmI stabilized by either 100 % glycerol, 50 % glycerol, or 50 % glycerol with 1X reaction buffer during layer assembly, with the addition of negative controls (lacking enzymes) to control for

inactivation of the enzymes. It was found that the 100 % glycerol helps retain enzyme function the most, shown in Figure 40C, resulting in the best yield of G-quadruplex and thus the highest colorimetric output at 420 nm. Additionally, upon increasing the volume of enzyme from 4 μL to 12 μL, as shown in Figure 40D, apparently enough enzyme survives the alkane deposition to give an RCA reaction that is no longer comparable to the negative control.

The whole reaction, whose assembly is shown in Figure 41A, was tested by slow incubation in a gradually warming heat bath (32 °C to 55 °C over the course of 1.5 hours). Once the reaction was complete, the combined wax layer was allowed to cool before the aqueous layer was collected and its absorbance was quantitated on a microplate reader. During the cooling process, it was noted that a gradient of green was consistently found in the tubes, with the most intense color seen in the wax-liquid interface. When the aqueous layers were collected and analyzed, the absorbance at 420 nm was frequently uniform across all samples, as can been seen in the four reactions shown in Figure 40B. The full reaction, a reaction that was run without the Target sequence, and a G-quadruplex containing positive control reaction all gave the same absorbance in the layer format, despite having been shown to catalyze ABTS oxidation at different rates in solution.

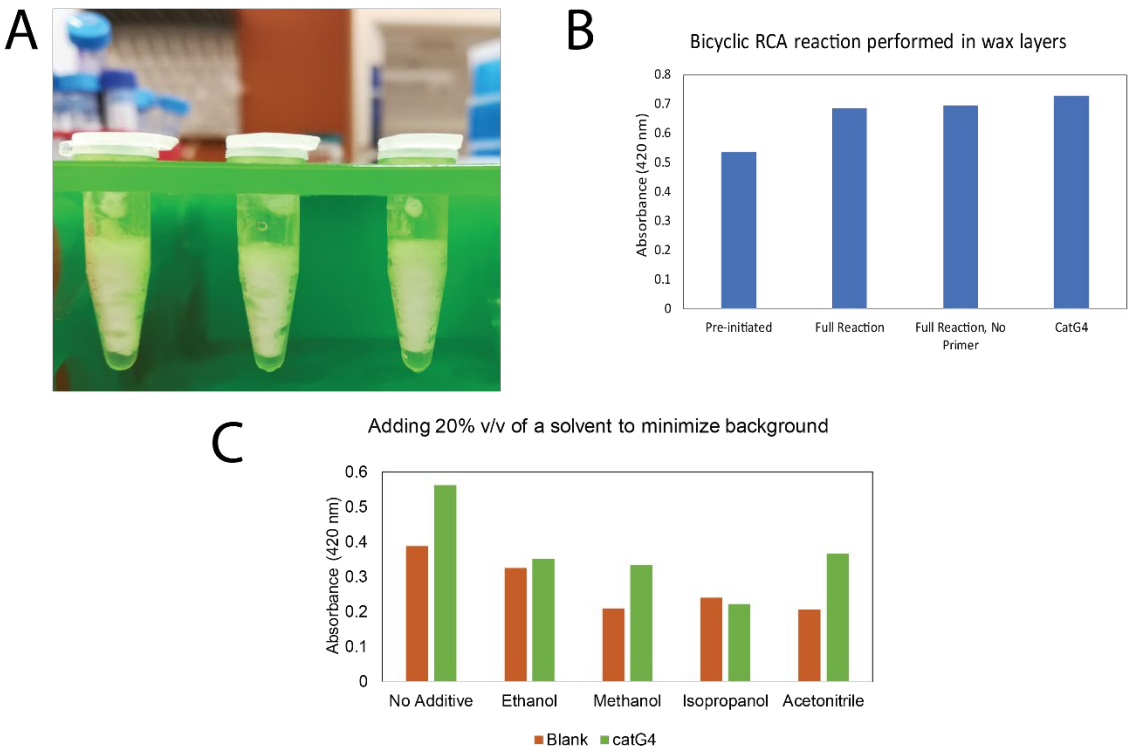

Figure 41: Photograph of the prepared alkane layers prior to target addition and melting (A). ABTS output from a pre-initiated reaction (Circle I ligated ahead of time), the full reaction in the presence and absence of the Target, as well as a reaction supplemented with 0.1 µM CatG4 (B). Significant improvement is then observed upon the addition of 20 % v/v organic solvents to the Hemin-ABTS layer (C). Background subtraction was done by subtracting the absorbance at 550 nm from that at 420 nm.

This background signal issue with the full reaction is potentially due to the hydrophobicity of ABTS, or potentially a consequence of the amount of time the reaction is kept at an elevated temperature, as it has been stated in literature that heating increased the chance that it might bypass the G-quadruplex and react with the hydrogen peroxide directly.[156] To optimize this, 20 % v/v organic solvents were added to the colorimetric detection buffer to help the background remain low,[157] as shown in Figure 42. When analyzing the results, we were looking for the two that had the greatest different between the blank and the G-quadruplex, as detection by eye is benefitted by having a larger color difference. Methanol

and Acetonitrile had the largest differences, and additionally helped prevent visible absorption of the ABTS into the wax layer that was believed to increase background.

The best performing solvents were then tested with the pre-prepared Circle I amplicon, prepared similarly to the FRET tests. As can be seen in Figure 42A, the RCA reactions had much higher signal than the background, and in the case of acetonitrile, we see a consistent dependence of the initial target concentration with the end absorbance of the ABTS. The addition of Hemin in the RCA stage of the reaction doesn't appear to help with the formation of the G-quadruplexes, as there is no discernable absorbance difference between the two sets.

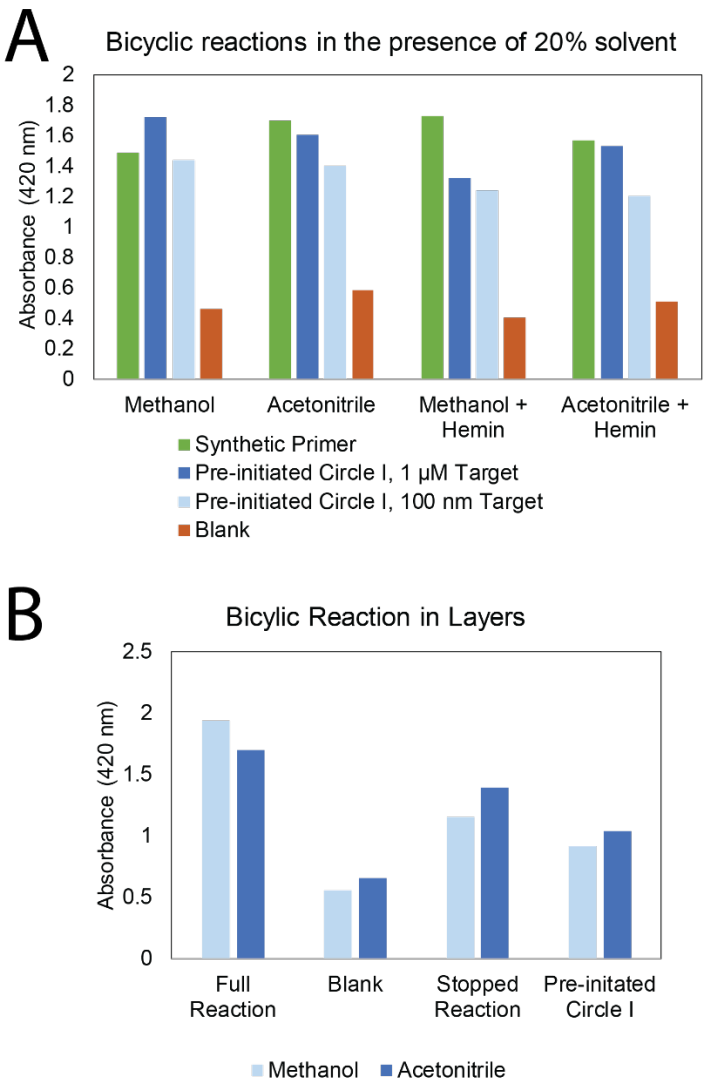

Figure 42: Bicyclic reaction performed in layers from pre-incubated Circle I RCA Amplicon or synthetic Circle II primer (A). Full bicyclic reaction performed in layers, either melted in one go (full) or stopped at the $CuSO_4$ stage and left to cleave overnight before continuing (B). Background subtraction was done by subtracting the absorbance at 550 nm from that at 420 nm.

The same test was then performed on the full reaction, with the layers assembled the same as in Figure 41, but with the exception of the additional 20 % v/v methanol or acetonitrile. The reaction was heated in a water bath from 35 °C to 55 °C over the course of an hour and a half for the full reaction and the blank. The 'Stopped' reaction was heated from 35 °C to 42 °C over the course of half an hour before being removed from the water bath for 16 hours to allow the RCA reaction and copper ion mediated cleavage to happen

slowly. The tube was then placed back at 42 °C and slowly ramped up to 55 °C over the course of an hour alongside the pre-prepared Circle I control. The background-subtracted absorbances are shown in Figure 42B.

The full reaction performed well, generating a large amount of G-quadruplex during just the 1.5 hours of the temperature ramp up. Even more importantly, the blank, which is identical to the full reaction but lacking any Target DNA, showed very low signal in both solvents. The stopped reaction also generated an absorbance above the blank, which is good because it shows that the enzymes can be kept functional as long as they are in the layers, allowing for the assay to be shipped at room temperature for short periods of time. There is significantly less output than in the full reaction, so likely some enzyme denatured.

5.4 Conclusion

This chapter demonstrated the development of a multi-pot reaction performed in one Eppendorf tube without the use of manual steps, using separately meltable alkane layers to enable sequential mixing of reaction components. The duration of each stage of the reaction can be modulated through heating at a controlled rate to control melting of different layers. The platform allows for slight changes in the reaction buffer to optimize discrete steps. To date, however, a high background signal remains a significant hurdle, as the ABTS reagent tends to partition into the melted wax, potentially oxidizing the ABTS in the process and resulting in a significant absorbance reading. Further work to help improve the signal through optimization of the composition of the ABTS solution to retain the molecule in the aqueous phase would allow for the application of this assay as a low-resource diagnostic.

6
Significance of Results and Future Prospects

Point of care (PoC) and clinical settings are increasingly dependent on low-cost minimal resource diagnostic tests, with DNA amplification techniques being in the forefront of this biosensor revolution. In this dissertation, a bicyclic amplification scheme using a DNAzyme to generate primers in situ for a second round of RCA was demonstrated. This was done through first analyzing the existing literature on amplification techniques (Chapter 1) and DNAzymes (Chapter 2) before testing four DNAzymes for their potential application to the bicyclic assay (Chapter 3). The bicyclic assay was then tested with a FRET-probe readout (Chapter 4) as well as producing G-quadruplexes for colorimetric signal generation (Chapter 5). The assay was additionally performed as a multistep, one-pot technique through the use of meltable wax layers that mix reagents sequentially (Chapter 5).

6.1 Development of a one-pot bicyclic nucleic acid amplification assay using DNAzyme-generated primers for Rolling Circle Amplification

Chapter 3 detailed the process by which DNAzymes were vetted for in situ primer generation. Chapter 4 demonstrated the design of an isothermal, one-pot, bicyclic RCA amplification assay that can be used to detect single stranded DNA or RNA targets, the scheme of which is shown in Figure 25. The scientific contributions of these chapters are as follows:

- Quantified the feasibility of using 4 different classes of DNAzymes to generate primers from an RCA amplicon in a complex reaction mixture.

- Demonstrated a rapid, sequence specific single stranded DNA detection scheme that uses bicyclic RCA to achieve polynomial amplification.
- Demonstrated that autocatalytic generation of RCA primers using a DNAzyme allows a non-enzymatic mechanism to improve the amplification provided by an RCA reaction.
- Obviating buffer changes or purification steps during the assay is an improvement over related work, in which incompatible buffer systems require purification of products or dialysis to proceed to the subsequent stages.
- The completely isothermal procedure presented here is advantageous for PoC applications, as opposed to other amplification assays that contain a melt step.

This assay will need to be further refined to see application in the field; in particular, the current overnight timeframe for detection does not yet provide the desired PoC 30-minute timescale. Optimization of the DNAzyme cleavage reaction should help to reduce this time significantly: the challenge is that the specificity of the DNAzyme cleavage and the stability of the reagents must be maintained while increasing the speed.

The assay is also designed to allow for multiplexing, to be able to detect multiple different targets in the same tube. This is especially useful with virus families, as in the flavivirus family encompassing Zika, Dengue, West Nile, Yellow Fever, etc. These are all mosquito-borne diseases that share the same infection hotspots, so a test that could detect each of them separately and simultaneously would reduce the equipment burden on clinics. As illustrated in Figure 43, this assay was designed to be very simple to alter for a new target sequence. A pair of Circle I and Circle II sequences can be redesigned quickly for

each target of interest, and they should support bicyclic RCA in solution with no crosstalk, as early tests have shown in Figure 43C.

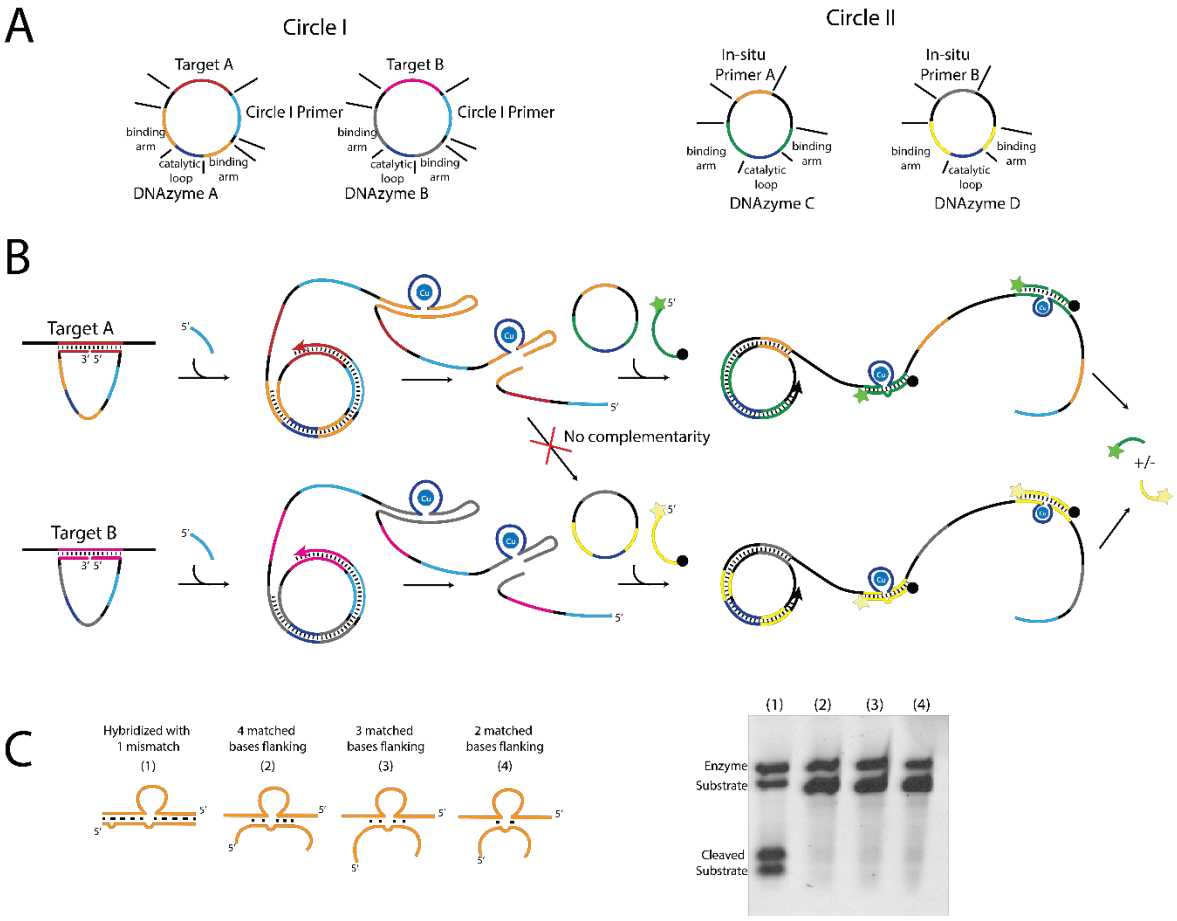

Figure 43: Proposed multiplexing of bicyclic RCA. The design of the Target I and II detection circles is shown (A) as well as a scheme demonstrating the parallel reactions with no consensus sequences, allowing for both targets to be detected in a single reaction with no crosstalk. Separate FRET probes designed with different fluorophores are used to quantitate which, or both, of the Targets are present in solution (B). Previous work testing the sequence specificity of the DNAzyme is shown in (C) with the arm sequences varied to have only a certain number of matched bases flanking the cut site.

6.2 Integration of an amplification multi-step assay into a one-pot, hands-free system

Chapter 6 detailed the development of a minimal-handling colorimetric test for the presence of target single stranded DNA or RNA, through merging the bicyclic RCA system with G-quadruplex synthesis and ABTS oxidation. The G-quadruplex is generated in the

second RCA, and activates the reaction of ABTS with added hydrogen peroxide. To manage the destructive effect of hydrogen peroxide on the other reagents, as well as to allow for long term storage of sensitive assay components like enzymes, the reaction components were separated by pure alkane waxes that can be melted sequentially by placement in a water bath and slow heating. The intellectual contributions of this part of the work are as follows:

- Optimized layer volumes and deposition techniques for future phase-change projects.
- Analyzed the compatibility of RCA system with the wax layers.
- Tested a variety of signal generation modalities for both real-time and endpoint quantitation of G-quadruplexes.
- Combined the RCA and G-quadruplex detection to develop the first one-pot, hands-free detection system for quantitation of a target oligonucleotide through chromogenic ABTS oxidation.

Deployment of this assay will require improved storage stability and automated deposition of layers. Currently the assay components must be refrigerated prior to use. To alleviate this requirement, future work can incorporate lyophilization of a simpler layered assay to reduce loss of activity of the enzymes long term. Previous work in the lab has demonstrated that lyophilization was possible on a smaller layered assay, and there was no loss of activity.[8]

Another possibility is to convert the assay to a paper-based modality, with the potential for quantification via paper SERS. Previous work in the White lab has shown that

fluorescently labeled short DNA can be mobilized through paper chromatography and quantified,[158] and lateral flow systems have also been developed to deposit the SERS-active molecules on a nanoparticle bed.[159] These techniques could be used to transfer the cleaved fluorescent or colorimetric DNAzyme cleavage products onto a detection strip.

6.4 Future Directions – Expansion to double stranded nucleic acids

The assay as it currently stands is designed to detect exclusively naturally single stranded DNA and RNA. Single stranded oligonucleotides are an easier target for detection, especially when trying to keep an assay isothermal, but we would like to broaden our range of targets to include genomic DNA or highly structured RNAs, two areas of significant interest in the biosensing space.[160] We propose a possible plan that uses Peptide Nucleic Acid (PNA) or Locked Nucleic Acid (LNA) brackets to open a single stranded pocket in the helix of a double stranded target, allowing for Circle I to hybridize and ligate. This proposal is shown in Figure 44 below.

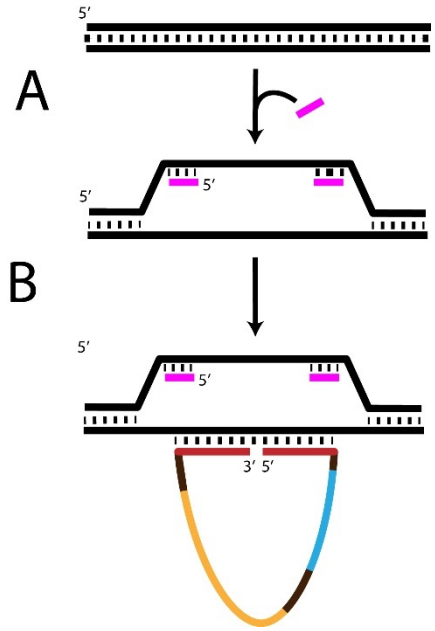

Figure 44: Proposal for opening the dsDNA helix using strand invasion by short PNA or LNA brackets (pink). The PNA or LNA brackets invade the dsDNA helix due to their higher binding affinity (A), thus allowing Circle I precursor to hybridize and ligate (B).

The use of PNA or LNA, due to their higher affinity for DNA than DNA has for itself,[161,162] would allow the brackets to invade the double stranded helix as it undergoes DNA breathing.[163] The use of PNA and LNA as strongly hybridizing alternatives in toehold invasion techniques is not new, and the concept is similar to this proposed work.[164,165] The implementation of this strategy will allow us to broaden the range of possible targets, and increase the impact of this technique.

6.5 Final advice for others embarking on PoC DNA amplification assay design.

During the course of this assay's development, several key problems were overcome. In this section I will try to impart some of the more useful lessons on PoC amplification design for anyone attempting a similar concept in the future.

When generating primers in situ in a reaction mixture, the resulting 3′ end is very significant, as primer extension strictly requires a 3′ hydroxyl. This thesis tested all four mechanisms of DNAzyme cleavage primarily by happenstance, but each one was additionally tested extensively with a range of polymerases to establish if a 3′ end cleanup was necessary, and if so, how to go about it. In the same vein, the polymerase used is also very significant, as results were made immensely more complex using polymerases that are highly active to the point of generating significant non-specific amplification (BST 3.0). Less processive polymerases (BST 2.0, Klenow (exo$^-$), and φ29) are strongly preferred for both the specificity of the assay as well as the comprehensibility of the data.

Secondary structure is complicated and will get in the way of everything. Keep things as unimolecular and as short as possible. Initially Circle I was designed to be 100 bases long, but it became clear relatively quickly that this length allowed for significant secondary structure formation in the circle, even when ligated. Due to the fragile nature of many DNAzymes' structure, this prevented their formation. The circles are now designed with a minimal sequence in mind, containing exclusively the splint and DNAzyme sequences with the occasional 5-6 base spacer as necessary between functional elements. Additionally, due to the fragility of the DNAzyme structures, keeping them unimolecular significantly increases the likelihood that the DNAzyme will actually fold into its catalytic form, as well as cuts the cleavage time.

One-pot reactions are difficult to orchestrate primarily because all components are present simultaneously, and great care much be taken so that they do not interfere with each other. It was additionally found during the course of this thesis that the different cofactors and stabilizers not only had detrimental effects that needed to be mitigated (zinc

is unpredictably insoluble, and copper ion mildly quenches FAM fluorescence for example) but also additional benefits that were unexpected (DMSO helps unfold G-blocks for the polymerase, as well as increasing color output). Extensive research into the potential impact of an additive on each step of the reaction assists in deciding whether to keep an additive that has a minor effect in one isolated stage, but a significant effect in another.

Appendices

List of Sequences

Table A1: List of DNA Sequences used	
Sequence Name	Sequence (5′→3′)
Universal Sequences	
Circle I Long Splint	TAATCAAGTA CACATACCAA AACAAAGTGG TAAAGGTCCT
Circle I Short Splint	TAATCAAGTA CACATACCAA AACAAAGTGGT
Circle II splint	CCTGTTCATCTTGCATTCGAGTA
Primer I	TTTTTTATGACCATAGGACA
3.2.1: 10-23	
10-23 Enzyme	CGCACCCAGGCTAGCTACAACGACTCTCTCC
10-23 Substrate	GGAGAGArGrArUrGGGTGCG
10-23 Substrate Ext	TCGATGTGGAGAGArGrArUrGGGTGCGAGCTC
10-23 Circle I	/5Phos/TTGGTATGTGTAGTTCTTAAAAAGAGGCCCAGACTCATTCTGAGTC GTATTAGAATTCGGAGAGAGTCGTTGTAGCTAGCCTGGGTGCGACCACTT TGTT
10-23 Circle I short	/5Phos/TTGGTATGTGTAGGAGAGAGTCGTTGTAGCTAGCCTTGGTGCGAGC TCACCACTTTGTT
10-23 Circle II	/5Phos/AAGATGAACAGGGGCCTCAAAATGTAGAACTACTTTGCGAGACTT TCAGTGTGGATCTCTCTCCACATCGATCGTTTCTACTCGAATGC
10-23 Circle 3′ end	GAGCTCGCACCCAGGCTAGCTACAACGACTCTCTCCTTACGAGTATTTAC ACATACCAA
10-23 Circle 5′ end	AACAAAGTGGTTATTTATGACCATAGGACAGTAACGTAGTTGAGCTCGCA CCCAGGCTAGCTACAACGACTCTCTCC
Interfering DNA	ACTACGTTACTGTCCTATGG
3.2.2: I-R3	
I-R3	GTAACGTAGTTGAGCTGTCACAGAATGTGACGTTGA^AGCGTTAC
I-R3 Circle I	/5Phos/TTGGTATGTGTAAATACTCGAATGCTGTAACGCT^TCAACGTCACA TTCTGTGACAGCTCAACTACGTTACTGTCCTATGGTCATAAATAACCACTT TGTT
I-R3 Circle II	/5Phos/ATTCTGTGACGGCCTCAAAATGTAGAACTCTCGTGCTGTGATGTGG AGACTAAGTAAAACATTTGCTGTTCTTATTTCTCAACGTCAC
3.2.3: 46mer	
46mer	GAATTCTAATACGACTCAGAATGAGTCTGGGCCTCTTTTTAAGAAC

46mer Circle I	/5Phos/TTGGTATGTGTAAATACTCGTGTTCTTAAAAAGAGGCCCAGACTCATTCTGAGTCGTATTAGAATTCTACTGTCCTATGGTCATAAATAACCACTTTGTT
3.2.4: F8-X	
F8-X Full	GAAAGTCTGCACACCGAATCGGTGTGTGGATGCCGGGTCCGACTTTCAGTGA
F8-X Substrate	GAAAGTCTGCACACCGA
F8-X Enzyme	TCGGTGTGTGGATGCCGGGTCCGACTTTCAGTGA
F8-X Circle I Full	/5Phos/TTGGTATGTCACTGAAAGTCGGACCCGGCATCCACACACCGATTCGGTGTGCAGACTTTACTTTGTT
F8-X Circle I ES	/5Phos/TTGGTATGTTCTACACTGAAAGTCGGACCCGGCATCCACACACCGATTTACTACTTTGTT
4	
F8-X Full	CGAATTAGAAAGTCTGCACACCGAATCGGTGTGTGGATGCCGGGTCCGACTTTCAGTGA
Target	TAATCAAGTACACATACCAAAACAAAGTGGT
F8-X precut primer	ACGAATTAGAAAGTC
Template I Splint	ACATACCAAAACAAAGT
Template I	/5Phos/CGATCGTTGCAGTGTAGAACGGACCCGGCATCCACTCGACTGAGTCCTCAGTCGAGCAGTTCTACACTGTCCGACGA
Template II Splint	CGAATTAGAAAGTCCGAATTAGAAAGTCTTTTTTTT
Template II G Version I	GACTTTCTAATTCGTCGAATGTTTTTCCCCAAAACCCCTTTTTGACTTTCTAATTCG
Template II G Version II	GACTTTCTAATTCGTCGAATGCTTTTTTTTCCCAACCCGCCCTACCCATTTTGACTTTCTAATTCG
Template II G Version III	GACTTTCTAATTCGTCGAATGCTTTTTTCCCCCTTTTTCCCCCTTTTTGACTTTCTAATTCG
Template II F8X	TTGGTATGTTCTACACTGAAAGTCGGACCCGGCATCCACACACCGATTTACTACTTTGTT
F8-X Substrate Ext	CTACACGAAAGTCTGCACACCGATTTA
FRET Probe	/56FAM/CTACACGAAAGTCTGCACACCGATTTA/3BQH-1/
5	
CatG4	TGGGTAGGGCGGGTTGGGAAA
c-myc	GAGGGTGGGGAGGGTGGGGAG
AG5A5G5A	AGGGGGAAAAAGGGGGA

TG5T5G5T	TGGGGGTTTTTGGGGGT
AG4A4G4A	AGGGGAAAAGGGGA-
TG4T4G4T	TGGGGTTTTGGGGT
Template II G5	GACTTTCTAATTCGTCGAATGCTTTTTTCCCCCTTTTTCCCCCTTTTTGACTTTCTAATTCG
Template II G4	GACTTTCTAATTCGTCGAATGCTTTTTTCCCCTTTTCCCCTTTTTGACTTTCTAATTCG
Template II CatG4	GACTTTCTAATTCGTCGAATGCTTTTTTTTCCCAACCCGCCCTACCCATTTTGACTTTCTAATTCG
Template II Splint	CGAATTAGAAAGTCCGAATTAGAAAGTC
Template I	/5Phos/TTGGTATGTTAGAAAGTTCGGACCCGGCATCCACACAGGCATGTGCCTGTGCAGACTTTCTAACTTTGTT
Template II Splint Tail	CGAATTAGAAAGTCCGAATTAGAAAGTCTTTTTTTT

Table A2: List of DNAzyme Sequences (5′→3′)

DNAzyme	Enzyme (Catalytic) Strand	Substrate (Cleaved) Strand
8-17[33]	NNNNTCCGAGCCGGACGANNNN	NNNNNrG^NNNN
10-23[49]	NNNNAGGCTAGCTACAACGANNNN	NNNNUrA^NNNN
GC DNAzyme[54]	NNNNCGGCCCGCGGCGCGANNNN	NNNNTrG^GGNNNN
S4[60]	NNNNCTAGGGTGGGGTTAGAGTGGANNNN	NNNNTrU^CGTGNNNN
S9[60]	NNNNCTACTGCTTTACTGGCGGCCANNNN	NNNNTrC^CGTGNNNN
S21[60]	NNNNAGTATATCAAGTGAATGGCANNNN	NNNNTrC^TGTNNNN
EtNa[59]	NNNTTCTCACAGCGTACTCGCTAAGGTTGTNNNN	NNNNTrA^TTNNNN
G3[71]	NNNNGGGACGAATTCTAATACGACTCACTATrA^GGAAGAGATGGCGACAACTCTTTACCCAAGAAGGGGTGCGTACTATGCTACCTTATTAACGTGACGGTAAGCTTGGCACCNNNN	
NaA43[72]	NNNNCAGGTCAAAGGTGGGTGAGGGGACGCCAAGAGTCCCCGCGGTNNNN	NNNNTrA^GGAANNNN
Ce13d[57]	NNNNAGGTGAAAGGTGGGGTGCGAGTTTTACTCGTTNNNN	NNNNrA^GGAAGNNNN
E6[58]	NNNNCAGCGATCCGGAACGGCACCCATGTNNNN	NNNNTrA^GGNNNN

CT10.3.29M[61]	CAAATGATCGGTGGGTAGCAACTGAAAGGCGGTTGCAATGCGGATGGATTGTACGGTC	GTCCGTGCTrU^TGGTTCAATTTG
S15[60]	NNNNAGTATATCAAGTGAATGGCANNNN	NNNNTrC^TGTNNNN
DZ1[70]	NNNNCTGGTACCGACTTATGGTCCTCCATAACATCGGGCTATGCGTANNNN	NNNNYGCYrU^TGGNNNN
DZ7[70]	NNNNGGCACGGCGGGGTCCTATGTGGAGACACCTTTAGGTAATGTGTGTANNNN	NNNNTGCYrG^YGGTTCNNNN
Ag10C[62]	NNNNTAGGTGATTTCCACGATTATGCGGAAACAGGGCAGCGTNNNN	NNNNrA^GGNNN
E_{Hg}0T[63]	NNNNTGTCGGGAAACCGACCTTCGACANNNN	NNNNTrA^GGAANNNN
39[64]	NNNNTGCAGTCGGGTAGTTAAACCGACCTTCAGACANNNN	NNNNArA^GGAANNNN
GR5[65]	NNNNTGAAGTAGCGCCGCCGTANNNN	NNNNArA^GGAANNNN
DEC22-18[67]	NNNNCGTTGTCATTGGCACACGGAGGTTTACTGAGTGGTAACCACGTAGCATGNNNN	NNNNCGTGCFrA^QGGTTCGNNNN
MgZ[68]	NNNNCAGGTCGGGGCCGAAATATAGGATATTTTGGGAGGCTATGNNNN	NNNNCFrA^QGNNNN
5J-A28[69]	NNNNTGATCGAGGAACCAAATATTGTAATATTGATGCCTGGCGGCAGTCGGTACCGAGGTCGGTACGCATGGCACCCGCATCG	NNNNGATGTGTCCGTGCFrA^QGGTCGATTCNNNN
DZ15WS[73]	NNNNTrA^GGAAGAGATGGCGACATCTCTTACAAACCCCAAACCTTCTCTT	
DZ27WS[73]	NNNNTrA^GGAAGAGATGGCGACATCTCCTCACCTCAAGCGACTTCTCTCG	
pH3DZ1[74]	GTAGTACGAGGAAATAGGGGGAGAGTGGTGTAGGCTTGAAGGTGCCACGTC	NNNNTGCFrA^QGGTTCGANNN
pH4DZ1[74]	GAGAAACATCTTTGAGGGATAAGCCGCCGATAGAGCGGAAGCGACTTGGTTGTAGCTG	NNNNTGCFrA^QGGTTCGANNN
pH5DZ1[74]	TGAATAGGGTCTCGGGCATAAATTACGGAAACGGTTTTAATTTTCTAGTGGAAAGGTCCGATAACGAG	NNNNTGCFrA^QGGTTCGANNN
Pistol-Like	NNNNATACGACTCAC^TATAGGAAGAGATGGCGACATAGTTAAGAGCTCGGGGTAGGCGGGAACAACGTTCACGTTGTGTNNNN	
PLDz[78]	GAATTCTAATACGA^CTCAGAATGAGCTGGGCCTCTTTTTAAGAAC	
F8-X[79]	NNNNC^TGCNNNNNNNNGTGTGTGGATGCCGGGTCCGNNN	
10MD5[82]	NNNNAACATAACTCCCTGTCGATATCGTTTGCGTGGGTGAATAGATGCNNNN	NNNNTATATG^TNNNN
Class I[81]	NNNNACGTAGTTGAGCTGTCNNNNNNNGACGTTGA^AGCGTNNNN	

Class II[81]	NNNN^AGCATCTTTGGCNNNNNGCTAGGGGAATAAATCTTTGGGCANNNN
RFA-EC1[101]	CACGGATCCTGACAAGGATGTGTGCGTTGTCGAGACCTGCGACCGGAACACT ACACTGTGTGGGATGGATT TCTTTACAGTTGTGCAGCTCCGTCCGACTCTTCCAGCFRQGGTTCGATCAAGA
AAI2-5[166]	GGAACGGTTAGATCTGATACCTTAGCGAAGGTGTGGTTGGC

^- cleavage site
F = Fluorophore (Fluorescein-dT), Q = Quencher (DABCYL-dT)

Table A3: pH drift of Tris upon heating[167]

5 °C	25 °C	37 °C
7.76	7.20	6.91
7.89	7.30	7.02
7.97	7.40	7.12
8.07	7.50	7.22
8.18	7.60	7.30
8.26	7.70	7.40
8.37	7.80	7.52
8.48	7.90	7.62
8.58	8.00	7.71
8.68	8.10	7.80
8.78	8.20	7.91
8.88	8.30	8.01
8.98	8.40	8.10
9.09	8.50	8.22
9.18	8.60	8.31
9.28	8.70	8.42

List of Buffers

Reaction Buffer (1X)

10 mM Tris HCl

10 mM $MgCl_2$

50 mM NaCl

pH 7.9 at 25 °C

Reaction Buffer – RCA (1X)

10 mM Tris HCl

10 mM $MgCl_2$

50 mM NaCl

1 mM ATP

1 mM of each dNTP

pH 7.9 at 25 °C

ABTS Imaging Buffer (1X)

10 mM Tris HCl

10 mM $MgCl_2$

50 mM NaCl

40 μM Hemin

6 mM ABTS

pH 7.0 at 25 °C

References

1. Tideman, P. A. *et al.* Impact of a regionalised clinical cardiac support network on mortality among rural patients with myocardial infarction. *Med. J. Aust.* **200**, 157–160 (2014).

2. Nerenz, R. D. & Gronowski, A. M. Qualitative Point-of-Care Human Chorionic Gonadotropin Testing: Can We Defuse This Ticking Time Bomb? *Clin. Chem.* **61**, 483–486 (2015).

3. Olansky, L. & Kennedy, L. Finger-Stick Glucose Monitoring. *Diabetes Care* **33**, 948–949 (2010).

4. Jyoti, B. & Devi, P. Detection of human immunodeficiency virus using oral mucosal transudate by rapid test. *Indian J. Sex. Transm. Dis.* **34**, 95–101 (2013).

5. R. W. Peeling, K. K. Holmes & D. Mabey. Rapid tests for sexually transmitted infections (STIs): the way forward. *Sex. Transm. Infect. J.* **82**, 1–6 (2006).

6. Wan, E. *et al.* Green Technologies for Room Temperature Nucleic Acid Storage. *Curr. Issues Mol. Biol.* **12**, 135–142 (2010).

7. Ferraz, A. S. *et al.* Storage and stability of IgG and IgM monoclonal antibodies dried on filter paper and utility in *Neisseria meningitidis* serotyping by Dot-blot ELISA. *BMC Infect. Dis.* **8**, 30 (2008).

8. Goertz, J. P. & White, I. M. Phase-Change Partitions for Thermal Automation of Multistep Reactions. *Anal. Chem.* 3708–3713 (2018).

9. Kuang, J., Yan, X., Genders, A. J., Granata, C. & Bishop, D. J. An overview of technical considerations when using quantitative real-time PCR analysis of gene expression in human exercise research. *PLOS ONE* **13**, e0196438 (2018).

10. Valones, M. A. A. *et al.* Principles and applications of polymerase chain reaction in medical diagnostic fields: a review. *Braz. J. Microbiol.* **40**, 1–11 (2009).

11. Petralia, S. & Conoci, S. PCR Technologies for Point of Care Testing: Progress and Perspectives. *ACS Sens.* **2**, 876–891 (2017).

12. Dove, A. PCR: Thirty-five years and counting. *Science | AAAS* (2018).

13. Guatelli, J. C. *et al.* Isothermal, in vitro amplification of nucleic acids by a multienzyme reaction modeled after retroviral replication. *Proc. Natl. Acad. Sci. U. S. A.* **87**, 1874–1878 (1990).

14. Fahy, E., Kwoh, D. Y. & Gingeras, T. R. Self-sustained sequence replication (3SR): an isothermal transcription-based amplification system alternative to PCR. *Genome Res.* **1**, 25–33 (1991).

15. Van Ness, J., Van Ness, L. K. & Galas, D. J. Isothermal reactions for the amplification of oligonucleotides. *Proc. Natl. Acad. Sci. U. S. A.* **100**, 4504–4509 (2003).

16. Wong, Y.-P., Othman, S., Lau, Y.-L., Radu, S. & Chee, H.-Y. Loop-mediated isothermal amplification (LAMP): a versatile technique for detection of micro-organisms. *J. Appl. Microbiol.* **124**, 626–643 (2018).

17. Notomi, T. *et al.* Loop-mediated isothermal amplification of DNA. *Nucleic Acids Res.* **28**, e63 (2000).

18. Vincent, M., Xu, Y. & Kong, H. Helicase-dependent isothermal DNA amplification. *EMBO Rep.* **5**, 795–800 (2004).

19. An, L. *et al.* Characterization of a thermostable UvrD helicase and its participation in helicase dependent amplification. *J. Biol. Chem.* **280**, 28952–28958 (2005).

20. Fire, A. & Xu, S. Q. Rolling replication of short DNA circles. *Proc. Natl. Acad. Sci. U. S. A.* **92**, 4641–4645 (1995).

21. Zhou, H. *et al.* Ultrasensitive genotyping with target-specifically generated circular DNA templates and RNA FRET probes. *Chem. Commun.* **51**, 11556–11559 (2015).

22. Xu, H. *et al.* Loopback rolling circle amplification for ultrasensitive detection of Kras gene. *Talanta* **164**, 511–517 (2017).

23. Beals, T. P., Smith, J. H., Nietupski, R. M. & Lane, D. J. A mechanism for ramified rolling circle amplification. *BMC Mol. Biol.* **11**, 94 (2010).

24. Xu, C. *et al.* Branched RCA coupled with a NESA-based fluorescence assay for ultrasensitive detection of miRNA. *New J. Chem.* **41**, 5355–5361 (2017).

25. Li, H., Xu, J., Wang, Z., Wu, Z.-S. & Jia, L. Increasingly branched rolling circle amplification for the cancer gene detection. *Biosens. Bioelectron.* **86**, 1067–1073 (2016).

26. Dahl, F. *et al.* Circle-to-circle amplification for precise and sensitive DNA analysis. *Proc. Natl. Acad. Sci. U. S. A.* **101**, 4548–4553 (2004).

27. Murakami, T., Sumaoka, J. & Komiyama, M. Sensitive isothermal detection of nucleic-acid sequence by primer generation–rolling circle amplification. *Nucleic Acids Res.* **37**, e19 (2009).

28. Hutchison, C. A., Smith, H. O., Pfannkoch, C. & Venter, J. C. Cell-free cloning using φ29 DNA polymerase. *Proc. Natl. Acad. Sci. U. S. A.* **102**, 17332–17336 (2005).

29. Dean, F. B., Nelson, J. R., Giesler, T. L. & Lasken, R. S. Rapid Amplification of Plasmid and Phage DNA Using Phi29 DNA Polymerase and Multiply-Primed Rolling Circle Amplification. *Genome Res.* **11**, 1095–1099 (2001).

30. Barzon, L. *et al.* Isolation of infectious Zika virus from saliva and prolonged viral RNA shedding in a traveller returning from the Dominican Republic to Italy, January 2016. *Eurosurveillance* **21**, 30159 (2016).

31. Bonaldo, M. C. *et al.* Isolation of Infective Zika Virus from Urine and Saliva of Patients in Brazil. *PLoS Negl. Trop. Dis.* **10**, e0004816 (2016).

32. Kruger, K. *et al.* Self-splicing RNA: Autoexcision and autocyclization of the ribosomal RNA intervening sequence of tetrahymena. *Cell* **31**, 147–157 (1982).

33. Breaker, R. R. & Joyce, G. F. A DNA enzyme that cleaves RNA. *Chem. Biol.* **1**, 223–229 (1994).

34. Caruthers, M. H. *et al.* Chemical synthesis of deoxyoligonucleotides by the phosphoramidite method. in *Methods in Enzymology* vol. 154 287–313 (Academic Press, 1987).

35. Nilsson, B. L., Soellner, M. B. & Raines, R. T. Chemical Synthesis of Proteins. *Annu. Rev. Biophys. Biomol. Struct.* **34**, 91–118 (2005).

36. Li, Y. & Breaker, R. R. Kinetics of RNA Degradation by Specific Base Catalysis of Transesterification Involving the 2′-Hydroxyl Group. *J. Am. Chem. Soc.* **121**, 5364–5372 (1999).

37. Victor A. Bloomfield, Donald M. Crothers & Ignacio Tinoco, Jr. *Nucleic Acids: Structures, Properties and Functions*. (Sausalito: University Science Books, 2000).

38. Ma, S., Tang, N. & Tian, J. DNA Synthesis, Assembly and Applications in Synthetic Biology. *Curr. Opin. Chem. Biol.* **16**, 260–267 (2012).

39. Lu, C.-H., Wang, F. & Willner, I. Zn^{2+}-Ligation DNAzyme-Driven Enzymatic and Nonenzymatic Cascades for the Amplified Detection of DNA. *J. Am. Chem. Soc.* **134**, 10651–10658 (2012).

40. Cuenoud, B. & Szostak, J. W. A DNA metalloenzyme with DNA ligase activity. *Nature* **375**, 611–614 (1995).

41. Purtha, W. E., Coppins, R. L., Smalley, M. K. & Silverman, S. K. General Deoxyribozyme-Catalyzed Synthesis of Native 3′−5′ RNA Linkages. *J. Am. Chem. Soc.* **127**, 13124–13125 (2005).

42. Camden, A. J., Walsh, S. M., Suk, S. H. & Silverman, S. K. DNA Oligonucleotide 3′-Phosphorylation by a DNA Enzyme. *Biochemistry* **55**, 2671–2676 (2016).

43. Chandrasekar, J. & Silverman, S. K. Catalytic DNA with phosphatase activity. *Proc. Natl. Acad. Sci. U. S. A.* **110**, 5315–5320 (2013).

44. Li, Y. & Sen, D. Toward an Efficient DNAzyme. *Biochemistry* **36**, 5589–5599 (1997).

45. Xiao, Y. *et al.* Catalytic Beacons for the Detection of DNA and Telomerase Activity. *J. Am. Chem. Soc.* **126**, 7430–7431 (2004).

46. Silverman, S. K. Catalytic DNA: Scope, Applications, and Biochemistry of Deoxyribozymes. *Trends Biochem. Sci.* **41**, 595–609 (2016).

47. M. Liu, D. Chang & Yingfu Li. Discovery and Biosensing Applications of Diverse RNA-Cleaving DNAzymes. *Acc. Chem. Res.* **50**, 2273–2283 (2017).

48. Morrison, D., Rothenbroker, M. & Li, Y. DNAzymes: Selected for Applications. *Small Methods* **2**, 1–12 (2018).

49. Santoro, S. W. & Joyce, G. F. A general purpose RNA-cleaving DNA enzyme. *Proc. Natl. Acad. Sci. USA* **94**, 4262–4266 (1997).

50. Schlosser, K. & Li, Y. A Versatile Endoribonuclease Mimic Made of DNA: Characteristics and Applications of the 8–17 RNA-Cleaving DNAzyme. *ChemBioChem* **11**, 866–879 (2010).

51. Liu, H. *et al.* Crystal structure of an RNA-cleaving DNAzyme. *Nat. Commun.* **8**, 2006 (2017).

52. Zaborowska, Z., Fürste, J. P., Erdmann, V. A. & Kurreck, J. Sequence Requirements in the Catalytic Core of the "10-23" DNA Enzyme. *J. Biol. Chem.* **277**, 40617–40622 (2002).

53. Schubert, S. *et al.* RNA cleaving '10-23' DNAzymes with enhanced stability and activity. *Nucleic Acids Res.* **31**, 5982–5992 (2003).

54. Schlosser, K. & Li, Y. DNAzyme-mediated catalysis with only guanosine and cytidine nucleotides. *Nucleic Acids Res.* **37**, 413–420 (2009).

55. Gao, J., Shimada, N. & Maruyama, A. MNAzyme-catalyzed nucleic acid detection enhanced by a cationic copolymer. *Biomater. Sci.* **3**, 716–720 (2015).

56. Gerasimova, Y. V. & Kolpashchikov, D. M. Nucleic Acid Detection using MNAzymes. *Chem. Biol.* **17**, 104–106 (2010).

57. Zhou, W., Zhang, Y., Huang, P.-J. J., Ding, J. & Liu, J. A DNAzyme requiring two different metal ions at two distinct sites. *Nucleic Acids Res.* **44**, 354–363 (2016).

58. Breaker, R. R. & Joyce, G. F. A DNA enzyme with Mg^{2+}-dependent RNA phosphoesterase activity. *Chem. Biol.* **2**, 655–660 (1995).

59. Zhou, W., Saran, R., Chen, Q., Ding, J. & Liu, J. A New Na+-Dependent RNA-Cleaving DNAzyme with over 1000-fold Rate Acceleration by Ethanol. *ChemBioChem* **17**, 159–163 (2016).

60. Schlosser, K., Gu, J., Lam, J. C. F. & Li, Y. In vitro selection of small RNA-cleaving deoxyribozymes that cleave pyrimidine–pyrimidine junctions. *Nucleic Acids Res.* **36**, 4768–4777 (2008).

61. Lam, J. C. F., Withers, J. B. & Li, Y. A Complex RNA-Cleaving DNAzyme That Can Efficiently Cleave a Pyrimidine–Pyrimidine Junction. *J. Mol. Biol.* **400**, 689–701 (2010).

62. Saran, R. & Liu, J. A Silver DNAzyme. *Anal. Chem.* **88**, 4014–4020 (2016).

63. Liu, J. & Lu, Y. Rational Design of "Turn-On" Allosteric DNAzyme Catalytic Beacons for Aqueous Mercury Ions with Ultrahigh Sensitivity and Selectivity. *Angew. Chem. Int. Ed.* **46**, 7587–7590 (2007).

64. Liu, J. *et al.* A catalytic beacon sensor for uranium with parts-per-trillion sensitivity and millionfold selectivity. *Proc. Natl. Acad. Sci. U. S. A.* **104**, 2056–2061 (2007).

65. Lan, T., Furuya, K. & Lu, Y. A highly selective lead sensor based on a classic lead DNAzyme. *Chem. Commun. Camb. Engl.* **46**, 3896–3898 (2010).

66. Huang, P.-J. J. & Liu, J. An Ultrasensitive Light-up Cu^{2+} Biosensor Using a New DNAzyme Cleaving a Phosphorothioate-Modified Substrate. *Anal. Chem.* **88**, 3341–3347 (2016).

67. Mei, S. H. J., Liu, Z., Brennan, J. D. & Li, Y. An Efficient RNA-Cleaving DNA Enzyme that Synchronizes Catalysis with Fluorescence Signaling. *J. Am. Chem. Soc.* **125**, 412–420 (2003).

68. Chiuman, W. & Li, Y. Simple Fluorescent Sensors Engineered with Catalytic DNA 'MgZ' Based on a Non-Classic Allosteric Design. *PLoS ONE* **2**, e1224 (2007).

69. Chiuman, W. & Li, Y. Evolution of High-Branching Deoxyribozymes from a Catalytic DNA with a Three-Way Junction. *Chem. Biol.* **13**, 1061–1069 (2006).

70. Lam, J. C. F., Kwan, S. O. & Li, Y. Characterization of non-8–17 sequences uncovers structurally diverse RNA-cleaving deoxyribozymes. *Mol. Biosyst.* **7**, 2139–2146 (2011).

71. Geyer, C. R. & Sen, D. Evidence for the metal-cofactor independence of an RNA phosphodiester-cleaving DNA enzyme. *Chem. Biol.* **4**, 579–593 (1997).

72. Torabi, S.-F. *et al.* In vitro selection of a sodium-specific DNAzyme and its application in intracellular sensing. *Proc. Natl. Acad. Sci. U. S. A.* **112**, 5903–5908 (2015).

73. Kasprowicz, A., Stokowa-Sołtys, K., Jeżowska-Bojczuk, M., Wrzesiński, J. & Ciesiołka, J. Characterization of Highly Efficient RNA-Cleaving DNAzymes that Function at Acidic pH with No Divalent Metal-Ion Cofactors. *ChemistryOpen* **6**, 46–56 (2017).

74. Liu, Z., Mei, S. H. J., Brennan, J. D. & Li, Y. Assemblage of Signaling DNA Enzymes with Intriguing Metal-Ion Specificities and pH Dependences. *J. Am. Chem. Soc.* **125**, 7539–7545 (2003).

75. Ali, Md. M., Kandadai, S. A. & Li, Y. Characterization of pH3DZ1 — An RNA-cleaving deoxyribozyme with optimal activity at pH 3. *Can. J. Chem.* **85**, 261–273 (2007).

76. Carmi, N., Shultz, L. A. & Breaker, R. R. In vitro selection of self-cleaving DNAs. *Chem. Biol.* **3**, 1039–1046 (1996).

77. Carmi, N., Balkhi, S. R. & Breaker, R. R. Cleaving DNA with DNA. *Proc. Natl. Acad. Sci. USA* **95**, 2233–2237 (1998).

78. Sun, Y. *et al.* New cofactors and inhibitors for a DNA-cleaving DNAzyme: superoxide anion and hydrogen peroxide mediated an oxidative cleavage process. *Sci. Rep.* **7**, (2017).

79. Wang, M. *et al.* In vitro selection of DNA-cleaving deoxyribozyme with site-specific thymidine excision activity. *Nucleic Acids Res.* **42**, 9262–9269 (2014).

80. Xiao, Y., Chandra, M. & Silverman, S. K. Functional Compromises Among pH Tolerance, Site Specificity, and Sequence Tolerance for a DNA-Hydrolyzing Deoxyribozyme. *Biochemistry* **49**, 9630–9637 (2010).

81. Gu, H., Furukawa, K., Weinberg, Z., Berenson, D. F. & Breaker, R. R. Small, Highly Active DNAs That Hydrolyze DNA. *J. Am. Chem. Soc.* **135**, 9121–9129 (2013).

82. Chandra, M., Sachdeva, A. & Silverman, S. K. DNA-catalyzed sequence-specific hydrolysis of DNA. *Nat. Chem. Biol.* **5**, 718–720 (2009).

83. Xiao, Y., Allen, E. C. & Silverman, S. K. Merely two mutations switch a DNA-hydrolyzing deoxyribozyme from heterobimetallic (Zn^{2+}/Mn^{2+}) to monometallic (Zn^{2+}-only) behavior. *Chem. Commun. Camb. Engl.* **47**, 1749–1751 (2011).

84. Haruki, M., Tsunaka, Y., Morikawa, M. & Kanaya, S. Cleavage of a DNA–RNA–DNA/DNA chimeric substrate containing a single ribonucleotide at the DNA–RNA junction with prokaryotic RNases HII. *FEBS Lett.* **531**, 204–208 (2002).

85. Elbaz, J., Moshe, M., Shlyahovsky, B. & Willner, I. Cooperative Multicomponent Self-Assembly of Nucleic Acid Structures for the Activation of DNAzyme Cascades: A Paradigm for DNA Sensors and Aptasensors. *Chemistry* **15**, 3411–3418 (2009).

86. Yin, B.-C., Ye, B.-C., Tan, W. & Xie, C.-C. An Allosteric Dual-DNAzyme Unimolecular Probe for Colorimetric Detection of Copper(II). *J. Am. Chem. Soc.* **131**, 14624–14625 (2009).

87. Martin, T. D. Determination of Trace Elements in Drinking Water by Axially Viewed Inductively Coupled Plasma-Atomic Emission Spectroscopy. *EPA Methods Report* 36 (2003).

88. Wang, S., Forzani, E. S. & Tao, N. Detection of Heavy Metal Ions in Water by High-Resolution Surface Plasmon Resonance Spectroscopy Combined with Anodic Stripping Voltammetry. *Anal. Chem.* **79**, 4427–4432 (2007).

89. Cerovac, S. *et al.* Trace level voltammetric determination of lead and cadmium in sediment pore water by a bismuth-oxychloride particle-multiwalled carbon nanotube composite modified glassy carbon electrode. *Talanta* **134**, 640–649 (2015).

90. Zeng, Y., Ren, J., Shen, A. & Hu, J. Field and Pretreatment-Free Detection of Heavy-Metal Ions in Organic Polluted Water through an Alkyne-Coded SERS Test Kit. *ACS Appl. Mater. Interfaces* **8**, 27772–27778 (2016).

91. Xu, W., Tian, J., Luo, Y., Zhu, L. & Huang, K. A rapid and visual turn-off sensor for detecting copper (II) ion based on DNAzyme coupled with HCR-based HRP concatemers. *Sci. Rep.* **7**, 43362 (2017).

92. Zhou, W., Zhang, Y., Ding, J. & Liu, J. In Vitro Selection in Serum: RNA-Cleaving DNAzymes for Measuring Ca^{2+} and Mg^{2+}. *ACS Sens.* **1**, 600–606 (2016).

93. Engvall, E. & Perlmann, P. Enzyme-linked immunosorbent assay (ELISA) quantitative assay of immunoglobulin G. *Immunochemistry* **8**, 871–874 (1971).

94. de la Rica, R. & Stevens, M. M. Plasmonic ELISA for the ultrasensitive detection of disease biomarkers with the naked eye. *Nat. Nanotechnol.* **7**, 821–824 (2012).

95. Verma, M. S. *et al.* Sliding-strip microfluidic device enables ELISA on paper. *Biosens. Bioelectron.* **99**, 77–84 (2018).

96. Saiki, R. K. *et al.* Enzymatic amplification of beta-globin genomic sequences and restriction site analysis for diagnosis of sickle cell anemia. *Science* **230**, 1350–1354 (1985).

97. Yang, L., Du, F., Chen, G., Yasmeen, A. & Tang, Z. A novel colorimetric PCR-based biosensor for detection and quantification of hepatitis B virus. *Anal. Chim. Acta* **840**, 75–81 (2014).

98. Ahrberg, C. D., Ilic, B. R., Manz, A. & Neužil, P. Handheld real-time PCR device. *Lab. Chip* **16**, 586–592 (2016).

99. Zhang, B., Liu, B., Zhuang, J. & Tang, D. Cleavage of Metal-Ion-Induced DNAzymes Released from Nanolabels for Highly Sensitive and Specific Immunoassay. *Bioconjug. Chem.* **24**, 678–683 (2013).

100. Huang Fu, Z.-Z. *et al.* Highly Sensitive Fluorescent Immunoassay of Human Immunoglobulin G Based on PbS Nanoparticles and DNAzyme. *Anal. Sci.* **29**, 499–504 (2013).

101. Zhang, W., Feng, Q., Chang, D., Tram, K. & Li, Y. In vitro selection of RNA-cleaving DNAzymes for bacterial detection. *Methods* **106**, 66–75 (2016).

102. Ali, M. M. *et al.* A Printed Multicomponent Paper Sensor for Bacterial Detection. *Sci. Rep.* **7**, 12335 (2017).

103. Liu, M. *et al.* Programming a topologically constrained DNA nanostructure into a sensor. *Nat. Commun.* **7**, 12074 (2016).

104. Liu, M. *et al.* A DNAzyme Feedback Amplification Strategy for Biosensing. *Angew. Chem. Int. Ed.* 6142–6146 (2017).

105. Peng, H. *et al.* DNAzyme-Mediated Assays for Amplified Detection of Nucleic Acids and Proteins. *Anal. Chem.* **90**, 190–207 (2018).

106. Jimenez, R. M., Polanco, J. A. & Lupták, A. Chemistry and biology of self-cleaving ribozymes. *Trends Biochem. Sci.* **40**, 648–661 (2015).

107. Santoro, S. W. & Joyce, G. F. Mechanism and Utility of an RNA-Cleaving DNA Enzyme. *Biochemistry* **37**, 13330–13342 (1998).

108. Das, U. & Shuman, S. Mechanism of RNA 2′,3′-cyclic phosphate end healing by T4 polynucleotide kinase–phosphatase. *Nucleic Acids Res.* **41**, 355–365 (2013).

109. Lee, Y. *et al.* DNA-Catalyzed DNA Cleavage by a Radical Pathway with Well-Defined Products. *J. Am. Chem. Soc.* **139**, 255–261 (2017).

110. Claussen, C. A. & Long, E. C. Nucleic Acid Recognition by Metal Complexes of Bleomycin. *Chem. Rev.* **99**, 2797–2816 (1999).

111. Burger, R. M. Cleavage of Nucleic Acids by Bleomycin. *Chem. Rev.* **98**, 1153–1170 (1998).

112. Stephen W. Santoro & Gerald F. Joyce. Mechanism and Utility of an RNA-Cleaving DNA Enzyme. *Biochemistry* **37**, 13330–13342 (1998).

113. Ota, N., Warashina, M., Hirano, K., Hatanaka, K. & Taira, K. Effects of helical structures formed by the binding arms of DNAzymes and their substrates on catalytic activity. *Nucleic Acids Res.* **26**, 3385–3391 (1998).

114. Schlosser, K., Gu, J., Sule, L. & Li, Y. Sequence-function relationships provide new insight into the cleavage site selectivity of the 8–17 RNA-cleaving deoxyribozyme. *Nucleic Acids Res.* **36**, 1472–1481 (2008).

115. Fischer, B. E., Häring, U. K., Tribolet, R. & Sigel, H. Metal Ion/Buffer Interactions. *Eur. J. Biochem.* **94**, 523–530 (1979).

116. Maruyama, A. *et al.* Characterization of Interpolyelectrolyte Complexes between Double-Stranded DNA and Polylysine Comb-Type Copolymers Having Hydrophilic Side Chains. *Bioconjug. Chem.* **9**, 292–299 (1998).

117. Vasudevamurthy, M. K., Lever, M., George, P. M. & Morison, K. R. Betaine structure and the presence of hydroxyl groups alters the effects on DNA melting temperatures. *Biopolymers* **91**, 85–94 (2009).

118. Seifi, T. *et al.* Amplification of GC-rich Putative Mouse PeP Promoter using Betaine and DMSO in Ammonium Sulfate Polymerase Chain Reaction Buffer. *Avicenna J. Med. Biotechnol.* **4**, 206–209 (2012).

119. Sandigursky, M. & Franklin, W. A. Exonuclease I of *Escherichia coli* Removes Phosphoglycolate 3′-End Groups from DNA. *Radiat. Res.* **135**, 229–233 (1993).

120. Inamdar, K. V. *et al.* Conversion of Phosphoglycolate to Phosphate Termini on 3′ Overhangs of DNA Double Strand Breaks by the Human Tyrosyl-DNA Phosphodiesterase hTdp1. *J. Biol. Chem.* **277**, 27162–27168 (2002).

121. Nagappa, L. K., Satha, P., Govindaraju, T. & Balaram, H. Phosphoglycolate phosphatase is a metabolic proof-reading enzyme essential for cellular function in Plasmodium berghei. *J. Biol. Chem.* **13**, 4997–5007 (2019).

122. Lizardi, P. M. *et al.* Mutation detection and single-molecule counting using isothermal rolling-circle amplification. *Nat. Genet.* **19**, 225 (1998).

123. Polidoros, A. N., Pasentsis, K. & Tsaftaris, A. S. Rolling circle amplification-RACE: a method for simultaneous isolation of 5′ and 3′ cDNA ends from amplified cDNA templates. *BioTechniques* **41**, 35–42 (2006).

124. Murakami, T., Sumaoka, J. & Komiyama, M. Sensitive RNA detection by combining three-way junction formation and primer generation-rolling circle amplification. *Nucleic Acids Res.* **40**, e22 (2012).

125. Kühnemund, M., Witters, D., Nilsson, M. & Lammertyn, J. Circle-to-circle amplification on a digital microfluidic chip for amplified single molecule detection. *Lab. Chip* **14**, 2983–2992 (2014).

126. Berg, J. M., Tymoczko, J. L. & Stryer, L. Enzymes Can Be Inhibited by Specific Molecules. in *Biochemistry.* (W. H. Freeman and Co., 2002).

127. Murphy, M. C., Rasnik, I., Cheng, W., Lohman, T. M. & Ha, T. Probing Single-Stranded DNA Conformational Flexibility Using Fluorescence Spectroscopy. *Biophys. J.* **86**, 2530–2537 (2004).

128. Marras, S. A. E., Kramer, F. R. & Tyagi, S. Efficiencies of fluorescence resonance energy transfer and contact-mediated quenching in oligonucleotide probes. *Nucleic Acids Res.* **30**, e122–e122 (2002).

129. Schwartz, J. J. & Quake, S. R. Single molecule measurement of the “speed limit” of DNA polymerase. *Proc. Natl. Acad. Sci.* U.S.A. **106**, 20294–20299 (2009).

130. Stefan, L., Denat, F. & Monchaud, D. Insights into how nucleotide supplements enhance the peroxidase-mimicking DNAzyme activity of the G-quadruplex/hemin system. *Nucleic Acids Res.* **40**, 8759–8772 (2012).

131. Liao, A. M. *et al.* A Simple Colorimetric System for Detecting Target Antigens by a Three-Stage Signal Transformation–Amplification Strategy. *Biochemistry* **57**, 5117–5126 (2018).

132. Wang, X.-P., Yin, B.-C., Wang, P. & Ye, B.-C. Highly sensitive detection of microRNAs based on isothermal exponential amplification-assisted generation of catalytic G-quadruplexDNAzyme. *Biosens. Bioelectron.* **42**, 131–135 (2013).

133. Li, H. *et al.* Ultrasensitive label-free amplified colorimetric detection of p53 based on G-quadruplex MBzymes. *Biosens. Bioelectron.* **50**, 180–185 (2013).

134. Du, Y.-C., Jiang, H.-X., Huo, Y.-F., Han, G.-M. & Kong, D.-M. Optimization of strand displacement amplification-sensitized G-quadruplex DNAzyme-based sensing system and its application in activity detection of uracil-DNA glycosylase. *Biosens. Bioelectron.* **77**, 971–977 (2016).

135. Jiang, H.-X., Liang, Z.-Z., Ma, Y.-H., Kong, D.-M. & Hong, Z.-Y. G-quadruplex fluorescent probe-mediated real-time rolling circle amplification strategy for highly sensitive microRNA detection. *Anal. Chim. Acta* **943**, 114–122 (2016).

136. Huang, J. *et al.* Sensitive fluorescent detection of DNA methyltransferase using nicking endonuclease-mediated multiple primers-like rolling circle amplification. *Biosens. Bioelectron.* **91**, 417–423 (2017).

137. Joon Lee, I., Goo, N.-I. & Kim, D.-E. Label/quencher-free detection of single-nucleotide changes in DNA using isothermal amplification and G-quadruplexes. *Analyst* **141**, 6503–6506 (2016).

138. Imlay, J. A., Chin, S. M. & Linn, S. Toxic DNA damage by hydrogen peroxide through the Fenton reaction in vivo and in vitro. *Science* **240**, 640–642 (1988).

139. Marchand, A. & Gabelica, V. Folding and misfolding pathways of G-quadruplex DNA. *Nucleic Acids Res.* **44**, 10999–11012 (2016).

140. Kong, D.-M., Cai, L.-L., Guo, J.-H., Wu, J. & Shen, H.-X. Characterization of the G-quadruplex structure of a catalytic DNA with peroxidase activity. *Biopolymers* **91**, 331–339 (2009).

141. You, H., Wu, J., Shao, F. & Yan, J. Stability and Kinetics of c-MYC Promoter G-Quadruplexes Studied by Single-Molecule Manipulation. *J. Am. Chem. Soc.* **137**, 2424–2427 (2015).

142. Anantha, N. V., Azam, M. & Sheardy, R. D. Porphyrin Binding to Quadruplexed T4G4. *Biochemistry* **37**, 2709–2714 (1998).

143. Guo, Y. *et al.* A Thermophilic Tetramolecular G-Quadruplex/Hemin DNAzyme. *Angew. Chem. Int. Ed.* **56**, 16636–16640 (2017).

144. Etz, E. S. & Robinson, R. A. Dissociation Constant of Protonated Tris(hydroxymethyl)aminomethane in N-Methylpropionamide and Related Thermodynamic Quantities from 10 to 55 °C. *J. Solut. Chem.* **2**, 405–415 (1973).

145. Li, W., Miyoshi, D., Nakano, S. & Sugimoto, N. Structural Competition Involving G-Quadruplex DNA and Its Complement. *Biochemistry* **42**, 11736–11744 (2003).

146. Yan, Y.-Y. *et al.* G-Quadruplex conformational change driven by pH variation with potential application as a nanoswitch. *Biochim. Biophys. Acta BBA - Gen. Subj.* **1830**, 4935–4942 (2013).

147. Manoj, K. M. *et al.* Atypical profiles and modulations of heme-enzymes catalyzed outcomes by low amounts of diverse additives suggest diffusible radicals' obligatory involvement in such redox reactions. *Biochimie* **125**, 91–111 (2016).

148. Edwards, D. N., Machwe, A., Wang, Z. & Orren, D. K. Intramolecular Telomeric G-Quadruplexes Dramatically Inhibit DNA Synthesis by Replicative and Translesion Polymerases, Revealing their Potential to Lead to Genetic Change. *PLOS ONE* **9**, e80664 (2014).

149. Nagesh, N. & Chatterji, D. Ammonium ion at low concentration stabilizes the G-quadruplex formation by telomeric sequence. *J. Biochem. Biophys. Methods* **30**, 1–8 (1995).

150. Hud, N. V., Schultze, P., Sklenář, V. & Feigon, J. Binding sites and dynamics of ammonium ions in a telomere repeat DNA quadruplex. *J. Mol. Biol.* **285**, 233–243 (1999).

151. Smirnov, I. V. & Shafer, R. H. Electrostatics dominate quadruplex stability. *Biopolymers* **85**, 91–101 (2007).

152. Edington, B. V., Whelan, S. A. & Hightower, L. E. Inhibition of heat shock (stress) protein induction by deuterium oxide and glycerol: Additional support for the abnormal protein hypothesis of induction. *J. Cell. Physiol.* **139**, 219–228 (1989).

153. Kim, D. & Lee, Y. J. Effect of glycerol on protein aggregation: Quantitation of thermal aggregation of proteins from CHO cells and analysis of aggregated proteins. *J. Therm. Biol.* **18**, 41–48 (1993).

154. Buyukkileci, C., Batur, A., Buyukkileci, A. O. & Hamamci, H. Temperature and Glycerol Formation: A Proposal to Explain the Causal Relationship Based on Glycolytic Enzyme Activities. *Am. J. Enol. Vitic.* **70**, 155–161 (2019).

155. Gekko, K. & Timasheff, S. N. Mechanism of protein stabilization by glycerol: preferential hydration in glycerol-water mixtures. *Biochemistry* **20**, 4667–4676 (1981).

156. Gao, F., Zhang, X., Wang, J., Sun, X. & Wang, C. Systematical characterization of functional and antioxidative properties of heat-induced polymerized whey proteins. *Food Sci. Biotechnol.* **27**, 1619–1626 (2018).

157. Applied Photophysics. Rational Optimization of Solvent Conditions for G-Quadruplex Oligonucleotides. (2019).

158. Hoppmann, E. P., Yu, W. W. & White, I. M. Detection of Deoxyribonucleic Acid (DNA) Targets Using Polymerase Chain Reaction (PCR) and Paper Surface-Enhanced Raman Spectroscopy (SERS) Chromatography. *Appl. Spectrosc.* **68**, 909–915 (2014).

159. Berger, A. G., Restaino, S. M. & White, I. M. Vertical-flow paper SERS system for therapeutic drug monitoring of flucytosine in serum. *Anal. Chim. Acta* **949**, 59–66 (2017).

160. Y. Zhao, F. Chen, Q. Li, L. Wang & C. Fang. Isothermal Amplification of Nucleic Acids. *Chem. Rev.* **115**, 12491–12545 (2015).

161. Ratilainen, T., Holmén, A., Tuite, E., Nielsen, P. E. & Nordén, B. Thermodynamics of Sequence-Specific Binding of PNA to DNA. *Biochemistry* **39**, 7781–7791 (2000).

162. Braasch, D. A. & Corey, D. R. Locked nucleic acid (LNA): fine-tuning the recognition of DNA and RNA. *Chem. Biol.* **8**, 1–7 (2001).

163. Metzler, R. & Ambjörnsson, T. Dynamic Approach to DNA Breathing. *J. Biol. Phys.* **31**, 339–350 (2005).

164. Zhang, X. *et al.* Ultraselective electrochemiluminescence biosensor based on locked nucleic acid modified toehold-mediated strand displacement reaction and junction-probe. *Analyst* **139**, 6109–6112 (2014).

165. Smolina, I. V., Demidov, V. V., Soldatenkov, V. A., Chasovskikh, S. G. & Frank-Kamenetskii, M. D. End invasion of peptide nucleic acids (PNAs) with mixed-base composition into linear DNA duplexes. *Nucleic Acids Res.* **33**, e146 (2005).

166. He, S. *et al.* Highly Specific Recognition of Breast Tumors by an RNA-Cleaving Fluorogenic DNAzyme Probe. *Anal. Chem.* **87**, 569–577 (2015).

167. pH vs Temperature For Tris Buffer. *New England Biolabs* https://www.neb.com/tools-and-resources/usage-guidelines/ph-vs-temperature-for-tris-buffer.